# CONTROLLING THE RADIATION SPECTRUM OF SOLE-SOURCE LIGHTING TO ELICIT DESIRABLE PHOTOMORPHOGENIC TRAITS AND REGULATE FLOWERING OF FLORICULTURE SEEDLINGS

By

Yujin Park

## A DISSERTATION

Submitted to
Michigan State University
in partial fulfillment of the requirements
for the degree of

Horticulture—Doctor of Philosophy

2018

#### **ABSTRACT**

# CONTROLLING THE RADIATION SPECTRUM OF SOLE-SOURCE LIGHTING TO ELICIT DESIRABLE PHOTOMORPHOGENIC TRAITS AND REGULATE FLOWERING OF FLORICULTURE SEEDLINGS

By

### Yujin Park

Application of sole-source light-emitting diode (LED) lighting in floricultural crop production is of increasing interest because of their high energy efficiency, longevity, and ability to deliver a customized radiation spectrum. One of the most important aspects of implementing LED lighting is to identify the radiation spectrum that elicits the desired plant characteristics. The objectives of this research were to investigate how sole-source lighting, with different spectral and intensity combinations, of blue (B, 400–500 nm), red (R, 600–700 nm), far-red (FR, 700–800 nm), and white (W) LEDs regulates photomorphogenic traits and flowering responses on a range of floriculture crops in highly controlled environments. During the first experiment, we investigated how the addition of FR radiation or partial substitution of R with FR radiation in B+R sole-source lighting influences seedling growth and subsequent flowering of geranium (Pelargonium ×hortorum), petunia (Petunia ×hybrida), snapdragon (Antirrhinum majus), and impatiens (*Impatiens walleriana*). As the R:FR (or estimated phytochrome photoequilibrium) of radiation treatments increased, seedling height in all species and total leaf area of geranium and snapdragon linearly decreased. In geranium and snapdragon, the increased total leaf area (by 7 %) with the addition of FR at the same photosynthetic photon flux density (PPFD) was accompanied by an increase in shoot dry weight (by 28–50%) while the increase of total leaf area (by 30–40%) with partial substitution of R with FR produced similar shoot dry weight compensating the

reduced PPFD (by 40%). In addition, inclusion of FR ( $\geq$  16 µmol·m<sup>-2</sup>·s<sup>-1</sup>) during seedling stage accelerated flowering of long-day plant snapdragon at finishing stage.

Two additional experiments were performed with geranium, petunia, and coleus (*Solenostemon scutellariodes*) to determine how different PPFDs and B photon flux densities regulate seedling growth and subsequent flowering responses to FR radiation. When B photon flux density was kept constant, decreasing R:FR with the addition of FR promoted stem elongation and leaf expansion, and subsequent dry mass accumulation, independently of PPFD. However, the promotive effect of low R:FR on flowering of long-day plant petunia was greater under the lower PPFD. Under the same PPFD, including a moderately high B photon flux density (80 µmol·m<sup>-2</sup>·s<sup>-1</sup>) diminished the effects of FR radiation on extension growth but had little effect on FR-mediated subsequent flowering promotion in long-day petunia.

In a final study, the utility of different shades of W radiation was evaluated, compared to a typical mixture of B+R radiation, considering their effects on human vision, photosynthetic photon efficacy, and plant growth and subsequent development in begonia (*Begonia* ×*semperflorens*), geranium, petunia, and snapdragon. While using W radiation generally increased the visual quality, seedling growth in all species was similar under B+R and W radiation treatments at the same PPFD. In addition, when W radiation treatments were created with the combination of mint W and R LEDs, they were energy efficient as much as B+R mixture in terms of producing plant dry mass per electrical energy input. Collectively, the results of this research generate new information on how the use of FR and W radiation can regulate plant growth and flowering responses with other wavebands to optimize the spectrum of solesource lighting to increase product quality of floriculture crops and potentially decrease crop production times.

#### **ACKNOWLEDGEMENTS**

I would like to first acknowledge my wonderful major professor Dr. Erik Runkle for his endless encouragement, support, and guidance throughout the past 4 years. I also want to thank my graduate committee members Dr. Bert Cregg, Dr. Thomas Sharkey, and Dr. Frank Telewski for their valuable inputs and suggestions for my Ph.D. program, research, and writing. I would like to thank Nate DuRussel for his kind and excellent assistance with my experiments. I also wish to thank to our floriculture groups, including Cathy Whitman, Dr. Roberto Lopez, Dr. Ryan Warner, and undergraduate students, for their great support, assistance, and friendship.

I was most fortunate to have so many great officemates, friends, and colleagues during my Ph.D., including Qingwu Meng, Mengzi Zhang, Charlie Garcia, QiuXia Chen, Brian Poel, Kellie Walters, Kristen Anderson, Shujun Ou, Diep Tran, María José Palma, Yingmei Ma, and also other HOGS friends. I really appreciate their support, friendship, and the beautiful memories with them. I also want to thank Dr. Diane Ebert-May, Dr. Brad Rowe, Dr. Roberto Lopez, Dr. Ryan Warner, and FAST Fellowship for giving me great teaching opportunities.

Finally, I would like to express my sincere gratitude to my beloved parents and brother for their infinite love, support, and encouragement. I also want to thank Mrs. Okran Han and Dr. Kyung-Hwan Han for their warm support and advice. In addition, I would like to thank Jong Hoon Park, Eun Sook Park, Seungeun Han, Sangho Jeon, Mrs. Thelma Hansen, Mrs. Besty Aho, The Korean Church of Lansing, The Peoples Church, and Dr. Kisun Kim.

# TABLE OF CONTENTS

| LIST OF TABLES   | vii |
|--|-----|
| LIST OF FIGURES  | ix  |
| SECTION I  |     |
| FAR-RED RADIATION PROMOTES GROWTH OF SEEDLINGS BY INCREASI |     |
| LEAF EXPANSION AND WHOLE-PLANT NET ASSIMILATION            |     |
| Abstract   | 3   |
| Introduction   |     |
| Materials and Methods                                      |     |
| Plant materials  |     |
| Radiation treatments and growth conditions                 | 9   |
| Growth conditions during the finish stage                  |     |
| Data collection and analysis                               |     |
| Results  |     |
| Discussion   |     |
| APPENDIX   |     |
| LITERATURE CITED   | 30  |
| SECTION II   | 37  |
| FAR-RED RADIATION AND PHOTOSYNTHETIC PHOTON FLUX DENSITY   |     |
| INDEPENDENTLY REGULATE SEEDLING GROWTH BUT INTERACTIVELY   |     |
| REGULATED FLOWERING  |     |
| Abstract   |     |
| Introduction   |     |
| Materials and Methods                                      |     |
| Plant materials  |     |
| Radiation treatments and growth conditions                 |     |
| Data collection for seedling growth                        |     |
| Leaf photosynthesis measurements                           |     |
| Growth conditions and data collection after transplant     |     |
| Statistical analysis                                       |     |
| Results and Discussion                                     |     |
| Stem length  |     |
| Leaf characteristics                                       |     |
| Chlorophyll  |     |
| Dry weight and photosynthesis                              |     |
| Subsequent flowering responses                             |     |
| APPENDIX   |     |
| LITERATURE CITED   | 67  |
| CECTION III  | 75  |

| BLUE RADIATION ATTENUATES THE PROMOTIVE EFFECTS OF FAR-RI | E <b>D</b> |
|---|------------|
| RADIATION ON EXTENSION GROWTH BUT NOT ON FLOWERING        | 75         |
| Abstract  | 77         |
| Introduction  | 78         |
| Materials and Methods                                     | 82         |
| Plant materials   |            |
| Radiation treatments and growth conditions                | 82         |
| Data collection for seedling growth                       | 83         |
| Growth conditions and data collection after transplant    | 84         |
| Statistical analysis                                      | 84         |
| Results   | 85         |
| Stem extension  | 85         |
| Leaf characteristics and photosynthesis                   | 86         |
| Plant dry weight  |            |
| Subsequent flowering responses                            | 87         |
| Discussion  |            |
| APPENDIX  | 92         |
| LITERATURE CITED  | 100        |
| SECTION IV  | 105        |
| SPECTRAL EFFECTS OF LIGHT-EMITTING DIODES ON PLANT GROWTH |            |
| VISUAL COLOR QUALITY, AND PHOTOSYNTHETIC PHOTON EFFICACY  |            |
| Abstract  |            |
| Introduction  |            |
| Materials and Methods                                     |            |
| Plant materials   |            |
| Radiation treatments and growth conditions                |            |
| Data collection and analysis                              | 113        |
| Results and Discussion                                    |            |
| Visual and color properties                               |            |
| Plant growth and development                              |            |
| Photosynthetic photon efficacy                            |            |
| APPENDIX.   |            |
| LITERATURE CITED  |            |

# LIST OF TABLES

| Table I-1. Spectral characteristics of six radiation treatments. The values after each light-emitting diode type (B=blue; R=red; FR=far red) indicate their intensity in $\mu$ mol·m <sup>-2</sup> ·s <sup>-1</sup> . Symbols are those used in Fig. 2 and 3   |
|--|
| Table I-2. Influence of the estimated phytochrome photoequilibria (PPE) of six radiation treatments on flowering characteristics. The values after each LED type (B=blue; R=red; FR=far red) indicate their intensity in $\mu$ mol·m <sup>-2</sup> ·s <sup>-1</sup> . Data represent the means of two replications (n = 20), and values with the same letter are not statistically different at $P = 0.05$   |
| Table II-1. Spectral characteristics of six sole-source lighting treatments. The values after each LED type (B=blue; R=red; FR=far red) indicate their photon flux density in $\mu$ mol·m <sup>-2</sup> ·s <sup>-1</sup> 58  |
| Table II-2. Actual mean air temperatures (°C, measured by thermocouples) and canopy temperatures (°C, measured by infrared sensors) during experimental replications. All means had a standard error $\pm 0.1$ °C.   |
| Table II-3. Analysis of variance for the effects of the estimated phytochrome photoequilibria (PPE), photosynthetic photon flux density (PPFD), or their interaction of sole-source lighting treatments on plant growth parameters of petunia, geranium, and coleus  |
| Table II-4. Influence of the estimated phytochrome photoequilibria (PPE), photosynthetic photon flux density (PPFD), or their interaction of sole-source lighting treatments on net assimilation (shoot DW per unit leaf area) and net $CO_2$ assimilation rate ( $A_n$ ) of seedlings. The values after each LED type (B=blue; R=red; FR=far red) indicate their photon flux density in $\mu$ mol·m <sup>-2</sup> ·s <sup>-1</sup> . Data represent the means of two replications with 10 subsamples (plants) for net assimilation and 5 subsamples for $A_n$ per replication and species. 61 |
| Table II-5. Influence of the estimated phytochrome photoequilibria (PPE), photosynthetic photon flux density (PPFD), or their interaction of sole-source lighting treatments on subsequent flowering characteristics of seedlings at finishing stage. The values after each LED type (B=blue; R=red; FR=far red) indicate their photon flux density in $\mu$ mol·m <sup>-2</sup> ·s <sup>-1</sup> . Data represent the mean of two replications for petunia and three replications for geranium with 10 subsamples (plants) per replication per species.                                       |
| Table III-1. Spectral characteristics of six radiation treatments. The values after each LED type (B=blue; R=red; FR=far red) indicate their intensity in μmol·m <sup>-2</sup> ·s <sup>-1</sup> . Symbols are those used in Fig. 2 - Fig. 8  |

| Table III-2. Analysis of variance for the effects of the estimated phytochrome photoequilibria (PPE), blue radiation (B, 400-500 nm), or their interaction on plant growth and flowering parameters of petunia, geranium, and coleus   |
|--|
| Table III-3. Influence of the estimated phytochrome photoequilibria (PPE) and blue (B, 400-500 nm) photon flux density of sole-source lighting treatments on total leaf area, leaf mass per area (LMA), and net assimilation of seedlings. The values after each LED type (B=blue; R=red; FR=far red) indicate their photon flux density in µmol·m <sup>-2</sup> ·s <sup>-1</sup> . Data represent the mean of two replications for coleus and three replications for petunia and geranium with 10 subsamples (plants) per replication and species |
| Table III-4. Influence of sole-source lighting treatments on subsequent flowering characteristics of seedlings. The values after each LED type (B=blue; R=red; FR=far red) indicate their photon flux density in $\mu$ mol·m <sup>-2</sup> ·s <sup>-1</sup> . Data represent the mean of two replications for petunia and coleus and three replications for geranium with 10 subsamples (plants) per replication and species 96  |
| Table IV-1. Spectral characteristics of sole-source lighting treatments delivered from mint white (MW), red (R), blue (B), and green (G) light-emitting diodes (LEDs) at total photosynthetic photon flux density (PPFD) = $160 \mu \text{mol} \cdot \text{m}^{-2} \cdot \text{s}^{-1}$ . The subscript values after each LED type indicate the percentages of the total PPFD delivered from each LED type   |
| Table IV-2. Photosynthetic photon efficacy (PPE) and dry weight gain per electric energy consumption (dry weight efficacy) for begonia 'Olympia Red', geranium 'Pinto Premium Deep Rose', snapdragon 'Liberty Classic Yellow', and petunia 'Wave Blue' seedlings grown for 34 d, 25 d, 24 d and 19 d, respectively, under six sole-source lighting treatments delivered by mint white (MW), red (R), blue (B), and green (G) light-emitting diodes. The values after each LED type represent their percentages of the total PPFD.                  |

# LIST OF FIGURES

| Figure I-1. The spectral distribution of six radiation treatments from blue (B), red (R), and farred (FR) light-emitting diodes (LEDs). The values after each LED type indicate their intensity in $\mu$ mol·m <sup>-2</sup> ·s <sup>-1</sup>  |
|--|
| Figure I-2. Influence of the estimated phytochrome photoequilibria (PPE) of six radiation treatments on seedling stem length, leaf area, and SPAD reading. Six radiation treatments were categorized into far-red (FR; 700-800 nm) substitution treatments ( $B_{32}+R_{96}+FR_{32}$ and $B_{32}+R_{64}+FR_{64}$ ), FR addition treatments ( $B_{32}+R_{128}+FR_{16}$ , $B_{32}+R_{128}+FR_{32}$ , and $B_{32}+R_{128}+FR_{64}$ ), and control treatment ( $B_{32}+R_{128}$ ). Each data point represents the mean and standard error of two replications with 10 subsamples (plants) per replication and species. Associated correlation coefficients ( $R^2$ ) and regression equations are presented when statistically significant (solid line) but not when not significant (dotted line). *, ***, *** indicate significant at $P < 0.05$ , 0.01 or 0.001, respectively |
| Figure I-3. Influence of the estimated phytochrome photoequilibria (PPE) of six radiation treatments on plant dry weight (DW). Six radiation treatments were categorized into far-red (FR; 700-800 nm) substitution treatments ( $B_{32}+R_{96}+FR_{32}$ and $B_{32}+R_{64}+FR_{64}$ ), FR addition treatments ( $B_{32}+R_{128}+FR_{16}$ , $B_{32}+R_{128}+FR_{32}$ , and $B_{32}+R_{128}+FR_{64}$ ), and control treatment ( $B_{32}+R_{128}$ ). Each data point represents the mean and standard error of two replications with 10 subsamples (plants) per replication and species. Associated correlation coefficients ( $R^2$ ) and regression equations are presented when statistically significant (solid line) but not when not significant (dotted line). NS, *, or ** indicate nonsignificant or significant at $P < 0.05$ or 0.01, respectively                  |
| Figure I-4. Influence of the calculated yield photon flux density of six radiation treatments on shoot dry weight (DW) per unit leaf area. Each data point represents the mean and standard error of two replications with 10 subsamples (plants) per replication and species. Associated correlation of coefficients ( $\mathbb{R}^2$ ) and regression equations are presented when statistically significant (solid line) but not when not significant (dotted line). NS, *, **, *** indicate nonsignificant or significant at $P < 0.05$ , 0.01 or 0.001, respectively  |
| Figure II-1. The spectral distribution of six sole-source lighting treatments consisting of blue (B, 400-500 nm), red (R, 600-700 nm), and far-red (FR, 700-800 nm) radiation delivered by light-emitting diodes. The value after each waveband indicate its photon flux density in μmol·m <sup>-2</sup> ·s <sup>-1</sup> .  |

Figure II-2. Influence of the estimated phytochrome photoequilibria (PPE) of sole-source lighting treatments on stem length and leaf characteristics of seedlings grown under a

| photosynthetic photon flux density (PPFD) of 96 or 288 $\mu$ mol·m <sup>2</sup> ·s <sup>3</sup> . Each data point represents the mean and standard error of two replications for petunia and three replications for geranium and coleus with 10 subsamples (plants) per replication per species. Associated correlation coefficients (R <sup>2</sup> ) and regression equations are presented when statistically significant (solid line) but not when not significant (dotted line). *, **, or *** indicate significant at $P < 0.05$ , 0.01, or 0.001, respectively  |
|--|
| Figure II-3. Influence of the estimated phytochrome photoequilibria (PPE) of sole-source lighting treatments on SPAD index, leaf chlorophyll (Chl) $a+b$ , and Chl $a/b$ of seedlings grown under a photosynthetic photon flux density (PPFD) of 96 or 288 $\mu$ mol·m <sup>-2</sup> ·s <sup>-1</sup> . Each data point represents the mean and standard error of two replications for petunia and three replications for geranium and coleus with 10 subsamples (plants) per replication per species for SPAD index and 5 subsamples per replication per species for Chl $a+b$ and Chl $a/b$ . Associated correlation coefficients (R <sup>2</sup> ) and regression equations are presented when statistically significant (solid line) but not when not significant (dotted line). *, ***, or *** indicate significant at $P < 0.05$ , 0.01, or 0.001, respectively  |
| Figure II-4. Influence of the estimated phytochrome photoequilibria (PPE) of sole-source lighting treatments on dry weights of seedlings grown under a photosynthetic photon flux density (PPFD) of 96 or 288 $\mu$ mol·m <sup>-2</sup> ·s <sup>-1</sup> . Each data point represents the mean and standard error of two replications for petunia and three replications for geranium and coleus with 10 subsamples (plants) per replication per species. Associated correlation coefficients (R <sup>2</sup> ) and regression equations are presented when statistically significant (solid line) but not when not significant (dotted line). * or ** indicate significant at $P < 0.05$ or 0.01, respectively  |
| Figure III-1. The spectral distribution of six radiation treatments from blue (B), red (R), and farred (FR) light-emitting diodes (LEDs). The values after each LED type indicate their photon flux density in $\mu$ mol·m <sup>-2</sup> ·s <sup>-1</sup>  |
| Figure III-2. Influence of the estimated phytochrome photoequilibria (PPE) of sole-source lighting on stem length and SPAD index of seedlings grown under a photosynthetic photon flux density of $160  \mu \text{mol} \cdot \text{m}^{-2} \cdot \text{s}^{-1}$ with red (R <sub>160</sub> ) or blue and red radiation (B <sub>80</sub> R <sub>80</sub> ). Data points represent the means of two replications for coleus and three replications for petunia and geranium, and vertical bars are standard errors of the means (n = 2 for coleus and n = 3 for petunia and geranium). Associated correlation coefficients (R <sup>2</sup> ) and regression equations are presented when statistically significant (solid line) but not when not significant (dashed line). *, **, or *** indicate significant at $P < 0.05$ , 0.01 or 0.001, respectively. $y_{BR}$ * indicates that the slopes of the regression lines are significantly different for the two B levels ( $P < 0.05$ ) |

| lighting on dry weight (DW) of seedlings grown under a photosynthetic photon flux density of $160 \mu\text{mol}\cdot\text{m}^{-2}\cdot\text{s}^{-1}$ with red (R <sub>160</sub> ) or blue and red radiation (B <sub>80</sub> R <sub>80</sub> ). Data points represent the means two replications for coleus and three replications for petunia and geranium, and vertical bars are standard errors of the means (n = 2 for coleus and n = 3 for petunia and geranium). Associated correlation coefficients (R <sup>2</sup> ) and regression equations are presented when statistically significant (solid line) but not when not significant (dashed line). * or ** indicate significant at $P$ < 0.05 or 0.01, respectively  |
|---|
| Figure IV-1. The spectral distribution of sole-source lighting treatments delivered from mint white (MW), red (R), blue (B), and green (G) light-emitting diodes (LEDs) at total photosynthetic photon flux density (PPFD) = $160 \mu \text{mol} \cdot \text{m}^{-2} \cdot \text{s}^{-1}$ . The subscript values after each LED type indicate the percentages of the total PPFD delivered from each LED type  |
| Figure IV-2. The 1931 CIE (x, y) chromaticity coordinates, correlated color temperature (CCT), and color rendering index (CRI) of six sole-source lighting treatments delivered from mint white (MW), red (R), blue (B), and green (G) light-emitting diodes (LEDs) at a total photosynthetic photon flux density (PPFD) = $160 \mu \text{mol} \cdot \text{m}^{-2} \cdot \text{s}^{-1}$ . The subscript values after each LED type indicate the percentages of the total PPFD delivered from each LED type. Black-body curve (black solid line) and CCT values (K) are presented in CIE 1931 chromaticity coordinates 125   |
| Figure IV-3. Plant height, total leaf area, fresh and dry weight for begonia 'Olympia Red', geranium 'Pinto Premium Deep Rose', snapdragon 'Liberty Classic Yellow', and petunia 'Wave Blue' seedlings grown for 34 d, 25 d, 24 d and 19 d, respectively, under six sole-source lighting treatments delivered by mint white (MW), red (R), blue (B), and green (G) light-emitting diodes. The values after each LED type represent their percentages of the total PPFD. Means with different letters are significantly different by Tukey's honestly significant difference test ( $P < 0.05$ ) and lack of mean separation indicates nonsignificance. Error bars indicate standard error of two replications with 10 subsamples (plants) per replication per species |
| Figure IV-4. Relative stem length and percent of plants that had visible buds of petunia 'Wave Blue' grown for 39 d and 45 d, respectively, under six sole-source lighting treatments delivered by mint white (MW), red (R), blue (B), and green (G) light-emitting diodes. The values after each LED type represent their percentages of the total PPFD. Means with different letters are significantly different by Tukey's honestly significant difference test ( $P < 0.05$ ). Error bars indicate standard error of two replications with 10 subsamples (plants) per replication per species   |
|   |

## **SECTION I**

FAR-RED RADIATION PROMOTES GROWTH OF SEEDLINGS BY INCREASING LEAF EXPANSION AND WHOLE-PLANT NET ASSIMILATION

Far-red Radiation Promotes Growth of Seedlings by Increasing Leaf Expansion and Whole-plant

Net Assimilation

Yujin Park<sup>1</sup> and Erik S. Runkle<sup>2</sup>

Department of Horticulture, 1066 Bogue Street, Michigan State University, East Lansing, MI

48824

This research is supported by Osram Opto Semiconductors; the USDA-ARS Floriculture and

Nursery Research Initiative; the USDA National Institute of Food and Agriculture, Hatch project

192266; Michigan State University's (MSU) AgBioResearch and Project GREEEN; and

horticulture companies supportive of MSU floriculture research. We thank C. Raker & Sons for

donation of plant material and Nate DuRussel for technical assistance. We also thank Dr. Bert

Cregg (Department of Horticulture, MSU) and Dr. Thomas Sharkey (Department of

Biochemistry and Molecular Biology, MSU) for valuable input on this manuscript.

<sup>1</sup>Graduate student.

<sup>2</sup>Corresponding author. Email address: runkleer@msu.edu.

2

#### **Abstract**

By definition, photosynthetically active radiation (PAR) includes wavelengths between 400 and 700 nm and thus, far-red radiation (FR, 700 to 800 nm) is excluded when the photosynthetic photon flux density (PPFD) is measured and reported. However, FR radiation [and the ratio of red (R; 600 to 700 nm) to FR] regulates phytochrome-mediated morphological and developmental plant responses to promote radiation capture and survival under shade. We postulated that the inclusion of FR in a radiation spectrum would have little effect on photosynthesis but would increase radiation capture and plant growth, while accelerating the subsequent flowering of shade-avoiding species. Geranium (*Pelargonium* × *hortorum*), petunia (*Petunia* × hybrida), snapdragon (*Antirrhinum majus*), and impatiens (*Impatiens walleriana*) were grown at 20 °C under an 18-h photoperiod provided by sole-source lighting from lightemitting diodes that included 32 µmol·m<sup>-2</sup>·s<sup>-1</sup> of blue and the following intensities of R and FR radiation:  $R_{128}$  (128 µmol·m<sup>-2</sup>·s<sup>-1</sup> of R),  $R_{128}$ +FR<sub>16</sub>,  $R_{128}$ +FR<sub>32</sub>,  $R_{128}$ +FR<sub>64</sub>,  $R_{96}$ +FR<sub>32</sub>, and R<sub>64</sub>+FR<sub>64</sub>. Plant height in all species studied and total leaf area of geranium and snapdragon linearly decreased as the R:FR (or the estimated phytochrome photoequilibrium) of each treatment increased. In geranium and snapdragon, the increase in total leaf area (by 7 %) with the addition of FR to the same PPFD subsequently increased shoot dry weight (DW) (by 28-50%) while the increase in total leaf area (by 30-40%) with the partial substitution of R with FR partly compensated for the reduction in PPFD (by 40%), producing a similar shoot DW. Whole-plant net assimilation of geranium, snapdragon, and impatiens increased with additional FR radiation, showing a linear relationship with the calculated yield photon flux density of each radiation treatment. In addition, inclusion of FR during seedling growth promoted flowering in the longday plant snapdragon. We conclude that FR radiation increases plant growth indirectly through

leaf expansion and directly through whole-plant net assimilation and in at least some species, promotes subsequent flowering.

*Keywords*: controlled environments; dry mass accumulation; flowering; phenotypic plasticity; shade-avoidance response

Abbreviations: B, blue radiation; FR, far-red radiation; LEDs, light-emitting diodes; PAR, photosynthetically active radiation; PPE, phytochrome photoequilibrium; PPFD, photosynthetic photon flux density; Pr, R-radiation-absorbing phytochrome; Pfr, FR-radiation-absorbing phytochrome; PSI, photosystem I; PSII, photosystem II; R, red; TPFD, total photon flux density; YPFD, yield photon flux density.

### Introduction

Plants use several classes of photoreceptors including red (R; 600-700 nm) and far-red (FR; 700-800 nm) radiation-absorbing phytochromes and blue (B; 400-500 nm) and UV radiation absorbing cryptochromes to perceive different aspects of the radiation environment (Possart et al., 2014; Keuskamp et al., 2010). Plant shading reduces the amount of photosynthetically active radiation (PAR) and changes the spectral composition. Photosynthetic pigments strongly absorb photosynthetically efficient B and R radiation but reflect or transmit most photosynthetically inefficient FR radiation (Casal, 2013a). Therefore, radiation under a plant canopy has a low R:FR (Gommers et al., 2013). The R:FR ratio is about 1.2 in daylight and is reduced to 0.2 under a typical canopy (Heraut-Bron et al., 1999). While FR photons are weakly or not effective at promoting the photosynthetic reaction, the low R:FR perceived by the

phytochrome photoreceptors can induce rapid changes in gene expression and physiological processes, which regulate the phenotypic plasticity (e.g., extension growth) of plants and enable them to better compete with neighboring plants (Keuskamp et al., 2010).

The shade-avoidance response of plants is mediated by phytochromes and typically includes elongation of internodes, petioles, and hypocotyls (often associated with a reduction in leaf development), apical dominance, and early flowering (Keuskamp et al., 2010; Ruberti et al., 2012). These growth and developmental responses can enable plants to outgrow shade and capture more photosynthetic radiation. In contrast, for plants that tolerate shade (a shade-tolerance response), leaf expansion increases to intercept more radiation with a concomitant reorganization of chlorophyll to improve photosynthetic efficiency (Dale, 1988). All of these plant responses to shade can promote radiation capture and subsequent survival under shade conditions (Nozue et al., 2015).

Phytochrome-regulated responses are often expressed in relation to the estimated phytochrome photoequilibrium (PPE), which is an indicator of the relative amount of active phytochrome in plants (Sager et al., 1988; Hogewoning et al., 2010). Phytochromes are photochromic biliproteins that exist in two photo-convertible isoforms: Pr, an R-radiation-absorbing form, and Pfr, a FR-radiation-absorbing form (Ciolfi et al., 2013). Upon absorption of R radiation, Pr is converted into the Pfr form (generally considered the biologically active form) that can absorb FR radiation and switch back to Pr (Ruberti et al., 2012). Following conversion to the Pfr form, phytochromes translocate to the nucleus to control several aspects of photomorphogenesis (Li et al., 2011). The total pool of phytochrome in light-grown plants is constant, but the relative amounts in the Pfr and Pr forms (or PPE) depend on the R:FR ratio and darkness incident on the plant. A high R:FR ratio creates a high PPE, and vice versa. Models

based on the distribution of incident spectral radiation have been developed to estimate the PPE and stem extension of a wide range of species and show an inverse linear relationship with estimated PPE. Therefore, the estimated PPE is useful in quantifying photomorphogenic responses to radiation quality (Smith, 1994; Runkle and Heins, 2001).

However, studies on the relationship between photomorphogenic response and estimated PPE have focused on shade-induced elongation. Overall plant growth and development in response to the estimated PPE is difficult to predict because the direction and extent of plastic responses to R:FR can differ among phytochrome-regulated plant responses. For example, unlike the inverse linear relationship between stem extension growth and the estimated PPE, the leaf expansion response to R:FR varies, ranging from inhibition to promotion, depending on growth conditions and species (Casal, 2013b; Demotes-Mainard et al., 2016). In addition, the acceleration of flowering was not correlated with the enhancement of elongation growth under a low R:FR in more than 100 accessions of arabidopsis (Arabidopsis thaliana), showing that ecotypes that responded strongly in elongation did not necessarily respond strongly in floral acceleration, and vice versa (Botto and Smith, 2002). Recent molecular studies have demonstrated that responses in different organs triggered by the same light signal are from distinct signaling cascades downstream of the activated photoreceptors in distinct tissues (Montgomery, 2016). Therefore, increased stem elongation does not necessarily correlate with leaf expansion or stimulation of flowering.

In many previous studies on plant responses to R:FR or shade, technically it was difficult to vary the R:FR ratio while maintaining other environmental constants, especially intensities of other radiation wavebands and the photosynthetic photon flux density (PPFD) (Dale, 1988).

Thus, plant responses to R:FR often involved complex interactions with the radiation intensity

and other wavebands, potentially confounding results. We utilized sole-source lighting from light-emitting diodes (LEDs) and highly controlled growth environments to determine how inclusion of FR in a radiation spectrum during seedling stage influences leaf area, radiation capture, and whole-plant net assimilation while also regulating characteristics relevant to the commercial production of seedlings such as plant habit (compactness) and subsequent growth and flowering after transplant. The wavelength specificity of LEDs technically enables us to investigate how a specific combination of wavelengths regulates plant growth and development without unintentionally confounding effects from differences in radiation intensities and other wavebands (Massa et al., 2008; Morrow, 2008). LEDs are increasingly being used for solesource lighting in commercial indoor plant production systems (Mitchell et al., 2015). One of the most cost-effective applications of LED sole-source lighting is young-plant production, in which high-value plants are grown at a high density and crop cycles are relatively short (e.g., 4 to 5 weeks). The vast majority of research with LED sole-source lighting has been published with only B and R radiation, and few studies have tested the benefits of including additional radiation wavebands (Mitchell et al., 2012; Randall and Lopez, 2014; Wollaeger and Runkle, 2015).

To determine the effects of FR addition on plant growth, we quantified plant growth by measuring dry weight (DW) gain, which is determined by the product of net assimilation and total leaf area (Gregory, 1917; Vernon and Allison, 1963; Radford, 1967; Hunt et al., 2002; Casal, 2013b; Snowden et al., 2016). In plant growth analysis, DW gain can be separated into two components: net assimilation and leaf area. Net assimilation rate, which is defined by Gregory (1917) as the rate of increase of DW per unit leaf area, is a useful measure of the photosynthetic efficiency of plants (Vernon and Allison, 1963; Radford, 1967; Hunt et al., 2002; Casal, 2013b; Snowden et al., 2016). We postulated that the addition of FR radiation would have

a negligible impact on whole-plant net assimilation, but as PPE decreased, changes in plant architecture (including leaf expansion and stem elongation) would increase radiation capture, potentially promoting plant growth. We also postulated that the inclusion of FR radiation during the seedling stage would promote the subsequent flowering of shade-avoiding species. We previously reported a subset of data for snapdragon (*Antirrhinum majus*) (Park and Runkle, 2016) which showed the impacts of FR radiation on plant architecture, whole-plant net assimilation, and shoot DW. Here we present a more comprehensive study with full results of snapdragon and other species. We anticipated results from this study would shed light on whether including FR radiation in a sole-source lighting spectrum elicited desirable plant responses including accelerated flowering and growth promotion.

#### **Materials and Methods**

## Plant materials

Geranium (*Pelargonium* ×*hortorum* 'Pinto Premium Orange Bicolor'), petunia (*Petunia* ×*hybrida* 'Wave Blue'), snapdragon (*Antirrhinum majus* 'Trailing Candy Showers Yellow'), and impatiens (*Impatiens walleriana* 'Super Elfin XP Red') were chosen for study based on commercial significance, shade tolerance, and photoperiodic flowering characteristics. Geranium, petunia, and snapdragon are shade-avoiding species while impatiens is shade-tolerant; petunia and snapdragon are long-day plants while geranium and impatiens are day-neutral plants. Seeds of each species were sown in 128-cell (2.7 × 2.7-cm; 12.0-mL volume) plug trays by a commercial young plant producer (C. Raker and Sons, Inc., Litchfield, MI), and trays were moved within 7 d to a research greenhouse at Michigan State University (East Lansing, MI) with a 16-h photoperiod at 20 °C (see finish stage conditions below). Upon emergence of the first true

leaves, each plug tray was then cut into four sections, each with  $\geq$ 30 seedlings, thinned to one plant per cell. The experiment was performed twice in time and for each replication, the days from seed sow until first true leaf emergence was (rep 1, 2): geranium (7, 7), snapdragon (9, 10), petunia (9, 10), and impatiens (13, 10).

Radiation treatments and growth conditions

The six LED modules were placed on open, metal mesh benches inside a refrigerated walk-in growth chamber. The top of each of six LED modules [described by Wollaeger and Runkle (2013) but with new LED panels contained a fan-cooled driver board with 80 LEDs each emitting B (peak = 447 nm), R (peak = 660 nm), and FR (peak = 731 nm) radiation and faced downward. Wire mesh was placed just below the middle half of the LED boards to provide a more uniform radiation intensity within each module. The intensities of the three LED types were adjusted manually by dimmer switches on the driver boards to create six radiation treatments based on an average of ten measurements from a spectroradiometer (PS-200; StellerNet,Inc., Tampa, FL) made at seedling-tray height at predetermined horizontal positions inside each module. The six radiation treatments were designed to determine the impacts of adding FR radiation to a typical B+R radiation spectrum (Table 1). The control treatment included 32  $\mu$ mol·m<sup>-2</sup>·s<sup>-1</sup> of B and 128  $\mu$ mol·m<sup>-2</sup>·s<sup>-1</sup> of R (B<sub>32</sub>+R<sub>128</sub>). The PPFD of 160  $\mu$ mol·m<sup>-</sup> <sup>2</sup>·s<sup>-1</sup> was the target radiation intensity to achieve a photosynthetic daily light integral (DLI) of 10 mol·m<sup>-2</sup>·s<sup>-1</sup>, which is the recommended minimum DLI to produce high-quality young plants (Runkle, 2007). The B radiation intensity (32 µmol·m<sup>-2</sup>·s<sup>-1</sup>) was kept constant for all radiation treatments so that responses were not confounded by differences in cryptochrome-mediated responses (Pierik et al., 2004; Keuskamp et al., 2011; Pedmale et al., 2016). The second and third treatments were created by partial substitution of R radiation with FR radiation (B<sub>32</sub>+R<sub>96</sub>+FR<sub>32</sub>,

and  $B_{32}+R_{64}+FR_{64}$ ) while keeping total photon flux density (TPF, 400-800 nm) identical to the control treatment. The other three treatments were created by the addition of FR radiation to a constant B+R radiation spectrum ( $B_{32}+R_{128}+FR_{16}$ ,  $B_{32}+R_{128}+FR_{32}$ , and  $B_{32}+R_{128}+FR_{64}$ ), and thus PPFD (400-700 nm) was identical to the control. At each replication, the six radiation treatments were randomly allocated to the LED modules. The random assignment of radiation treatments was carried out separately in each replication to decrease any positional effects of each LED module inside the growth chamber. In addition, plug trays were rotated daily to reduce any positional effects inside each LED module. For each radiation treatment, the yield photon flux density (YPFD), which is the product of radiation intensity and relative quantum efficiency (in  $\mu$ mol·m<sup>-2</sup>·s<sup>-1</sup>), was calculated based on McCree (1972) and Sager et al. (1988); the R:FR was calculated with 100-nm wavebands; and the PPE was estimated with the spectra in Fig. 1, as described by Sager et al. (1988) (Table 1).

Plants were grown at a constant 20 °C under an 18-h photoperiod as controlled by a data logger (CR10; Campbell Scientific, Logan, UT). In each treatment, air and plant canopy temperature were measured by thermocouples (0.13-mm type E; Omega Engineering, Stamford, CT) above the plant canopy and infrared (IR) sensors (Type K, OS36-01; Omega Engineering) positioned 20 cm above the module bottom and pointing at a downward angle toward the canopy of the closest plant tray, respectively. Radiation intensity was measured continuously in each module by quantum sensors (LI-190R, LI-COR, Lincoln, NE) at plug tray level. The IR sensors, thermocouples, and quantum sensors were connected to the same data logger and environmental data were recorded every 10 s. The data logger recorded means every 10 min throughout the duration of the experimental replications. Average air/canopy temperatures during the experiment periods were 20.4/20.4°C, 20.4/20.5°C, 20.2/20.2°C, 20.4/20.5°C, 20.5/20.5°C, and

 $20.5/20.7^{\circ}$ C for the  $B_{32}+R_{128}$ ,  $B_{32}+R_{128}+FR_{16}$ ,  $B_{32}+R_{128}+FR_{32}$ ,  $B_{32}+R_{128}+FR_{64}$ ,  $B_{32}+R_{96}+FR_{32}$ , and  $B_{32}+R_{64}+FR_{64}$  treatments, respectively. All temperatures had standard deviations (SD)  $\leq \pm 0.8^{\circ}$ C. Plants were irrigated as needed, every two or three days, through subsurface irrigation with deionized water supplemented with a water-soluble fertilizer providing (in mg·L<sup>-1</sup>) 50 N, 19 P, 50 K, 23 Ca, 4 Mg, 1 Fe, 0.5 Mn, 0.5 Zn, 0.5 Cu, 0.3 B, and 0.1 Mo (MSU Plug Special; GreenCare Fertilizers, Inc., Kankakee, IL).

Growth conditions during the finish stage

At the end of the seedling stage, ten seedlings from each treatment and replication were randomly selected and transplanted into 10-cm pots containing a 70% peatmoss, 21% perlite, and 9% vermiculite potting media (SUREMIX; Michigan Grower Products, Inc., Galesburg, MI) to determine whether the sole-source radiation treatments during the seedling stage had any subsequent effects on flowering when grown in a common greenhouse environment. Pots were randomly placed on benches in a glass-glazed, environmentally controlled greenhouse at a constant temperature set point of 20 °C. Supplemental lighting provided by 400-W high-pressure sodium lamps delivered a PPFD of 77 (SD  $\pm$ 13)  $\mu$ mol·m<sup>-2</sup>·s<sup>-1</sup> at plant height and a 16-h photoperiod. The high-pressure sodium lamps were controlled by an environmental control computer and were automatically switched on from 0600 to 2200 HR when the ambient solar PPFD was <185  $\mu$ mol·m<sup>-2</sup>·s<sup>-1</sup> and off when it was >370  $\mu$ mol·m<sup>-2</sup>·s<sup>-1</sup>.

Data collection and analysis

The experiment was performed twice. In each replication, 20 random plants of each species in each treatment were used for data collection: ten plants at the end of the seedling stage and ten plants at the finishing stage. At the end of the seeding stage, ten random plants of each species in each treatment, usually excluding outer guard rows, were harvested the following

number of days after seed sow (rep 1, 2): geranium (29, 30), snapdragon (35, 37), petunia (31, 31), and impatiens (37, 35). The following data were collected on plants in each treatment: leaf (at node) number, total leaf area [using a leaf-area meter (LI-3000; LI-COR)], SPAD index [using a portable chlorophyll meter (SPAD-502, Minolta corporation, Ltd., Osaka, Japan)], plant height (from media level to apical meristem), and shoot and root DW (after plants were dried in an oven at ≥66 °C for ≥5 d and using a Mettler Toledo PG5002 scale, Columbus, OH). Wholeplant net assimilation was calculated by dividing shoot DW by total leaf area (g·m<sup>-2</sup>) for each plant (Gregory, 1917; Vernon and Allison, 1963; Radford, 1967; Hunt et al., 2002; Casal, 2013b; Snowden et al., 2016). A visible leaf that was 25% or greater unfolded was counted in leaf number. SPAD index measurements were taken at the central point of the leaflet between the midrib and the leaf margin of the second or third fully expanded leaves from the apical shoot. Three readings per leaf per plant were taken and averaged to a single SPAD value for each plant. During the finishing stage, data collected on ten plants of each species in each treatment included date of first flowering, flower bud or inflorescence number, and length of the primary stem at first flowering.

The experiment used a randomized complete block design with two blocks and ten subsamples per block. Each replication was regarded as a block. Each LED module was regarded as the experimental unit for the radiation treatment. Within each LED module, ten individual seedlings per species were the sub-samples or observational units. Data were analyzed with the SAS (version 9.4; SAS Institute, Inc., Cary, NC). Regression analysis was performed with the PROC REG procedure to relate the plant data parameters to the estimated PPE and YPFD of the radiation treatments. In regression analysis, the mean for each replication was treated as a single data point and included 12 data points for the six radiation treatment effects (2 replications × 6

treatments) in Fig. 2, 3, and 4; 8 data points for the FR addition effects (2 replications  $\times$  4 treatments) in Fig. 3; and 6 data points for the FR substitution effects (2 replications  $\times$  3 treatments) in Fig. 3. Flowering data were analyzed with the PROC MIXED procedure [with a fixed factor for radiation treatments, a random factor of blocks (or replications), and a random factor for interaction between blocks and radiation treatments] that provided pairwise comparisons between treatments by using Tukey's honestly significant test at  $P \le 0.05$ .

## **Results**

Seedling stem length decreased linearly as the estimated PPE of each treatment increased from 0.69 to 0.88, although the magnitude of the increase varied by species (Fig. 2). Stem length of geranium, petunia, snapdragon, and impatiens decreased by 41, 95, 41 and 24%, respectively, as the estimated PPE of each treatment increased from 0.69 to 0.88. The largest increase in stem length of petunia under the lowest PPE (0.69) in this study was accompanied by an upright growth habit while the plants under the other treatments showed a rosette growth habit.

At least for geranium and snapdragon, total leaf area also decreased linearly as the estimated PPE of each treatment increased, but to a lesser extent than stem extension (Fig. 2). Treatment did not affect the number of leaves except for petunia, in which plants under light with a PPE=0.69 had 0.7-1.3 fewer leaves than those under other light treatments (data not shown). Thus, the decrease in total leaf area with increasing PPE can be attributed to a decrease in individual leaf size.

SPAD value, which is an index of chlorophyll concentration per unit leaf area, was correlated positively with the estimated PPE of each treatment for geranium, petunia, and snapdragon, but not impatiens (Fig. 2). When chlorophyll content per leaf was estimated by

multiplying SPAD value by total leaf area, the values were similar among treatments in all species (data not shown).

When the PPFD of each treatment was the same, shoot DW of geranium, petunia, and snapdragon showed similar inverse linear relationships with estimated PPE as those observed for stem elongation and leaf expansion (Fig. 3). In other words, DW increased with the addition of FR radiation. When the PPFD was reduced by up to 40% as R radiation was partially substituted with FR, shoot DW of these three species was similar among radiation treatments. In contrast, shoot DW of impatiens was similar when the total PPFD of each treatment was the same while shoot DW decreased under the lowest PPE (0.69) compared to under other treatments.

Shoot DW per unit leaf area or whole-plant net assimilation of geranium and snapdragon was negatively correlated with the estimated PPE of each treatment when PPFD of each treatment was the same (Fig. 3), indicating that the increase in shoot DW with additional FR radiation was related to an increase in whole-plant net assimilation. Under the FR substitution treatments, as both PPFD and PPE decreased, dry shoot weight per unit leaf area of geranium decreased linearly. In addition, shoot DW per unit leaf area of geranium, snapdragon, and impatiens showed a positive correlation with the calculated YPFD of each treatment (Fig. 4).

There was little to no effect of FR addition or partial substitution for R radiation (and thus, PPE) on root DW (data not shown). With few significant effects of light treatments on root DW, total (root+shoot) DW showed a similar pattern as shoot DW in relation to the PPE (data not shown). The shoot to root ratio (S:R) decreased linearly as the estimated PPE of each treatment increased from 0.69 to 0.88 in snapdragon but the trend was not significant in other species (Fig. 3).

In the long-day plant snapdragon, subsequent flowering was promoted by 10 to 12 d when treatments included  $\geq 16~\mu mol \cdot m^{-2} \cdot s^{-1}$  of FR radiation (and the resulting PPE was  $\leq 0.85$ ) (Table 3). The earlier flowering of snapdragon was accompanied by a shorter stem length at flowering. In the long-day plant petunia, the number of visible buds at flowering under the lowest PPE (0.69) in this study was significantly less than those grown under a higher PPE, but flowering time and stem length at flowering were not influenced by the seedling treatments. In contrast, days to flower, flower bud or inflorescence number, and stem length at flowering in the day-neutral species geranium and impatiens did not show a treatment response.

#### **Discussion**

Stem elongation in all species studied and leaf expansion of geranium and snapdragon showed an inverse linear relationship with the estimated PPE regardless of differences in the PPFD among treatments (Fig. 2). The linearity between PPE and plant responses suggests that R:FR and phytochrome directly regulated responses. Green leaves absorb radiation strongly in the range of PAR (400 to 700 nm) but reflect or transmit most FR radiation, and thus the extent of the reduction in R:FR or PPE is quantitatively related to the density and proximity of neighboring vegetation (Smith and Whitelam, 1997; Casal, 2013a). In response to the reduced R:FR or PPE, shade-avoiding species promote and direct extension growth in an attempt to better harvest available sunlight (Smith, 1994; Franklin, 2008), while shade-tolerant species typically display few or no shade-avoidance traits, such as elongation responses in stems and petioles, compared to shade-avoiding or open-habitat species (Gommers et al., 2013). In our study, in stem length and total leaf area, the shade-avoiding geranium, petunia, and snapdragon were sensitive to the changes in PPE, as indicated by the steep slopes of the regression lines, while

shade-tolerant impatiens was the least responsive to the PPE, as indicated by relatively flat slope and no correlation with PPE (Fig. 2). In the shade-avoiding geranium and snapdragon, the slope of the line in both stem elongation and total leaf area was similar, showing similar sensitivity to R:FR or PPE. The inverse linear relationship between stem elongation and the estimated PPE has been reported in many species (Smith, 1994), and the magnitude of stem elongation mostly involves increased cellular expansion (Sasidharan et al., 2008). In contrast, FR radiation addition (or a lower R:FR ratio) increased or decreased total leaf area, depending on species and growth conditions (Demotes-Mainard et al., 2016). In our study, decreasing R:FR or PPE increased the total leaf area of geranium and snapdragon and it was attributed to the increase in individual leaf size, not leaf number.

In large white petunia (*Petunia axilaris*), leaf expansion in FR-treated plants (FR=52 μmol·m<sup>-2</sup>·s<sup>-1</sup>, PPFD=180 μmol·m<sup>-2</sup>·s<sup>-1</sup>) was related to the late phase of leaf growth and larger cells (Casal et al., 1987). Low R:FR-grown (R:FR=0.1, PPFD=130 μmol·m<sup>-2</sup>·s<sup>-1</sup>) leaves of arabidopsis displayed enhanced cell expansion of all cell types, suggesting that the regulation of leaf growth was mediated primarily by changes in cell expansion (Patel et al., 2013). In a separate study, the reduced leaf size of arabidopsis grown under low R:FR (R:FR=0.1, PPFD=27 μmol·m<sup>-2</sup>·s<sup>-1</sup>) was caused by a decreased cell number with a negligible effect on cell size (Carabelli et al., 2007). In addition, the inhibitory effect of FR radiation on leaf expansion in several species was, in part, attributed to the consequence of competition for resources with the elongated stem, which reduced the carbon supply to leaf growth (Casal et al., 1987). In general, the leaves deprived of photosynthate or nutrients developed fewer cells than plants with a greater carbon supply because cell division in plants has been correlated with carbohydrate supply (Van Volkenburgh, 1999). These results indicate that leaf expansion is promoted under low R:FR

when the PPFD is sufficient for growth while it is inhibited under low R:FR when the PPFD is excessively low and thus, when the carbon supply for leaf growth is limited. This suggests that the contrasting effect of low R:FR in leaf expansion in previous reports can be attributed to the PPFD of the shade treatments and their effect on the subsequent carbon supply for leaf growth. The consistent increase in leaf size with decreasing R:FR and PPE in our study is therefore likely from an increase in the cell expansion because the PPFD was sufficient for growth and thus, the carbon supply for leaf cell division was adequate.

Dry mass accumulation of plants is a function of the incident radiation, the efficiency of incident radiation interception, and conversion of captured radiation into biomass through photosynthesis, as well as other environmental and cultural conditions (Heraut-Bron et al., 1999; Maliakal et al., 1999; Richards, 2000; Casal, 2013b). The efficiency of radiation capture is primarily affected by plant architecture and especially by leaf area because radiation capture increases with increasing leaf area (Cope et al., 2014). In plant growth analysis, growth has been interpreted as the product of net assimilation and total leaf area (Gregory, 1917; Vernon and Allison, 1963; Radford, 1967; Hunt et al., 2002; Casal, 2013b; Snowden et al., 2016). Several studies showed that plant growth is determined more by parameters related to leaf area, such as total leaf area of plants, specific leaf area (the ratio of leaf area to leaf dry mass), and leaf area index (the leaf area per unit ground surface area), than by area-based photosynthesis, indicating that leaf area is an important parameter in determining plant growth (Klassen et al., 2003; Hogewoning et al., 2010; Weraduwage et al., 2015; Snowden et al., 2016). In our study, in geranium and snapdragon, the addition of FR to the same PPFD, which reduced the PPE, increased total leaf area (by 7%) and subsequently increased shoot DW (by 28-50%) (Fig. 2 and 3). Also, an increase in leaf area (by 30-40%) under FR substitution treatments partly

compensated for the 40% decrease in PPFD, enabling plants to produce a similar shoot biomass (as measured by DW) under more light-limiting conditions (Fig. 2 and 3). The promotive effect of FR radiation on leaf expansion and subsequent dry mass accumulation has been previously reported including in lettuce (*Lactuca sativa*) (Li and Kubota, 2009; Stutte et al., 2009) and arabidopsis (Patel et al., 2013). Together, these results suggest that FR radiation can indirectly promote biomass accumulation by establishing a canopy with a larger effective leaf area and thus, better radiation interception.

Different wavelengths have different quantum yields for CO<sub>2</sub> fixation. R radiation generally has the highest quantum yield, but it decreases dramatically at longer red wavelengths (above 680 nm), and FR radiation alone is considered inefficient at driving photosynthesis (McCree, 1972). However, our results showed that the additional FR radiation increased wholeplant net assimilation (Fig. 3). YPFD has been suggested as a more accurate predictor of photosynthesis than PPFD; it includes a broader waveband (300 to 800 nm) and photons of each wavelength are weighed by the relative quantum efficiency (RQE) (McCree, 1972; Sager et al., 1988; Cope and Bugbee, 2013). In our study, the RQE value at the emission peak of the FR LED (731 nm) was 0.15 while it was 0.93 for the R LED (660 nm). Thus, compared to the calculated YPFD under B+R, YPFD decreased by 34% when 50% of R radiation was substituted with FR and increased by up to 8% when FR radiation was added to B+R radiation (Table 1). The wholeplant net assimilation in three species showed a positive correlation with the calculated YPFD, within the range from 96 to 157 µmol·m<sup>-2</sup>·s<sup>-1</sup> (Fig. 4). When YPFD decreased by 34% in FR substitution treatments, whole-plant net assimilation decreased by 22-33%. When YPFD increased by 8% in FR addition treatments, whole-plant net assimilation increased by 20-37%. Considering the increase in whole-plant net assimilation for FR addition treatments was caused

only by the increase in YPFD by the addition of the photons in FR region, this result shows that a small increase in quantum yield with FR photons can have large direct effects on whole-plant net assimilation.

FR radiation has a low quantum yield because of insufficient excitation of photosystem II (PSII) with photosystem I (PSI) overexcitation (Emerson and Lewis, 1943; Duysens et al., 1961; Pettai et al., 2005; Thapper et al., 2009). PSII, which preferentially absorbs wavelengths between 400-680 nm and maximally at around 680 nm, and PSI, which absorbs FR maximally at around 700 nm, operate in series to carry out photosynthesis in algae and higher plants (Duysens et al., 1962; Evans and Anderson, 1987; Hogewoning et al., 2012; Laisk et al., 2014). Since PSII determines the rate of electron supply to PSI, insufficient excitation of PSII only with FR radiation strictly limits the overall quantum yield of photosynthesis (Duysens et al., 1961; Blankenship, 2002; Pettai et al., 2005). It is postulated that for stable operation with high efficiency, electron transport rates through these two photosystems should be balanced and any imbalance in excitation of the two photosystems decreases quantum yield (Allen, 2003; Pfannschmidt, 2005; Hogewoning et al., 2012). Although the peaks of the R LED (peak = 660 nm) and FR LED (peak = 731 nm) used in this study are slightly different from the paradigm peaks of PSII and PSI, they are within the range of their absorption spectrum. Thus, the added FR radiation possibly contributed to increased net assimilation by balancing the excitation between PSI and PSII while without FR, B+R radiation overexcited PSII relative to PSI.

However, the increase of net assimilation by FR radiation could be a consequence of the acclimation process of leaf architecture to a low R:FR. In our study, low R:FR or PPE increased leaf area and decreased SPAD value (an index of chlorophyll concentration per unit leaf area) (Fig. 2). In previous studies, although leaf area responses to R:FR have varied (ranging from an

increase to a decrease), generally a decrease in R:FR decreases chlorophyll content per unit area (Heraut-Bron et al., 1991; Demotes-Mainard et al., 2016), increases specific leaf area, and reduces leaf thickness (Smith and Whitelam, 1997; Gommers et al., 2013). In general, thinner shade leaves showed lower light compensation points and lower maintenance respiration rates compared to thicker sun-acclimated leaves, maintaining a higher net photosynthesis (gross photosynthesis minus respiration) under lower light than sun leaves (Chapin et al., 2011; Weraduwage et al., 2015). Also, under high R:FR, leaf mass per area and stomatal density increased, increasing photosynthesis in response to a higher PPFD (Boccalandro et al., 2009). These results suggest that low R:FR signals plants to adjust their leaf architecture and subsequent photosynthetic properties to shade conditions (lower PPFD and R:FR). Considering that the photosynthetic radiation intensity (PPFD = 96-160 µmol·m<sup>-2</sup>·s<sup>-1</sup>) in this study was relatively low for both shade-avoiding and shade-tolerant species, the leaves developed under low R:FR with FR radiation addition might contribute to the increase in whole-plant net assimilation under low PPFD conditions.

The acceleration of flowering by low R:FR is one characteristic of the shade-avoidance response (Smith and Whitelam, 1997; Morelli and Ruberti, 2000; Nozue et al., 2015). Our results are not consistent with this paradigm; while other shade-avoidance responses were regulated by low R:FR or PPE, flowering of three crops was not influenced by the R:FR or PPE within the range studied while in snapdragon, FR promoted flowering but the response was apparently saturated by  $16 \ \mu mol \cdot m^{-2} \cdot s^{-1}$  (or PPE  $\leq 0.85$ ; Table 3). This result is consistent with the existence of separate signaling mechanisms regulating phytochrome-mediated changes in plant architecture and floral induction (Botto and Smith, 2002; Cerdan and Chory, 2003; Nozue et al., 2015). In arabidopsis, while CONSTITUTIVELY PHOTOMORPHOGENIC1 (COP1) and the

four SUPPRESSOR OF PHYA-105 (SPA) genes are essential for hypocotyl and leaf petiole elongation in response to low R:FR, the acceleration of flowering in response to a low R:FR was normal in cop1 and spa mutants, demonstrating that the pathways of flowering time in response to low R:FR were different from those of elongation responses (Rolauffs et al., 2012). Also in arabidopsis (a long-day plant), a low R:FR shade signal promoted flowering partially through activation of the photoperiodic pathway (Kim et al., 2008) and low R:FR had little effect on acceleration of flowering under a short day compared to a long day (Wollenberg et al., 2008). In our study, the photoperiod of the radiation treatments was 18 hours, and the short night length combined with a lower R:FR during the day maximally accelerates flowering of at least some long-day plants, such as snapdragon. Also, the values of the effective PPE for promoting flowering of snapdragon in our study (0.69 to 0.85; Table 3) were similar with those most effective for night interruption lighting (0.63-0.80) in long-day plants including snapdragon and petunia (Petunia ×hybrida) (Craig and Runkle, 2016). These results suggest that including FR radiation in a light spectrum can regulate subsequent flowering independently from photomorphogenic responses such as extension growth of leaves and stems.

Here we showed that inclusion of FR promoted plant growth indirectly through leaf expansion and directly through an increase in whole-plant net assimilation. In addition, inclusion of FR during seedling growth promoted subsequent flowering in one long-day species. Although the effects of FR (and subsequent estimated PPE) on phytochrome-mediated responses was quantitatively different for some characteristics measured (such as between stem elongation and leaf expansion) or independent for others (such as between stem elongation and acceleration of flowering), the estimated PPE of the radiation spectrum showed an inverse linear relationship with several plant morphological traits including leaf expansion and stem elongation. In addition,

the calculated YPFD positively correlated with whole-plant net assimilation. These results indicate that inclusion of FR radiation in a radiation spectrum, whether from conventional incandescent lamps or more modern LEDs, can promote plant size and growth while regulating morphological and flowering characteristics as desired.

# **APPENDIX**

Table I-1. Spectral characteristics of six radiation treatments. The values after each light-emitting diode type (B=blue; R=red; FR=far red) indicate their intensity in  $\mu$ mol·m<sup>-2</sup>·s<sup>-1</sup>. Symbols are those used in Fig. 2 and 3.

| Radiation treatment          | Symbol   | PPFD <sup>a</sup> | TPFD <sup>b</sup> | YPFD <sup>c</sup> | R:FR <sup>d</sup> | PPE <sup>e</sup> |
|------------------------------|----------|-------------------|-------------------|-------------------|-------------------|------------------|
| $B_{32}+R_{128}$ (control)   |          | 160               | 160               | 146               | 1:0               | 0.88             |
| $B_{32}+R_{96}+FR_{32}$      | •        | 128               | 160               | 122               | 3:1               | 0.81             |
| $B_{32}+R_{64}+FR_{64}$      | •        | 96                | 160               | 96                | 1:1               | 0.69             |
| $B_{32} + R_{128} + FR_{16}$ | $\nabla$ | 160               | 176               | 149               | 8:1               | 0.85             |
| $B_{32} + R_{128} + FR_{32}$ | $\nabla$ | 160               | 192               | 150               | 4:1               | 0.83             |
| $B_{32}+R_{128}+FR_{64}$     | $\nabla$ | 160               | 224               | 157               | 2:1               | 0.78             |

<sup>&</sup>lt;sup>a</sup>PPFD: Photosynthetic photon flux density (photon flux integral between 400 and 700 nm, in μmol·m<sup>-2</sup>·s<sup>-1</sup>).

<sup>&</sup>lt;sup>b</sup>TPFD: Total photon flux density (photon flux integral between 400 and 800 nm, in  $\mu$ mol·m<sup>-2</sup>·s<sup>-1</sup>).

<sup>&</sup>lt;sup>c</sup>YPFD: Yield photon flux density, which is the product of TPFD and relative quantum efficiency (in μmol·m<sup>-2</sup>·s<sup>-1</sup>) based on McCree (1972) and Sager et al. (1988).

<sup>&</sup>lt;sup>d</sup>R:FR: Ratio of photon flux integral of red (R; 600-700 nm) and far red (FR; 700-800 nm) radiation.

<sup>&</sup>lt;sup>e</sup>PPE: Phytochrome photoequilibria, which is the estimated  $P_{FR}/P_{R+FR}$  following Sager et al. (1988).

Table I-2. Influence of the estimated phytochrome photoequilibria (PPE) of six radiation treatments on flowering characteristics. The values after each LED type (B=blue; R=red; FR=far red) indicate their intensity in  $\mu$ mol·m<sup>-2</sup>·s<sup>-1</sup>. Data represent the means of two replications (n = 20), and values with the same letter are not statistically different at P = 0.05.

| Radiation treatment                                | Days to flower                          | Stem length (cm) | Flower bud or inflorescence no. |  |  |  |
|--|---|------------------|---------------------------------|--|--|--|
| Geranium 'Pinto Premium Orar                       | Geranium 'Pinto Premium Orange Bicolor' |                  |                                 |  |  |  |
| $B_{32}+R_{128}$ (control)                         | 56.1                                    | 19.7             | 3.2                             |  |  |  |
| $B_{32}+R_{96}+FR_{32}$                            | 54.6                                    | 19.6             | 3.0                             |  |  |  |
| B <sub>32</sub> +R <sub>64</sub> +FR <sub>64</sub> | 54.8                                    | 18.5             | 3.7                             |  |  |  |
| $B_{32}+R_{128}+FR_{16}$                           | 54.9                                    | 19.2             | 3.0                             |  |  |  |
| $B_{32}+R_{128}+FR_{32}$                           | 54.0                                    | 19.8             | 2.9                             |  |  |  |
| $B_{32}+R_{128}+FR_{64}$                           | 53.6                                    | 19.2             | 2.9                             |  |  |  |
| Significance                                       | NS                                      | NS               | NS                              |  |  |  |
| Petunia 'Wave Blue'                                |   |                  |                                 |  |  |  |
| $B_{32}+R_{128}$ (control)                         | 34.2                                    | 8.4              | 18.7 a                          |  |  |  |
| $B_{32}+R_{96}+FR_{32}$                            | 26.6                                    | 7.0              | 9.3 a                           |  |  |  |
| B <sub>32</sub> +R <sub>64</sub> +FR <sub>64</sub> | 25.8                                    | 7.8              | 8.0 b                           |  |  |  |
| $B_{32}+R_{128}+FR_{16}$                           | 29.6                                    | 7.7              | 17.1 a                          |  |  |  |
| $B_{32}+R_{128}+FR_{32}$                           | 30.0                                    | 6.7              | 14.9 a                          |  |  |  |
| $B_{32}+R_{128}+FR_{64}$                           | 28.2                                    | 5.7              | 13.4 a                          |  |  |  |
| Significance                                       | NS                                      | NS               | *                               |  |  |  |
| Snapdragon 'Trailing Candy Sh                      | owers Yellow'                           |                  |                                 |  |  |  |
| $B_{32}+R_{128}$ (control)                         | 31.1 a                                  | 17.5 a           | 14.8                            |  |  |  |
| $B_{32}+R_{96}+FR_{32}$                            | 18.8 b                                  | 12.6 b           | 9.3                             |  |  |  |
| B <sub>32</sub> +R <sub>64</sub> +FR <sub>64</sub> | 20.8 b                                  | 14.4 b           | 8.2                             |  |  |  |
| $B_{32}+R_{128}+FR_{16}$                           | 18.6 b                                  | 13.3 b           | 8.7                             |  |  |  |
| $B_{32}+R_{128}+FR_{32}$                           | 18.7 b                                  | 13.0 b           | 10.4                            |  |  |  |
| $B_{32}+R_{128}+FR_{64}$                           | 18.3 b                                  | 12.8 b           | 10.6                            |  |  |  |
| Significance                                       | ***                                     | **               | NS                              |  |  |  |
| Impatiens 'Super Elfin XP Red'                     |   |                  |                                 |  |  |  |
| $B_{32}+R_{128}$ (control)                         | 17.2                                    | 4.9              | 11.8                            |  |  |  |
| $B_{32}+R_{96}+FR_{32}$                            | 16.7                                    | 5.1              | 13.6                            |  |  |  |
| $B_{32}+R_{64}+FR_{64}$                            | 17.8                                    | 5.5              | 15.6                            |  |  |  |
| $B_{32}+R_{128}+FR_{16}$                           | 18.1                                    | 5.9              | 13.6                            |  |  |  |
| $B_{32}+R_{128}+FR_{32}$                           | 19.5                                    | 5.6              | 18.9                            |  |  |  |
| $B_{32}+R_{128}+FR_{64}$                           | 16.2                                    | 5.1              | 14.9                            |  |  |  |
| Significance                                       | NS                                      | NS               | NS                              |  |  |  |

NS, \*, \*\*, or \*\*\* Nonsignificant or significant at P < 0.05, 0.01 or 0.001, respectively.

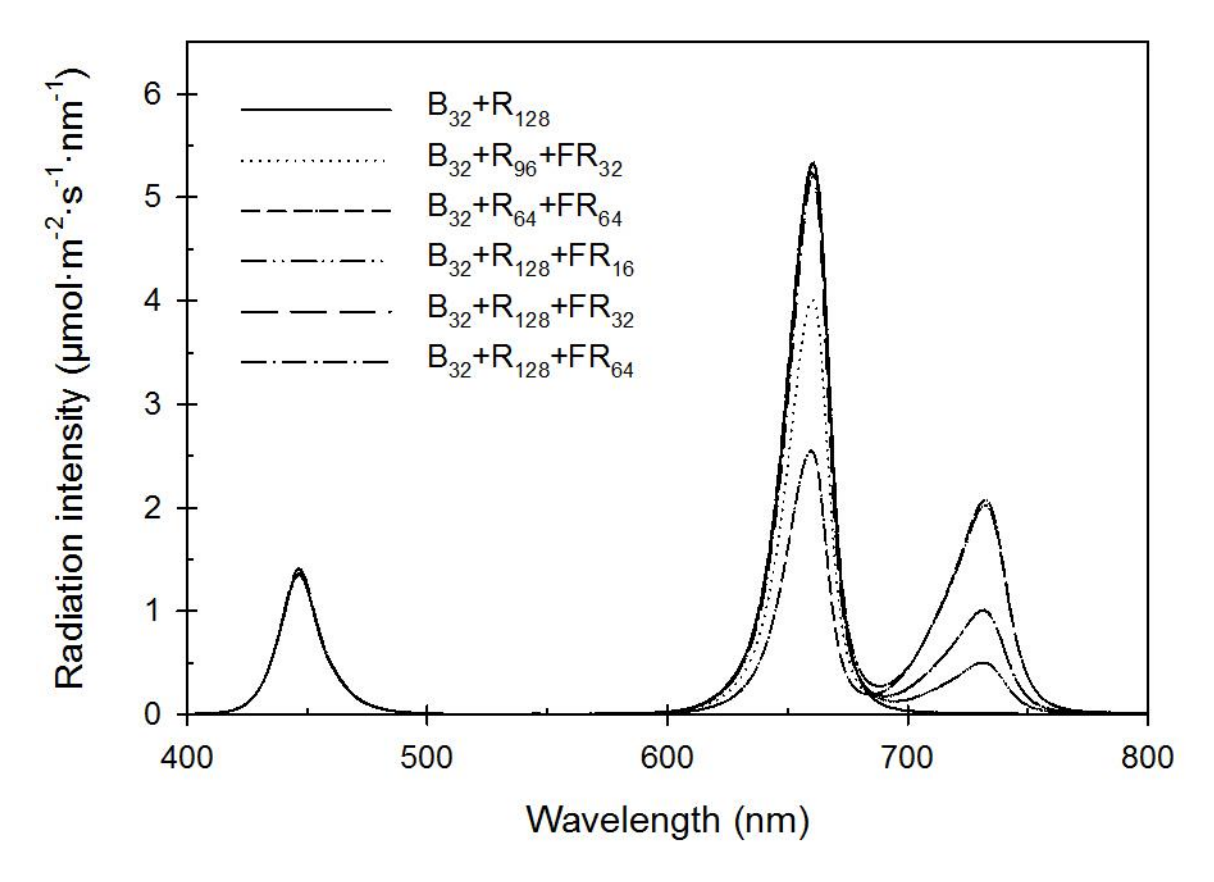


Figure I-1. The spectral distribution of six radiation treatments from blue (B), red (R), and farred (FR) light-emitting diodes (LEDs). The values after each LED type indicate their intensity in  $\mu mol \cdot m^{-2} \cdot s^{-1}$ .

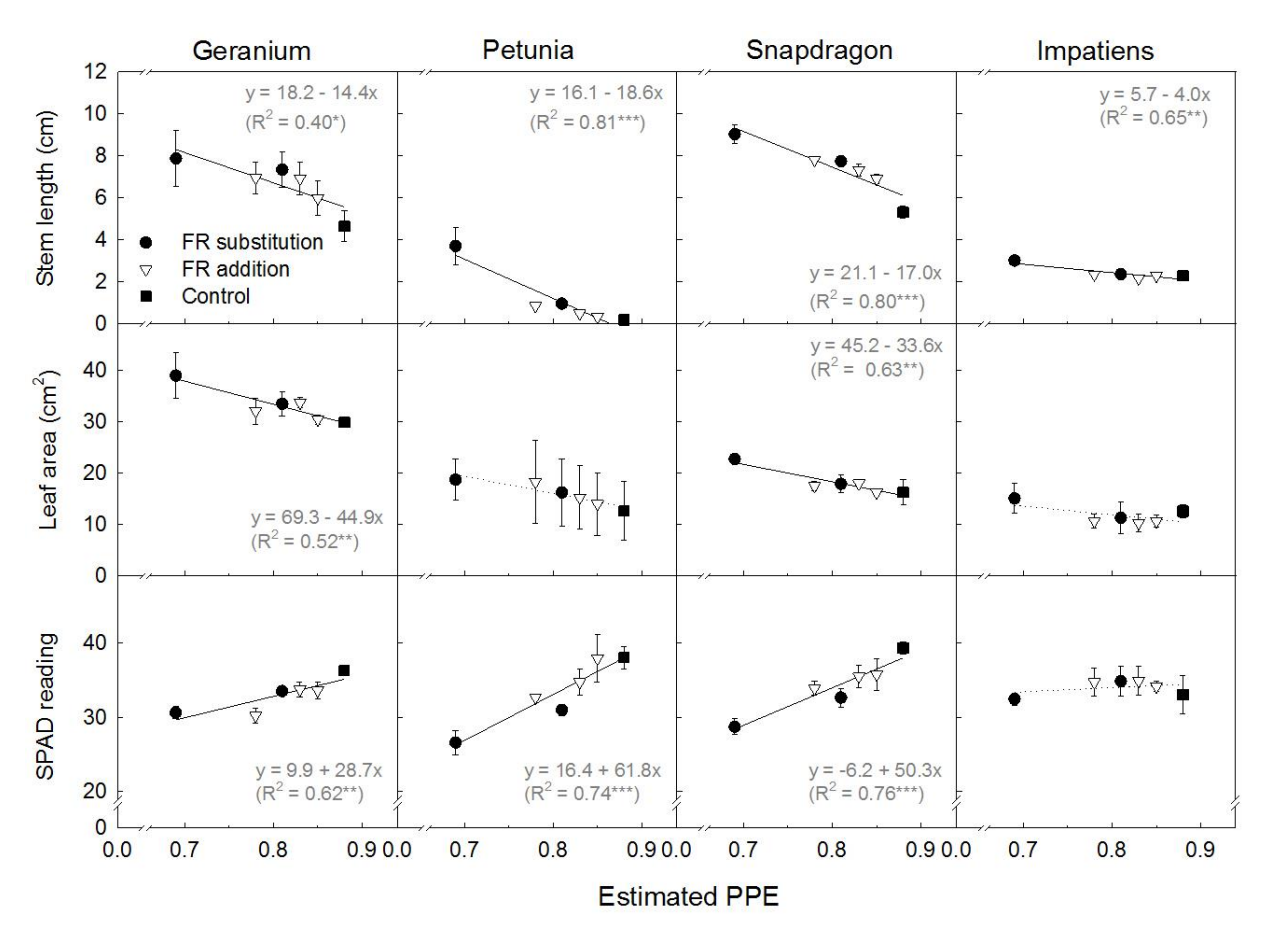


Figure I-2. Influence of the estimated phytochrome photoequilibria (PPE) of six radiation treatments on seedling stem length, leaf area, and SPAD reading. Six radiation treatments were categorized into far-red (FR; 700-800 nm) substitution treatments ( $B_{32}+R_{96}+FR_{32}$  and  $B_{32}+R_{64}+FR_{64}$ ), FR addition treatments ( $B_{32}+R_{128}+FR_{16}$ ,  $B_{32}+R_{128}+FR_{32}$ , and  $B_{32}+R_{128}+FR_{64}$ ), and control treatment ( $B_{32}+R_{128}$ ). Each data point represents the mean and standard error of two replications with 10 subsamples (plants) per replication and species. Associated correlation coefficients ( $R^2$ ) and regression equations are presented when statistically significant (solid line) but not when not significant (dotted line). \*, \*\*\*, \*\*\* indicate significant at P < 0.05, 0.01 or 0.001, respectively.

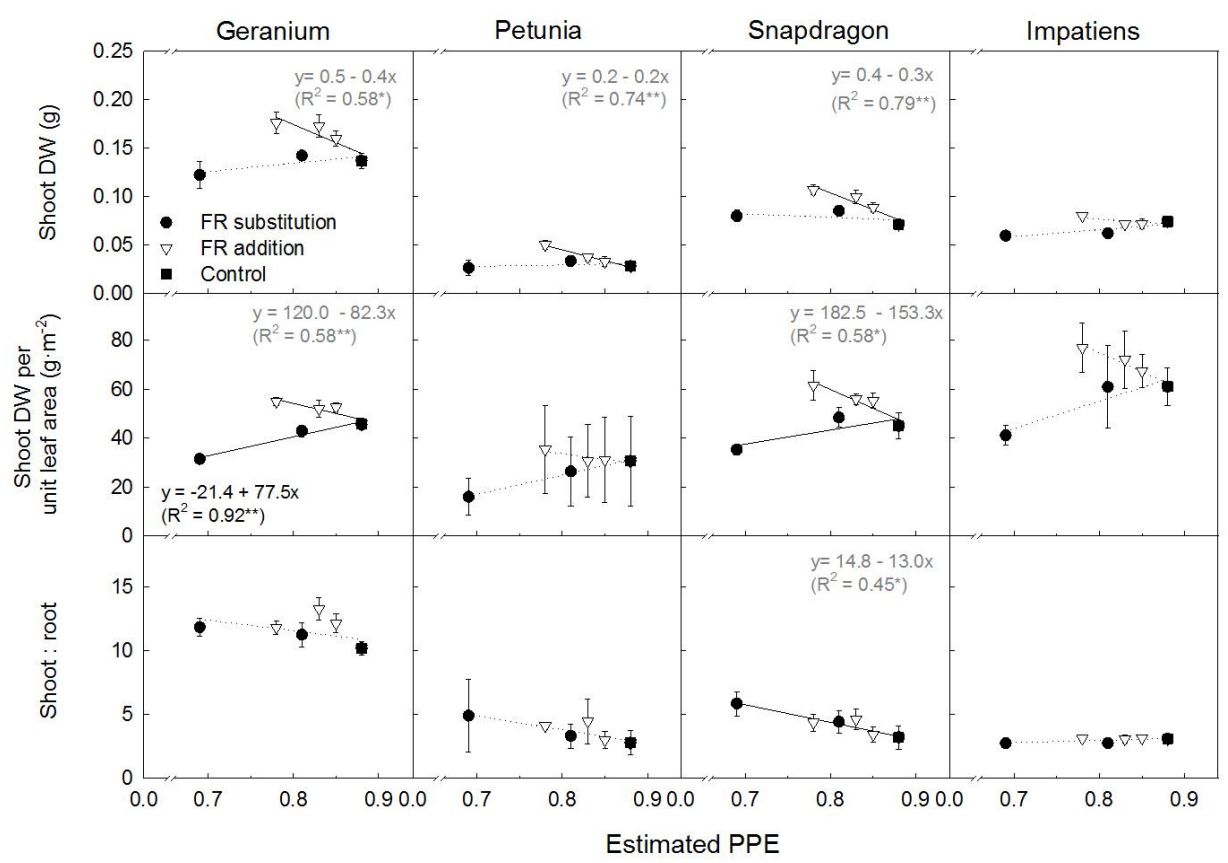
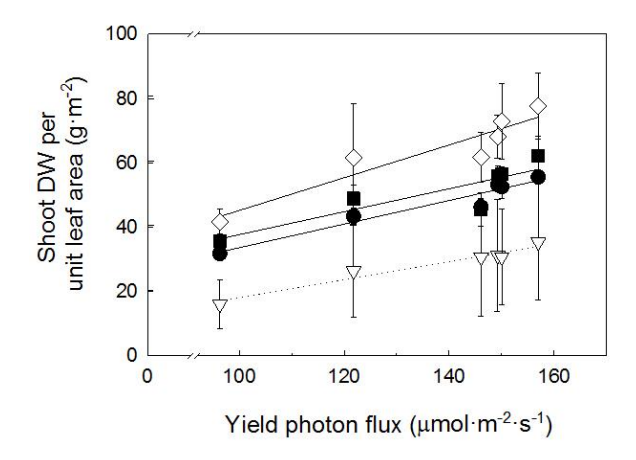


Figure I-3. Influence of the estimated phytochrome photoequilibria (PPE) of six radiation treatments on plant dry weight (DW). Six radiation treatments were categorized into far-red (FR; 700-800 nm) substitution treatments ( $B_{32}+R_{96}+FR_{32}$  and  $B_{32}+R_{64}+FR_{64}$ ), FR addition treatments ( $B_{32}+R_{128}+FR_{16}$ ,  $B_{32}+R_{128}+FR_{32}$ , and  $B_{32}+R_{128}+FR_{64}$ ), and control treatment ( $B_{32}+R_{128}$ ). Each data point represents the mean and standard error of two replications with 10 subsamples (plants) per replication and species. Associated correlation coefficients ( $R^2$ ) and regression equations are presented when statistically significant (solid line) but not when not significant (dotted line). NS, \*, or \*\* indicate nonsignificant or significant at P < 0.05 or 0.01, respectively.



| Species    | Symbol     | Regression equation | $\mathbb{R}^2$ |  |
|------------|------------|---------------------|----------------|--|
| Geranium   | •          | y = -3.0 + 0.4x     | 0.88***        |  |
| Petunia    | $\nabla$   | y = -10.2 + 0.3x    | NS             |  |
| Snapdragon |            | y = -1.9 + 0.4x     | 0.63**         |  |
| Impatiens  | $\Diamond$ | y = -5.7 + 0.5x     | 0.48*          |  |
|            |            |                     |                |  |

Figure I-4. Influence of the calculated yield photon flux density of six radiation treatments on shoot dry weight (DW) per unit leaf area. Each data point represents the mean and standard error of two replications with 10 subsamples (plants) per replication and species. Associated correlation of coefficients ( $\mathbb{R}^2$ ) and regression equations are presented when statistically significant (solid line) but not when not significant (dotted line). NS, \*, \*\*, \*\*\* indicate nonsignificant or significant at P < 0.05, 0.01 or 0.001, respectively.

LITERATURE CITED

#### LITERATURE CITED

- Allen, J.F. 2003. State transitions—A question of balance. Science 299:1530–1532.
- Blankenship, R.E. 2002. History and early development of photosynthesis. In Molecular mechanisms of photosynthesis. Blackwell Science, Oxford, pp. 26–41.
- Botto, J.F. and H. Smith. 2002. Differential genetic variation in adaptive strategies to a common environmental signal in Arabidopsis accessions: phytochrome-mediated shade avoidance. Plant Cell Environ. 25:53–63.
- Boccalandro, H.E., M.L. Rugnone, J.E. Moreno, E.L. Ploschuk, L. Serna, M.J. Yanovsky, and J.J. Casal. 2009. Phytochrome B enhances photosynthesis at the expense of water-use-efficiency in Arabidopsis. Plant Physiol. 150:1083–1092.
- Bourget, M.C., 2008. An introduction to light-emitting diodes. HortScience 43:1944–1946.
- Casal, J.J., P.J. Aphalo, and R.A. Sanchez. 1987. Phytochrome effects on leaf growth and chlorophyll content in *Petunia axillaris*. Plant Cell Environ. 10:509–514.
- Casal, J.J., 2013a. Photoreceptor signaling networks in plant responses to shade. Annu. Rev. Plant Biol. 64:403–27.
- Casal, J.J., 2013b. Canopy light signals and crop yield in sickness and in health. ISRN Agron. 2013:650439.
- Cerdan, P.D. and J. Chory. 2003. Regulation of flowering time by light quality. Nature 423:881–885.
- Chapin, F.S., P.A. Matson, P.M. Vitousek, and M.C. Chapin. 2011. Principles of terrestrial ecosystem ecology. 2nd ed. Springer, New York, pp. 97–122.
- Ciolfi, A., G. Sessa, M. Sassi, M. Possenti, S. Salvucci, M. Carabelli, G. Morelli, and I. Ruberti. 2013. Dynamics of the shade-avoidance response in Arabidopsis. Plant Physiol. 163:331–353.
- Cope, K.R. and B. Bugbee. 2013. Spectral effects of three types of white light-emitting diodes on plant growth and development: Absolute versus relative amounts of blue light. HortScience 48:504–509.
- Cope, K.R., M.C. Snowden, and B. Bugbee. 2014. Photobiological interactions of blue light and photosynthetic photon flux: effects of monochromatic and broad-spectrum light source. Photochem. Photobiol. 90:574–584.

- Craig, D.S. and E.S. Runkle. 2016. An intermediate phytochrome photoequilibria from night-interruption lighting optimally promotes flowering of several long-day plants. Environ. Exp. Bot. 121:132–138.
- Dale, J.E. 1988. The control of leaf expansion. Ann. Rev. Plant Physiol. Plant Mol. Biol. 39:267–295.
- Demotes-Mainard, S., T. Peron, A. Corot, J. Bertheloot, J. Le Gourrierec, S. Travier, L. Crespel, P. Morel, L. Huche-Thelier, R. Boumaza, A. Vian, V. Guerin, N. Leduc, and S. Sakr. 2015. Plant responses to red and far-red lights, applications in horticulture. Environ. Exp. Bot. 121:4–21.
- Duysens, J.N.M., J. Amesz, and B.M. Kamp. 1961. Two photochemical systems in photosynthesis. Nature 190:510–511.
- Duysens, L.N.M. and J. Amesz. 1962. Function and identification of two photochemical systems in photosynthesis. Biochim. Biophys. Acta. 64:243–260.
- Emerson, R. and C.M. Lewis. 1943. The dependence of the quantum yield of Chlorella photosynthesis on wavelength of light. Am. J. Bot. 30:165–78.
- Gommers, C.M.M., E.J.W. Visser, K.R. St Onge, L.A.C.J. Voesenek, and R.Pierik. 2013. Shade tolerance: when growing tall is not an option. Trends Plant Sci. 18:65–71.
- Gregory, F.G. 1917. Physiological conditions in cucumber houses. 3rd Ann. Exp. Res. Stn. Rep. Cheshunt, England. pp. 19–28.
- Heraut-Bron, V., C. Robin, C. Varlet-Grancher, D. Afif, and A. Guckert. 1999. Light quality (red:far-red ratio): does it affect photosynthetic activity, net CO<sub>2</sub> assimilation, and morphology of young white clover leaves? Can. J. Bot. 77:1425–1431.
- Hogewoning, S.W., P. Douwstra, G. Trouwborst, W. van Ieperen, and J. Harbinson. 2010. An artificial solar spectrum substantially alters plant development compared with usual climate room irradiance spectra. J. Exp. Bot. 61:1267–1276.
- Hogewoning, S.W., E. Wientjes, P. Douwstra, G. Trouwborst, W. van Ieperen, R. Croce, and J. Harbinson. 2012. Photosynthetic quantum yield dynamics: from photosystems to leaves. Plant Cell 24:1921–1935.
- Hunt, R., D.R. Causton, B. Shipley, and A.P. Askew. 2002. A modern tool for classical plant growth analysis. Ann. Bot. 90:485–488.
- Keuskamp, D.H., R. Sasidharan, and R. Pierik. 2010. Physiological regulation and functional significance of shade avoidance responses to neighbors. Plant Signal. Behav. 5:655–662.

- Keuskamp, D.H., R. Sasidharan, I. Vos, A.J.M. Peeters, L.A.C.J. Voesenek, and R. Pierik. 2011. Blue-light-mediated shade avoidance requires combined auxin and brassinosteroid action in Arabidopsis seedlings. Plant J. 67:208–217.
- Kim, S.Y., X. Yu, and S.D. Michaels. 2008. Regulation of CONSTANS and FLOWERING LOCUS T expression in response to changing light quality. Plant Physiol. 148:269–279.
- Klassen, S., G. Ritchie, J. Frantz, D. Pinnock, and B.Bugbee. 2003. Real-time imaging of ground cover: relationships with radiation capture, canopy photosynthesis, and daily growth rate. Digital imaging and spectral techniques: applications to precision agriculture and crop physiology. 2003:3–14.
- Li, Q. and C. Kubota. 2009. Effects of supplemental light quality on growth and phytochemical of baby leaf lettuce. Environ. Exp. Bot. 67:59–64.
- Li, J., G. Li, H. Wang, and X.W. Deng. 2011. Phytochrome signaling mechanisms. Arabidopsis Book:e0148.
- Laisk, A., V. Oja, and L.Dall'Osto. 2014. Action spectra of photosystems II and I and quantum yield of photosynthesis in leaves in State 1. Biochim. Biophys. Acta 1837:315–325.
- Maliakal, S.K., K. McDonnell, S.A. Dudley, and J. Schmitt. 1999. Effects of red to far-red ratio and plant density on biomass allocation and gas exchange in *Impatiens capensis*. International J. Plant Sci. 160:723–733.
- Massa, G.D., H.H. Kim, R.M. Wheeler, and C.A. Mitchell. 2008. Plant productivity in response to LED lighting. HortScience 43:1951–1956.
- Morrow, R.C. 2008. LED lighting in horticulture. HortScience 43:1947–1950.
- McCree, K.J. 1972. The action spectrum, absorbance and quantum yield of photosynthesis in crop plants. Agr. Meteorol. 9:191–216.
- Mitchell, C., A.-J. Both, M. Bourget, J. Burr, C. Kubota, R. Lopez, R. Morrow, and E. Runkle. 2012. LEDs: The future of greenhouse lighting! Chronica Hort. 52:6–11.
- Montgomery, B.L., 2016. Spatiotemporal phytochrome signaling during photomorphogenesis: From physiology to molecular mechanisms and back. Front. Plant Sci. 7:480.
- Morelli, G. and I. Ruberti. 2000. Shade avoidance responses. Driving auxin along lateral routes. Plant Physiol. 122:621–626.
- Nozue, K., A.V. Tat, U. Kumar Devisetty, M. Robinson, M.R. Mumbach, Y. Ichihashi, S. Lekkala, and J.N. Maloof. 2015. Shade avoidance components and pathways in adult plants revealed by phenotypic profiling. PLoS Genet. 11:e1004953.

- Park, Y. and E.S.Runkle. 2016. Investigating the merit of including far-red radiation in the production of ornamental seedlings grown under sole-source lighting. Acta Hortic. 1134:259–266.
- Patel, D., M. Basu, S. Hayes, I. Majlath, F.M. Hetherington, T.J. Tschaplinski, and K.A. Franklin. 2013. Temperature-dependent shade avoidance involves the receptor-like kinase ERECTA. The Plant J. 73:980–992.
- Pedmale, U.V., S.S.C. Huang, M. Zander, B.J. Cole, J. Hetzel, K. Ljung, P.A.B. Reis, P. Sridevi, K. Nito, J.R. Nery, J.R. Ecker, and J. Chory. 2016. Cryptochromes interact directly with PIFs to control plant growth in limiting blue light. Cell 164:233–245.
- Pettai, H., V. Oja, A. Freiberg, and A. Laisk. 2005. Photosynthetic activity of far-red light in green plants. Biochem. Biophy. Acta. 1708:311–321.
- Pfannschmidt, T., 2005. Acclimation to varying light qualities: Toward the functional relationship of state transitions and adjustment of photosystem stoichiometry. J. Phycol. 41:723–725.
- Pierik, R., G.C. Whitelam, L.A.C.J. Voesenek, H. de Kroon, and E.J.W. Visser. 2004. Canopy studies on ethylene-insensitive tobacco identify ethylene as a novel element in blue light and plant-plant signalling. Plant J. 38:310–319.
- Possart, A., C. Fleck, and A. Hiltbrunner. 2014. Shedding (far-red) light on phytochrome mechanisms and responses in land plants. Plant Sci. 217–218:36–46.
- Radford, P.J. 1967. Growth analysis formulae-their use and abuse. Crop Sci. 7:171–175.
- Randall, W.C. and R.G. Lopez, 2014. Comparison of supplemental lighting from high-pressure sodium lamps and light-emitting diodes during bedding plant seedling production. Hortscience 49:589–595.
- Richards, R.A. 2000. Selectable traits to increase crop photosynthesis and yield of grain crops. J. Exp. Bot. 51:447–458.
- Rolauffs, S., P. Fackendahl, J. Sahm, G. Fiene, and U. Hoecker. 2012. Arabidopsis COP1 and SPA genes are essential for plant elongation but not for acceleration of flowering time in response to a low red light to far-red light ratio. Plant Physiol. 160:2015–2027.
- Ruberti I., G. Sessa, A. Ciolfi, M. Possenti, M. Carabelli, and G. Morelli. 2012. Plant adaptation to dynamically changing environment: the shade avoidance response. Biotechnol. Adv. 30:1047–1058.
- Runkle, E.S. and R.D. Heins. 2001. Specific functions of red, far red, and blue light in flowering and stem extension of long-day plants. J. Amer. Soc. Hort. Sci. 126:275–282.

- Runkle, E.S. 2007. Maximizing supplemental lighting. Greenhouse Product News 17:66.
- Sager, J.C., W.O. Smith, J.L. Edwards, and K.L. Cyr. 1988. Photosynthetic efficiency and phytochrome photoequilibria determination using spectral data. Trans. Amer. Soc. Agr. Eng. 31:1882–1889.
- Sasidharan, R., C.C. Chinnappa, L.A.C.J. Voesenek, and R. Pierik. 2008. The regulation of cell wall extensibility during shade avoidance: A study using two contrasting ecotypes of *Stellaria longipes*. Plant Physiol. 148:1557–1569.
- Smith, H. 1994. Sensing the light environment: The functions of the phytochrome family. In Photomorphogenesis in plants, 2nd edn. Kendrick, R.E. and Kronenberg, G.H.M. eds. (Dordrecht, the Netherlands: Kluwer Academic Publishers), pp. 377–416.
- Smith, H. and G.C. Whitelam. 1997. The shade avoidance syndrome: multiple responses mediated by multiple phytochromes. Plant Cell Environ. 20:840–844.
- Snowden, M.C., K.R. Cope, and B. Bugbee. 2016. Sensitivity of seven diverse species to blue and green light: interactions with photon flux. PLoS ONE 11:e0163121.
- Stutte, G.W., S. Edney, and T.Skerritt. 2009. Photoregulation of bioprotectant content of red leaf lettuce with light emitting diodes. HortScience 44:79–82.
- Thapper, A, F. Mamedov, F. Mokvist, L. Hammarstrom, and S. Styring. 2009. Defining the farred limit of photosystem II in spinach. Plant Cell 2:2391–2401.
- Van Volkenburgh, E. 1999. Leaf expansion: An integrating plant behavior. Plant Cell Environ. 22:1463–1473.
- Vernon, A.J. and J.C.S. Allison. 1963. A method of calculating net assimilation rate. Nature 200:814.
- Weraduwage, S.M., J. Chen, F.C. Anozie, A. Morales, S.E. Weise, and T.D. Sharkey. 2015. The relationship between leaf area growth and biomass accumulation in *Arabidopsis thaliana*. Front. Plant Sci. 6:167.
- Wollaeger, H.M. and E.S. Runkle. 2013. Growth response of ornamental annual seedlings under different wavelengths of red light provided by light-emitting diodes. HortScience 48:1478–1483.
- Wollaeger, H.M. and E.S. Runkle. 2015. Growth and acclimation of impatiens, salvia, petunia, and tomato seedlings to blue and red light. HortScience 50:522–529.
- Wollenberg, A.C., B. Strasser, P.D. Cerdan, and R.M. Amasino. 2008. Acceleration of flowering during shade avoidance in Arabidopsis alters the balance between FLOWERING LOCUS

C-mediated repression and photoperiodic induction of flowering. Plant Physiol. 148: 1681–1694.

## **SECTION II**

FAR-RED RADIATION AND PHOTOSYNTHETIC PHOTON FLUX DENSITY INDEPENDENTLY REGULATE SEEDLING GROWTH BUT INTERACTIVELY REGULATED FLOWERING

Far-red Radiation and Photosynthetic Photon Flux Density Independently Regulate Seedling

Growth but Interactively Regulate Flowering

Yujin Park<sup>1</sup> and Erik S. Runkle<sup>2</sup>

Department of Horticulture, 1066 Bogue Street, Michigan State University, East Lansing, MI

48824

This research was supported by Osram Opto Semiconductors; the USDA-ARS Floriculture and

Nursery Research Initiative; the USDA National Institute of Food and Agriculture, Hatch project

192266; Michigan State University's (MSU) AgBioResearch and Project GREEEN; and

horticulture companies supportive of MSU floriculture research. We thank C. Raker & Sons for

donation of plant material and Nate DuRussel for technical assistance. We thank Dr. Sasha

Kravchenko (Department of Plant, Soil and Microbial Sciences, MSU) and Statistical Consulting

Center (CANR Biometry Group, MSU) for statistical advice.

<sup>1</sup>Graduate student.

<sup>2</sup>Corresponding author. Email address: runkleer@msu.edu.

38

#### **Abstract**

Shade-avoidance responses can be triggered by a decrease in the red (R, 600–700 nm) to far-red (FR, 700–800 nm) radiation ratio, by a decrease in photosynthetic photon flux density (PPFD), or both. The effects of decreased PPFD on plant responses are often confounded with the effects of reduced blue (B, 400–500 nm) photon flux density, which is another signaling factor for shade-avoidance responses. We postulated that PPFD would not influence R:FRmediated shade-avoidance responses if B photon flux density was constant... We grew seedlings of geranium (*Pelargonium* ×hortorum), petunia (*Petunia* ×hybrida), and coleus (Solenostemon scutellariodes) under three R:FR (1:0, 2:1, and 1:1) at two PPFDs (96 and 288 μmol·m<sup>-2</sup>·s<sup>-1</sup>), all with a B photon flux density of 32 μmol·m<sup>-2</sup>·s<sup>-1</sup>. As R:FR decreased, stem length in all species increased. Decreasing R:FR increased individual leaf area and chlorophyll concentration of petunia, and shoot dry weight of petunia and coleus decreased. Increasing PPFD decreased chlorophyll concentration and increased leaf mass per area, net CO<sub>2</sub> assimilation, whole-plant net assimilation, and dry weight in at least two species, independent of R:FR. In petunia, a long day plant, decreasing R:FR promoted subsequent flowering at both PPFDs, but to a greater extent under the lower PPFD. In day-neutral geranium, the addition of FR had no effect on flowering, irrespective of PPFD. We conclude that with a constant B photon flux density, decreases in R:FR promote stem elongation and leaf expansion, and subsequent dry mass accumulation, independent of PPFD. However, for flowering of long-day plant petunia, the promotive effect of low R:FR is greater under lower PPFD.

*Keywords*: far-red radiation, photosynthetic photon flux density, phytochrome, red to far-red ratio, shade-avoidance, sole-source lighting

#### Abbreviations:

*A*<sub>n</sub>, net assimilation rate; B, blue radiation; Chl, chlorophyll; DW, dry weight; DLI, daily light integral: FR, far-red radiation; HPS, high-pressure sodium; LEDs, light-emitting diodes; LHC, light-harvesting chlorophyll protein complexes; LMA, leaf mass per area; PAR, photosynthetically active radiation; PPE, phytochrome photoequilibrium; PPFD, photosynthetic photon flux density; Pr, R-radiation-absorbing phytochrome; Pfr, FR-radiation-absorbing phytochrome; PhyB, phytochrome B; PSI, photosystem I; PSII, photosystem II; R, red; TPFD, total photon flux density; YPFD, yield photon flux density.

#### Introduction

Photosynthetic pigments efficiently absorb blue (B; 400-500 nm) and red (R; 600-700 nm) radiation but reflect or transmit most far-red (FR; 700-800nm) radiation (Casal, 2013).

Therefore, the R:FR ratio is reduced under vegetative shade, which elicits shade-avoidance responses (Ballaré et al., 1987; Smith and Whitelam, 1997). A low R:FR can increase elongation of internodes, petioles, and hypocotyls, regulate leaf expansion, promote apical dominance, suppress branching, and accelerate flowering, which generally enable plants to better capture radiation and survive under shade (Franklin, 2008; Casal, 2012). Although FR radiation is often assumed to have a negligible impact on net photosynthesis because of its low quantum yield (McCree, 1972), adding FR radiation to a B+R radiation spectrum increased long-term whole-plant net assimilation in several ornamental seedlings (Park and Runkle, 2017).

Phytochromes play a predominant role in the perception of the R:FR signal and regulate subsequent plant responses (Franklin and Quail, 2010; Kami et al., 2010). Phytochromes are

synthesized in the cytosol in their inactive R-absorbing form, Pr. Upon R radiation absorption, Pr converts to the active, FR-absorbing form, Pfr, and Pfr form, in turn, can be converted back to Pr by FR radiation or darkness. The active Pfr form translocates to the nucleus where it leads to rapid changes in gene expression, and becomes degraded (Jang et al., 2010; Li et al., 2011). Therefore, the R:FR of the incident radiation determines a dynamic photoequilibrium of the Pfr and Pr forms within the plants, which can be described as the relative amount of Pfr in the total phytochrome pool [the phytochrome photoequilibrium (PPE)].

Models have been developed to estimate PPE based upon the absorption of Pr and Pfr and the spectral distribution of incident radiation (Smith and Holmes, 1977; Sager et al., 1988). According to these models, the estimated PPE value for sunlight is 0.73 and decreases to as low as 0.15, depending on the degree of shade (Smith and Holmes, 1977; Smith, 1982). Typical PPE values under common electric light sources used in plant production and research include 0.64 under an incandescent lamp (Runkle and Heins, 2003; Meng and Runkle, 2014), 0.80-0.85 under a metal halide lamp (Sager et al., 1988; Dougher and Bugbee, 2001), 0.85-0.86 under a highpressure sodium (HPS) lamp (Sager et al., 1988; Dougher and Bugbee, 2001), and 0.85 under a fluorescent lamp (Wollaeger and Runkle, 2014). Several phytochrome-regulated responses, including stem elongation, chlorophyll (Chl) concentration, and flowering, have been expressed in relation to the estimated PPE (Smith, 1982; Sager et al., 1988; Craig and Runkle, 2016). For example, stem extension of a wide range of species commonly have an inverse linear relationship with estimated PPE (Smith, 1994; Runkle and Heins, 2001). The estimated PPE, therefore, is a useful indicator to quantify phytochrome-mediated plant responses to the radiation spectrum.

While plant responses to vegetative shade have commonly been studied as a function of R:FR and PPE, the photosynthetic photon flux density (PPFD) can also regulate shade-avoidance responses. In general, increasing PPFD decreases the magnitude of plant responses to the R:FR. For example, internode elongation of sunflower (*Helianthus annuus*) seedlings increased by reducing the R:FR (from 4.52 to 0.85) under both a low PPFD (157 μmol·m<sup>-2</sup>·s<sup>-1</sup>) and moderate PPFD (421 μmol·m<sup>-2</sup>·s<sup>-1</sup>), but the response was attenuated under the higher PPFD (Kurepin et al., 2007). Similarly, R:FR signaling through phytochrome B (phyB) promoted branching of arabidopsis (*Arabidopsis thaliana*) under a low PPFD (160 μmol·m<sup>-2</sup>·s<sup>-1</sup>), but effects were diminished under a higher PPFD (280 μmol·m<sup>-2</sup>·s<sup>-1</sup>), indicating that the high PPFD at least partly overrides the effects of phytochrome-mediated signaling on branching (Su et al., 2011).

However, most studies on the effect of PPFD on shade-avoidance responses used neutral shading, which reduced the quantity of radiation homogeneously and thus, reduced the photon flux density of each radiation waveband (e.g., B radiation). Therefore, PPFD-regulated plant responses could be at least partly confounded by changes in photon flux densities of specific wavebands, rather than a wholesale change in the PPFD. In particular, a reduction in B radiation (without changes in total PPFD) can induce shade-avoidance responses similar to those under a low R:FR or/and low PPFD, including elongation of hypocotyls (Djakovic-Petrovic et al., 2007; Pierik et al., 2009; Keuskamp et al., 2011) and stem elongation (Pierik et al., 2004; Sasidharan et al., 2008; Wollaeger and Runkle, 2015). Therefore, it is less clear whether the attenuated plant responses to R:FR under higher PPFD can be attributed to the increase in PPFD or specifically to the increase in B photon flux density. This point makes less clear how R:FR and its interaction with PPFD regulate plant growth and development without the confounding effects from B radiation.

Our primary research object was to determine whether the attenuation of R:FR responses from increased PPFD could be specifically attributed to a decrease in the photon flux of B radiation. We performed research in a highly controlled environment to investigate how PPFD interacts with FR radiation at a constant B photon flux density to regulate plant architecture, photosynthesis, growth, and subsequent flowering of species with different photoperiodic and shade tolerance responses. We postulated that when B photon flux density is kept constant, increasing the PPFD would not influence FR-mediated shade-avoidance responses (including stem elongation, leaf expansion, and early flowering) and thus, regardless of PPFD, increases in FR radiation would promote plant growth and accelerate subsequent flowering similarly. We also postulated that increases in FR radiation would increase photosynthesis and thus, plant growth.

#### **Materials and Methods**

## Plant materials

Geranium (*Pelargonium* ×*hortorum* 'Pinto Premium Orange Bicolor'), petunia (*Petunia* ×*hybrida* 'Wave Blue'), and coleus (*Solenostemon scutellariodes* 'Wizard Golden') were chosen for study based on commercial significance, shade tolerance, and photoperiodic flowering response. Geranium and petunia are shade-avoiding species while coleus is shade-tolerant; and geranium, petunia, and coleus are categorized as day-neutral, long-day, and short-day plants, respectively (Erwin et al., 2017). Seeds of each species were sown in 128-cell (2.7 × 2.7-cm; 12.0-mL volume) plug trays by a commercial young plant producer (C. Raker and Sons, Inc., Litchfield, MI). Trays were moved to Michigan State University (East Lansing, MI) 7 d after sow. Each plug tray of geranium and coleus was cut into three sections (each with ≥40 seedlings) and petunia trays were cut into four sections (each with ≥30 seedlings). Seedlings were thinned

to one plant per cell and placed under radiation treatments. The experiment was performed twice for petunia and three times for geranium and coleus.

Radiation treatments and growth conditions

The top of each of six LED modules [described by Wollaeger and Runkle (2013) but with new LED panels] contained LEDs emitting B (peak = 447 nm), R (peak = 660 nm), and FR (peak = 731 nm) radiation and faced downward. Wire mesh was placed just below the middle half of the LED boards to provide a more uniform photon flux density within each module. The intensities of the three LED types were independently adjusted by dimmer switches on the driver boards to create six radiation treatments based on a mean of 10 measurements from a spectroradiometer (PS-200; StellerNet, Inc., Tampa, FL) made at seedling-tray height at predetermined horizontal positions inside each module. The six radiation treatments were designed to test three R:FR ratios (1:0, 2:1, and 1:1) at two PPFDs [96 µmol·m<sup>-2</sup>·s<sup>-1</sup> (PPFD 96) and 288 µmol·m<sup>-2</sup>·s<sup>-1</sup> (PPFD 288)], each with 32 µmol·m<sup>-2</sup>·s<sup>-1</sup> of B radiation. The treatments delivered the following photon flux densities of R and FR radiation:  $R_{64}$  (64  $\mu$ mol·m<sup>-2</sup>·s<sup>-1</sup> of R),  $R_{64}+FR_{32}$ ,  $R_{64}+FR_{64}$ ,  $R_{256}$ ,  $R_{256}+FR_{128}$ , and  $R_{256}+FR_{256}$  (Fig. 1 and Table 1). For each radiation treatment, the yield photon flux density (YPFD), which is the product of photon flux density and relative quantum efficiency, was calculated based on McCree (1972) and Sager et al. (1988); the R:FR was calculated with 100-nm wavebands; and the PPE was estimated as described by Sager et al. (1988) (Table 1). The B photon flux density was kept constant for all radiation treatments so that responses to PPFD were not confounded by the effects of B radiation through cryptochrome (Pierik et al., 2004; Keuskamp et al., 2011; Pedmale et al., 2016). Subsequently, the relative portion of B radiation in the entire spectrum (400-800 nm) was higher at PPFD 96 (20-33% of B) than at PPFD 288 (6-11% of B), which decreased the estimated PPE by 0.01 at

the same R:FR (Table 1). The six LED modules were on open, metal mesh benches inside a refrigerated walk-in growth chamber. Plug trays were rotated daily to further reduce any positional effects inside each LED module.

Plants were grown at a constant 20 °C under an 18-h photoperiod as controlled by a data logger (CR10; Campbell Scientific, Logan, UT). In each treatment, thermocouples (0.13-mm type E; Omega Engineering, Stamford, CT) measured air temperature and infrared sensors (Type K, OS36-01; Omega Engineering), positioned 20 cm above the module bottom and pointing at a downward angle toward the canopy of the closest plant tray, measured canopy temperature. Quantum sensors (LI-190R; LI-COR, Lincoln, NE) measured PPFD in each module at plug tray level. The infrared sensors, thermocouples, and quantum sensors were connected to the same data logger and environmental data were recorded every 10 s (Table 2). The data logger recorded means every 10 min throughout the duration of the experimental replications. Plants were irrigated as needed, every two or three days, through subsurface irrigation with deionized water supplemented by water-soluble fertilizer providing (in mg·L<sup>-1</sup>) 50 N, 19 P, 50 K, 23 Ca, 4 Mg, 1 Fe, 0.5 Mn, 0.5 Zn, 0.5 Cu, 0.3 B, and 0.1 Mo (MSU Plug Special; GreenCare Fertilizers, Inc., Kankakee, IL). The EC and pH of the nutrient solution was 0.43 mS·cm<sup>-1</sup> and 6.2, respectively. To prevent nutrient deficiency in geranium and chlorosis in petunia, the EC of the nutrient solution for geranium was increased to 0.92 mS·cm<sup>-1</sup> (16, 9, or 9 d after seed sow in rep 1, 2, or 3, respectively) and the pH of the nutrient solution for petunia was decreased to 5.5 (18 or 13 d after seed sow in rep 1 or 2, respectively).

Data collection for seedling growth

At the end of the seeding stage, 15 random plants (10 plants for seedling growth parameter measurement and 5 plants for Chl extraction and measurement) of each species in

each treatment, usually excluding outer guard rows, were harvested the following number of days after seed sow (rep 1, 2, 3): geranium (39, 36, 36), petunia (35, 33), and coleus (34, 30, 38). The harvest times were determined when the seedlings were ready for transplanting (when the roots had grown sufficiently so that the seedlings could be easily pushed out of the trays with the entire root zone intact) and varied presumably because of differences in vigor of seed lots. The following data were collected on 10 plants in each treatment: leaf (at node) number, total leaf area, SPAD index, plant height (from media level to apical meristem), and shoot, leaf, and root dry weight (DW). A visible leaf that was 25% or greater unfolded was counted in leaf number and included in leaf area and leaf DW measurement. Total leaf area per plant was measured using a leaf-area meter (LI-3000; LI-COR). Average individual leaf area was determined by dividing total leaf area by leaf number for each plant. SPAD index was measured using a portable Chl meter (SPAD-502; Minolta corporation, Ltd., Osaka, Japan) at the central point of the leaflet between the midrib and the leaf margin of the second or third fully expanded leaf from the base of the main stem. Three readings per leaf per plant were averaged to a single SPAD value for each plant. For DW measurement, after the shoot was excised from the rooting medium, the medium was carefully washed off to separate the roots. The separated leaves, remainder of the shoot, and roots were placed in separate envelopes and dried in an oven at  $\ge 66$  °C for  $\ge 5$  d and weighed using an analytical balance (AG245; Mettler Toledo, Columbus, OH). We also calculated leaf mass per area (LMA, leaf DW divided by total leaf area) for all three species.

Chl concentration was measured on 5 plants of each species in each treatment. For each plant, one leaf disc (0.75 cm<sup>2</sup>) was cut from the central point of the leaflet between the midrib and the leaf margin (avoiding the leaf margin and midrib) of the second or third fully expanded leaf from the base of the main stem. Each leaf disc was placed into a 2 mL-tube and stored in a

freezer at -69 °C. Leaf Chl concentrations were extracted in 95 % ethanol and measured on a UV-Vis spectrophotometer (GENESYS 10S; Thermo Fisher Scientific, Waltham, MA) according to procedures by Zhang and Sharkey (2009). Chl a and b concentrations were calculated from leaf absorbance at 649 and 665 nm using the following equations (Wellburn and Lichtenthaler, 1984): Chl a (mg·L<sup>-1</sup>) = 13.95  $A_{665}$  – 6.88  $A_{649}$ ; Chl b (mg·L<sup>-1</sup>) = 24.96  $A_{649}$  – 7.32  $A_{665}$ .

## Leaf photosynthesis measurements

Leaf gas exchange was measured on geranium and coleus during the second and third replications 35 d after seed sow (geranium, for both rep 2 and 3) and 29 or 37 d after seed sow (coleus, rep 2 or 3, respectively). The date for leaf photosynthesis measurement was determined when the second leaf from the base of the main stem was fully expanded. Measurements were made on 5 random plants of each species in each treatment using a portable photosynthesis system (LI 6400XT; LI-COR). To measure net CO<sub>2</sub> assimilation at growth irradiance, a 6 cm<sup>2</sup> clear chamber (6400-08 Clear Chamber; LI-COR) was clamped onto the second fully expanded leaf (from the base of the main stem) under the six radiation treatments. Because the leaf did not cover the entire leaf chamber opening (2 cm × 3 cm), the leaf area inside the chamber during a measurement was determined by taking a photograph and using software (https://sketchandcalc.com), and CO<sub>2</sub> assimilation values were recomputed using the corrected leaf area. The mean PPFD transmitted through the clear chamber, measured by the LI 6400 XT, was  $48 \pm 0 \,\mu\text{mol}\cdot\text{m}^{-2}\cdot\text{s}^{-1}$  for PPFD 96 treatments and  $115 \pm 1 \,\mu\text{mol}\cdot\text{m}^{-2}\cdot\text{s}^{-1}$  for the PPFD 288 treatments. In the measurement chamber, the reference CO<sub>2</sub> concentration was 500 µmol·mol<sup>-1</sup>, flow rate was 400 µmol·mol<sup>-1</sup>, and relative humidity was between 40% and 60%.

Growth conditions and data collection after transplant

At the end of the seedling stage, 10 seedlings were randomly selected and transplanted into 10-cm pots containing a 70% peatmoss, 21% perlite, and 9% vermiculite potting media (SUREMIX; Michigan Grower Products, Inc., Galesburg, MI). Pots were randomly placed on benches in a glass-glazed, environmentally controlled greenhouse at a constant temperature set point of 20 °C. Supplemental lighting provided by HPS lamps delivered a mean PPFD of 77  $\pm$  3  $\mu$ mol·m<sup>-2</sup>·s<sup>-1</sup> at plant height and a 16-h photoperiod. The HPS lamps were controlled by an environmental control computer and were automatically switched on from 0600 to 2200 HR when the ambient solar PPFD was <185  $\mu$ mol·m<sup>-2</sup>·s<sup>-1</sup> and off when it was >370  $\mu$ mol·m<sup>-2</sup>·s<sup>-1</sup>. The following data were collected when each plant flowered: date, flower bud or inflorescence number, and length of the primary stem.

# Statistical analysis

The experiment used a randomized complete block design: each replication was regarded as a block; each LED module was regarded as the experimental unit for the radiation treatment; and within each LED module, each individual seedling per species was the sub-sample or observational unit. Data were analyzed with SAS (version 9.4; SAS Institute, Inc., Cary, NC). The response of plant growth, photosynthesis, and flowering to PPE, PPFD, and their interaction were compared by analysis of variance (ANOVA) using SAS PROC MIXED procedure [with two fixed factors for PPFD and R:FR, two random factors of blocks (or replications) and interaction between blocks, PPFD, and R:FR]. Results from the full ANOVA analysis are in Table 2, 3 and 4. PPE effects on growth, photosynthesis, and flowering were modeled using linear regression for each PPFD level by SAS PROC REG. The mean for each replication was treated as a single data point. Simple linear regression analysis at each PPFD included nine data

points (3 replications  $\times$  3 different PPEs) for geranium and coleus or six data points (2 replications  $\times$  3 different PPEs) for petunia.

## **Results and Discussion**

Our objective was to carefully dissect the independent and interactive effects of PPE and PPFD on 14 growth parameters and subsequent flowering, without potentially confounding effects from changes in B photon flux density. We studied three species with different photoperiodic flowering responses and tolerances to shade in case diverging responses. Overall, there were significant main effects of both PPE and PPFD for many growth parameters, while PPE and PPFD interacted to influence only leaf number in petunia and geranium (Table 3). In at least two species, PPE and PPFD independently influenced individual leaf area, SPAD index, shoot DW, and plant DW; PPE affected stem elongation and total leaf area; and PPFD impacted leaf number, LMA, Chl *a+b*, leaf DW, and root DW.

Stem length

Stem elongation under canopy shade has been primarily attributed to the decrease in the R:FR, but studies have also attributed it to the decrease in PPFD. For example, internode length of white mustard ( $Sinapis\ alba$ ) increased when PPFD of  $\geq 1000\ \mu mol \cdot m^{-2} \cdot s^{-1}$  decreased by around 50% (Ballaré et al., 1991), and stem length of tobacco ( $Nicotiana\ tabacum$ ) increased when PPFD decreased from 120  $\mu mol \cdot m^{-2} \cdot s^{-1}$  to 30  $\mu mol \cdot m^{-2} \cdot s^{-1}$  (Pierik et al., 2004). In this study, when PPFD decreased from 288 to 96  $\mu mol \cdot m^{-2} \cdot s^{-1}$  by lowering R radiation (and keeping B photon flux density constant), stem elongation of all species decreased with estimated PPE under both PPFD level, but the decrease in PPFD only promoted stem elongation of petunia (Fig. 2 and Table 3).

The effects of decreased PPFD on stem elongation could be at least partly attributed to the decrease in B radiation (Ballaré et al., 1991; Pierik et al., 2004; Pierik and de Wit, 2014).

Numerous studies have reported a strong B-mediated suppression of stem elongation, including in arabidopsis (Keller et al., 2011); longstalk starwort (*Stellaria longipes*) (Sasidharan et al., 2008); impatiens (*Impatiens walleriana*), salvia (*Salvia splendens*), and petunia (Wollaeger and Runkle, 2015); and radish (*Raphanus sativus*) and soybean (*Glycine max*) (Cope and Bugbee, 2013). Considering the commonality of B radiation suppressing stem elongation, we attribute the lack of a stem-extension response to PPFD in geranium and coleus specifically to the constant B photon flux density in the two PPFDs delivered in this study. In contrast, in petunia, decreasing PPFD increased stem length independent of B photon flux density.

## Leaf characteristics

Regardless of PPE, decreasing PPFD increased individual leaf area and decreased leaf number in shade-avoiding petunia and geranium, resulting in similar total leaf areas at the two PPFDs (Fig. 2 and Table 3). In shade-tolerant coleus, decreasing PPFD did not influence leaf number and decreased individual and total leaf area. At both PPFDs, individual leaf area of petunia decreased linearly as the estimated PPE increased (Fig. 2). Similar trends only occurred in coleus at PPFD 96. Total leaf area of petunia at PPFD 288 and coleus at PPFD 96 also decreased linearly with increasing PPE, showing similar trends for individual leaf area. In geranium, there was little to no effect of PPE on individual leaf area and total leaf area (Fig. 2 and Table 3). In past studies, the promotive or inhibitive effect of FR radiation on leaf expansion was partly dependent on carbon supply or PPFD (Kozuka et al., 2005; Wiese et al., 2007; Pantin et al., 2011; Gong et al., 2014). A reduced R:FR usually increased leaf area when the PPFD was sufficient to support leaf growth, but when the PPFD was excessively low and carbon supply was

limited, there was minimal effect of the R:FR (Casal et al., 1987; Carabelli et al., 2007; Patel et al., 2013). For example, decreasing R:FR from 2.4 to 0.4 increased individual leaf area of white clover (*Trifolium repens*) under a PPFD of 320 μmol·m<sup>-2</sup>·s<sup>-1</sup> but not under 110 μmol·m<sup>-2</sup>·s<sup>-1</sup> (Heraut-Bron et al., 1999). In our study, a PPFD of 96 μmol·m<sup>-2</sup>·s<sup>-1</sup> was sufficiently high in at least petunia that individual leaves expanded in response to a decreasing R:FR and PPE.

Plants grown under low light generally produce larger and thinner leaves (creating a lower LMA), thereby optimizing light interception per unit of leaf biomass (Evans and Pooter, 2001; Walters, 2005). We observed this phenomenon in all species (Fig. 2 and Table 3). Several genetic studies have indicated that the PPFD-mediated regulation of leaf thickness occurs without the involvement of photoreceptors including phytochromes, cryptochromes, and phototropins (Ferjani et al., 2008). For example, leaf thickness of *phyB* arabidopsis mutants increased with an increase in PPFD (Kim et al., 2005). In addition, single and double mutants of cryptochromes (cry1 and cry2) and phototropins (phot1 and phot2) showed normal leaf thickness responses (Weston et al. 2000; Lopéz-Juez et al. 2007). This explains why a reduction in PPFD without changes in B photon flux density decreased LMA of the three species studied while minimally affecting photoreceptor-mediated stem elongation of geranium and coleus. *Chlorophyll* 

A decrease in leaf Chl concentration is another characteristic of the shade-avoidance response (Smith and Whitelam, 1997). In shade-avoiding species, including arabidopsis (Patel et al., 2013), papaya (*Carica papaya*) (Buisson and Lee, 1993), and sunflower (Rousseaux et al., 1996), plants grown under decreased R:FR ratios accumulated less Chl. The regulation of Chl accumulation is mediated in part by phytochromes (Briggs et al., 1988; Huq et al., 2004; Stephenson and Terry, 2008; Inagaki et al., 2015). A decreased R:FR ratio decreased Chl

synthesis (McCormac and Terry, 2002; Stephenson and Terry, 2008; Inagaki et al., 2015) and increased Chl degradation (Okada et al., 1992). In this study, decreasing PPE linearly decreased Chl concentration (per unit leaf area) in shade-avoiding petunia (SPAD index and Chl a+b) and geranium (SPAD index) under both PPFDs (Fig. 3 and Table 3).

In shade-tolerant coleus, there was no significant correlation between Chl concentration (SPAD value and Chl a+b) and the estimated PPE (Fig. 3 and Table 3). Instead, Chl a/b of coleus linearly decreased with a decreasing PPE at both PPFDs (Fig. 3). The decreased Chl a/b ratio indicates changes in the stoichiometry and antenna size of the two photosystems (Terashima and Inone, 1985; Murchie and Horton 1997; Pons and de Jong-van Berkel., 2004; Patel et al., 2013). A decrease in R:FR excites photosystem I (PSI) more than photosystem II (PSII), causing an imbalance between the two photosystems (Evans and Anderson, 1987; Hogewoning et al., 2012). Restoring the imbalanced excitation of the two photosystems under a low R:FR leads to a relative increase in PSII and decrease in PSI (Walters and Horton, 1994; Anderson et al., 1995). Chl b is mostly located in the light-harvesting antenna complexes of PS II and consequently, an increase in PSII:PSI under low R:FR increases Chl b and reduces the Chl a/b ratio (Anderson et al., 1995; Yamazaki et al., 2005; Wagner et al., 2008). In both shadeavoiding and shade-tolerant species, a reduced R:FR ratio decreased the Chl a/b ratio (Pons and de Jong-van Berkel., 2004; Gommers et al., 2013). Our results show that in shade-tolerant coleus, decreasing R:FR reduced Chl a/b while in shade-avoiding petunia and geranium, decreasing R:FR primarily decreased leaf Chl concentration.

Independent of PPE, the decrease in PPFD increased Chl concentration in all species (Chl *a*+*b* in petunia and coleus and SPAD index in geranium) (Fig. 3 and Table 3). Similarly, a decrease in PPFD increased leaf chlorophyll concentration (per unit leaf area or unit mass) in

rhododendron (*Rhododendron*× 'Pink Ruffles') (Andersen et al., 1991), mountain laurel (*Kalmia* latifolia) (Brand, 1997), and petunia (Wollaeger and Runkle, 2013). Plants acclimate to different light intensities by adjusting the size of the light-harvesting chlorophyll protein complexes (LHCs), which contain Chl a and Chl b (Chow et al., 1990). In general, plants grown under lower light had a bigger LHC antenna and accumulated more chlorophylls compared to the plants grown under higher light (Bjorkman et al., 1972; Leong and Anderson, 1984). Increases in LHCs antenna size and chlorophyll content under a low light provided an efficient light harvesting capacity (Lei et al., 1996; Lei and Lechowicz, 1997). Light intensity regulation of LHCs is mainly mediated by the reduced state of the plastoquinone pool, which increases with increasing PPFD (Escoubas et al., 1995; Yang et al., 2001; Frigerio et al., 2007). In addition, a higher PPFD decreased LHC in cry1, cry2, and cry1/cry2 double mutants of arabidopsis (Weston et al. 2000). The increase in chlorophyll concentration with decreasing PPFD in our study is therefore likely regulated photosynthetically, not necessarily with the involvement of changes in B photon flux density. These results suggest that independent of PPE, the reduced PPFD increased chlorophyll concentrations, enabling plants to acclimate to the given light quantity. Dry weight and photosynthesis

Decreasing PPE linearly increased shoot DW in petunia and coleus at both PPFDs (Fig. 4 and Table 3). In contrast, PPE had a minimal effect on root DW of all species except for geranium at PPFD 96. Therefore, plant (shoot + root) DW showed a similar inverse linear relationship with the estimated PPE as the shoot DW (data not shown). In plant growth analysis, plant DW accumulation is determined by total leaf area and net assimilation (Vernon and Allison, 1963; Bugbee, 2016; Snowden et al., 2016). Net assimilation can be calculated as the ratio of plant DW to total leaf area. In addition to single-leaf photosynthetic rate, net assimilation has

been used to quantify whole-plant photosynthesis or photosynthetic efficiency (Bugbee, 2016). YPFD estimates (integrates) the relative quantum efficiency of photons from 300 to 800 nm and therefore is considered a more accurate estimate of the net radiation driving photosynthesis than PPFD when light quality is varied (Sager et al., 1988). In this study, increasing FR radiation increased YPFD by 13% at each PPFD, but the increased YPFD at each PPFD had little to no effect on whole-plant net assimilation in any species, or on net  $CO_2$  assimilation rate ( $A_n$ ) in geranium and coleus (Table 4). Only increasing PPFD increased whole-plant net assimilation in petunia and coleus and  $A_n$  in geranium. These results indicate that the additional FR had little influence on short- and long-term photosynthetic efficiency and thus, the promotive effects of FR on DW accumulation can be primarily attributed to an increase in leaf area. In petunia, shoot DW increased linearly with total leaf area at both PPFDs (data not shown).

# Subsequent flowering responses

The radiation treatments during the seedling stage minimally affected plant height at flowering of petunia and geranium (Table 5) or subsequent plant height of coleus (data not shown). The inclusion of FR radiation in the 18-h photoperiod during the seedling stage promoted subsequent flowering of the long-day petunia under both PPFDs when PPE was ≤0.78 (Table 5). Flowering of long-day plants was promoted under similar PPE values of sole-source lighting during the seedling stage (0.65-0.85) (Park and Runkle, 2017) and of photoperiodic lighting during the finishing stage (0.63-0.80) (Craig and Runkle, 2016). Phytochromes are involved in the perception of photoperiod and an intermediate R:FR or PPE accelerated flowering in some long-day plants (Sullivan and Deng, 2003; Craig and Runkle, 2016). In arabidopsis (a long-day plant), early flowering induced by a low R:FR was mediated by the

photoperiod-signaling pathway, indicating that similar mechanisms regulate shade-avoidance and photoperiodic flowering responses (Wollenberg et al., 2008).

In addition to R:FR or PPE, PPFD can also regulate flowering time (Levy and Dean, 1998; Castro Marín et al., 2011; Feng et al., 2016). Several studies showed increasing daily light integral (DLI) during the seedling stage of some ornamental species accelerated subsequent flowering, regardless of photoperiodic response (Pramuk and Runkle, 2005; Lopez and Runkle, 2008). For example, as mean DLI during the seedling stage increased from 4.1 to 14.2 mol·m<sup>-2</sup>·d<sup>-1</sup>, flowering occurred 4-12 d earlier in French marigold (*Tagetes patula*), celosia (*Celosia argentea*), impatiens (*Impatiens walleriana*), and pansy (Pramuk and Runkle, 2005). Similarly, in our study, increasing PPFD from 96 to 288 μmol·m<sup>-2</sup>·s<sup>-1</sup> increased DLI from 6.2 to 18.7 mol·m<sup>-2</sup>·d<sup>-1</sup>, which decreased flowering time in petunia and geranium by 2-8 d and 4-9 d, respectively, depending on the PPE (Table 5). In long-day petunia, the promotion of flowering from a decrease in PPE was greater under PPFD 96 (by 11 d) than under PPFD 288 (by 7 d). The late flowering of petunia under PPFD 96 without FR radiation was accompanied by an increase in number of flower buds.

In the day-neutral geranium, the addition of FR radiation during the seedling stage did not promote flowering (Table 5; Park and Runkle, 2017). However, the combination of FR radiation (PPE  $\leq$ 0.78) and the higher PPFD accelerated flowering of geranium more than plants grown under the lower PPFD when the PPE  $\geq$ 0.77. Compared to long-day plants (such as arabidopsis) and short-day plants [such as rice (*Oryza sativa*)], the underlying mechanisms of flowering of day-neutral plants [such as tomato (*Solanum lycopersicum*)] and the functions of phytochromes in flowering control are not well understood (Mizoguchi et al., 2007; Cao et al., 2016). However, in day-neutral maize (*Zea mays*), a loss of PHYB function accelerated

flowering under both long and short days (Sheehan et al., 2007). Similarly, in tomato 'Micro-Tom' (MT), the phytochrome deficient *aurea* mutant flowered one week earlier compared to the wild type, suggesting the involvement of phytochromes in flowering control (Carvalho et al., 2011). Considering the addition of FR radiation specifically promoted flowering under the higher PPFD in our study, and that flowering is determined by the cumulative effects of multiple external and internal signals (Wollenberg et al., 2008), it is possible that a low R:FR and the higher PPFD synergistically promoted flowering in geranium.

In conclusion, when B photon flux density is kept constant, the addition of FR radiation (or decreasing PPE) increased stem length, leaf area, and shoot dry weight of ornamental seedlings independently of PPFD. The addition of FR had little influence on instantaneous leaf photosynthesis and long-term whole-plant photosynthesis, and the promotive effects of FR on dry mass accumulation were primarily attributed to an increase in leaf area. Increasing PPFD without changes in B radiation decreased chlorophyll concentration, increased LMA, net CO<sub>2</sub> assimilation, whole-plant net assimilation, and dry weight independently of PPE. However, in the long-day plant petunia, the effects of decreasing PPE during seedling stage on accelerating subsequent flowering were greater under the lower PPFD.

# **APPENDIX**

Table II-1. Spectral characteristics of six sole-source lighting treatments. The values after each LED type (B=blue; R=red; FR=far red) indicate their photon flux density in  $\mu$ mol·m<sup>-2</sup>·s<sup>-1</sup>.

| ·jp · (_ · · · · · · · · · · · |                   | <i>)</i> | P          |                   |           |
|--------------------------------|-------------------|----------|------------|-------------------|-----------|
| Radiation treatment            | PPFD <sup>a</sup> | $TPFD^b$ | $YPFD^{c}$ | R:FR <sup>d</sup> | $PPE^{e}$ |
| $B_{32}+R_{64}$                | 96                | 96       | 84         | 1:0               | 0.87      |
| $B_{32}+R_{64}+FR_{32}$        | 96                | 128      | 89         | 2:1               | 0.77      |
| $B_{32}+R_{64}+FR_{64}$        | 96                | 160      | 95         | 1:1               | 0.70      |
| $B_{32}+R_{256}$               | 288               | 288      | 262        | 1:0               | 0.88      |
| $B_{32}+R_{256}+FR_{128}$      | 288               | 416      | 282        | 2:1               | 0.78      |
| $B_{32}+R_{256}+FR_{256}$      | 288               | 576      | 297        | 1:1               | 0.70      |

<sup>&</sup>lt;sup>a</sup>PPFD: Photosynthetic photon flux density (photon flux integral from 400 to 700 nm, in μmol·m<sup>-2</sup>·s<sup>-1</sup>).

<sup>&</sup>lt;sup>b</sup>TPFD: Total photon flux density (photon flux integral from 400 to 800 nm, in µmol·m<sup>-2</sup>·s<sup>-1</sup>).

<sup>&</sup>lt;sup>c</sup>YPFD: Yield photon flux density, which is the product of TPFD and relative quantum efficiency (in μmol·m<sup>-2</sup>·s<sup>-1</sup>) based on McCree (1972) and Sager et al. (1988).

<sup>&</sup>lt;sup>d</sup>R:FR: Ratio of photon flux integral of R (600-700 nm) and FR (700-800 nm) radiation.

<sup>&</sup>lt;sup>e</sup>PPE: Phytochrome photoequilibria following Sager et al. (1988).

Table II-2. Actual mean air temperatures (°C, measured by thermocouples) and canopy temperatures (°C, measured by infrared sensors) during experimental replications. All means had a standard error  $\pm 0.1$  °C.

| Radiation treatment -     | Replication 1 |        | Replication 2 |        | Replication 3 |        |
|---------------------------|---------------|--------|---------------|--------|---------------|--------|
| Radiation treatment       | Air           | Canopy | Air           | Canopy | Air           | Canopy |
| $B_{32}+R_{64}$           | 20.4          | 20.7   | 20.1          | 20.3   | 20.2          | 20.0   |
| $B_{32}+R_{64}+FR_{32}$   | 20.7          | 20.7   | 20.7          | 20.9   | 20.3          | 20.3   |
| $B_{32}+R_{64}+FR_{64}$   | 20.8          | 20.7   | 20.5          | 20.4   | 20.8          | 20.3   |
| $B_{32}+R_{256}$          | 21.1          | 21.4   | 21.2          | 21.2   | 21.3          | 21.7   |
| $B_{32}+R_{256}+FR_{128}$ | 21.4          | 21.7   | 21.4          | 22.0   | 21.2          | 21.5   |
| $B_{32}+R_{256}+FR_{256}$ | 22.0          | 22.9   | 21.8          | 21.6   | 21.6          | 21.8   |

Table II-3. Analysis of variance for the effects of the estimated phytochrome photoequilibria (PPE), photosynthetic photon flux density (PPFD), or their interaction of sole-source lighting treatments on plant growth parameters of petunia, geranium, and coleus.

|                      |                  | Petunia |              |     | Geranium |              |     | Coleus |              |
|----------------------|------------------|---------|--------------|-----|----------|--------------|-----|--------|--------------|
| Factor               | PPE              | PPFD    | PPE×<br>PPFD | PPE | PPFD     | PPE×<br>PPFD | PPE | PPFD   | PPE×<br>PPFD |
| Stem length          | *** <sup>a</sup> | *       | NS           | *** | NS       | NS           | *** | NS     | NS           |
| Individual leaf area | *                | **      | NS           | NS  | *        | NS           | *   | **     | NS           |
| Leaf number          | NS               | ***     | *            | *   | ***      | *            | NS  | NS     | NS           |
| Total leaf area      | *                | NS      | NS           | NS  | NS       | NS           | *   | **     | NS           |
| Leaf mass per area   | *                | ***     | NS           | NS  | *        | NS           | NS  | ***    | NS           |
| SPAD index           | ***              | **      | NS           | *** | *        | NS           | NS  | NS     | NS           |
| Chlorophyll a+b      | **               | **      | NS           | NS  | NS       | NS           | NS  | ***    | NS           |
| Chlorophyll a/b      | NS               | NS      | NS           | NS  | NS       | NS           | NS  | NS     | NS           |
| Leaf dry weight (DW) | NS               | ***     | NS           | NS  | NS       | NS           | *   | ***    | NS           |
| Shoot DW             | *                | ***     | NS           | NS  | NS       | NS           | **  | ***    | NS           |
| Root DW              | NS               | ***     | NS           | NS  | ***      | NS           | NS  | ***    | NS           |
| Plant DW             | *                | ***     | NS           | NS  | NS       | NS           | **  | ***    | NS           |
| Shoot DW:root DW     | NS               | **      | NS           | NS  | NS       | NS           | NS  | NS     | NS           |

<sup>&</sup>lt;sup>a</sup>NS, \*, \*\*, or \*\*\* Nonsignificant or significant at P < 0.05, 0.01, or 0.001, respectively.

Table II-4. Influence of the estimated phytochrome photoequilibria (PPE), photosynthetic photon flux density (PPFD), or their interaction of sole-source lighting treatments on net assimilation (shoot DW per unit leaf area) and net  $CO_2$  assimilation rate ( $A_n$ ) of seedlings. The values after each LED type (B=blue; R=red; FR=far red) indicate their photon flux density in  $\mu$ mol·m<sup>-2</sup>·s<sup>-1</sup>. Data represent the means of two replications with 10 subsamples (plants) for net assimilation and 5 subsamples for  $A_n$  per replication and species.

| Radiation treatment                                  | Net assimilation (g⋅m <sup>-2</sup> ) | $A_{\rm n}$ (µmol ${ m CO_2 \cdot m^{-2} \cdot s^{-1}}$ ) |  |  |
|--|---------------------------------------|---|--|--|
|  | Petunia                               | 7   |  |  |
| $B_{32}+R_{64}$                                      | 21.5 b <sup>a</sup>                   | _b  |  |  |
| $B_{32}+R_{64}+FR_{32}$                              | 22.1 b                                | -   |  |  |
| B <sub>32</sub> +R <sub>64</sub> +FR <sub>64</sub>   | 22.5 b                                | -   |  |  |
| $B_{32}+R_{256}$                                     | 55.5 a                                | -   |  |  |
| $B_{32}+R_{256}+FR_{128}$                            | 54.2 a                                | -   |  |  |
| B <sub>32</sub> +R <sub>256</sub> +FR <sub>256</sub> | 51.9 a                                | -   |  |  |
| Significance   |                                       |   |  |  |
| PPE  | $NS^c$                                | -   |  |  |
| PPFD   | ***                                   | -   |  |  |
| PPE×PPFD   | NS                                    | -   |  |  |
|  | Geranium                              |   |  |  |
| $B_{32}+R_{64}$                                      | 50.6 a                                | 1.5 b   |  |  |
| $B_{32}+R_{64}+FR_{32}$                              | 51.9 a                                | 2.0 b   |  |  |
| $B_{32}+R_{64}+FR_{64}$                              | 53.6 a                                | 2.2 b   |  |  |
| $B_{32}+R_{256}$                                     | 71.8 a                                | 3.1 a   |  |  |
| $B_{32}+R_{256}+FR_{128}$                            | 83.0 a                                | 3.0 a   |  |  |
| $B_{32}+R_{256}+FR_{256}$                            | 84.9 a                                | 3.3 a   |  |  |
| Significance   |                                       |   |  |  |
| PPE  | NS                                    | NS  |  |  |
| PPFD   | *                                     | ***   |  |  |
| PPE×PPFD   | NS                                    | NS  |  |  |
|  | Coleus                                |   |  |  |
| $B_{32}+R_{64}$                                      | 26.1 b                                | 1.9 a   |  |  |
| $B_{32}+R_{64}+FR_{32}$                              | 25.9 b                                | 2.3 a   |  |  |
| B <sub>32</sub> +R <sub>64</sub> +FR <sub>64</sub>   | 26.7 b                                | 2.2 a   |  |  |
| $B_{32}+R_{256}$                                     | 52.8 a                                | 3.5 a   |  |  |
| $B_{32}+R_{256}+FR_{128}$                            | 52.6 a                                | 4.3 a   |  |  |
| B <sub>32</sub> +R <sub>256</sub> +FR <sub>256</sub> | 49.7 a                                | 4.8 a   |  |  |
| Significance   |                                       |   |  |  |
| PPE  | NS                                    | NS  |  |  |
| PPFD   | ***                                   | *   |  |  |
| PPE×PPFD   | NS                                    | NS  |  |  |

<sup>&</sup>lt;sup>a</sup>Means with different letters are significantly different by Tukey's honestly significant difference test (P < 0.05).

b-, not determined.

 $<sup>^{</sup>c}NS$ , \*, \*\*, or \*\*\* Nonsignificant or significant at P < 0.05, 0.01, or 0.001, respectively.

Table II-5. Influence of the estimated phytochrome photoequilibria (PPE), photosynthetic photon flux density (PPFD), or their interaction of sole-source lighting treatments on subsequent flowering characteristics of seedlings at finishing stage. The values after each LED type (B=blue; R=red; FR=far red) indicate their photon flux density in  $\mu$ mol·m<sup>-2</sup>·s<sup>-1</sup>. Data represent the mean of two replications for petunia and three replications for geranium with 10 subsamples (plants) per replication per species.

| Radiation treatment       | Dave to flower      | Flower bud or     | Plant height at flowering |  |  |  |  |
|---------------------------|---------------------|-------------------|---------------------------|--|--|--|--|
| Kadiation deathlent       | Days to flower      | inflorescence no. |                           |  |  |  |  |
| Petunia                   |                     |                   |                           |  |  |  |  |
| $B_{32}+R_{64}$           | $26.5 a^a$ $24.4 a$ |                   | 9.2 a                     |  |  |  |  |
| $B_{32}+R_{64}+FR_{32}$   | 16.3 c              | 4.9 b             | 7.3 ab                    |  |  |  |  |
| $B_{32}+R_{64}+FR_{64}$   | 15.7 c              | 3.6 b             | 8.5 ab                    |  |  |  |  |
| $B_{32}+R_{256}$          | 18.9 b              | 5.5 b             | 6.7 ab                    |  |  |  |  |
| $B_{32}+R_{256}+FR_{128}$ | 13.9 cd             | 3.2 b             | 5.6 b                     |  |  |  |  |
| $B_{32}+R_{256}+FR_{256}$ | 11.8 d              | 3.0 b             | 6.8 ab                    |  |  |  |  |
| Significance              |                     |                   |                           |  |  |  |  |
| PPE                       | ***b                | ***               | NS                        |  |  |  |  |
| PPFD                      | ***                 | **                | **                        |  |  |  |  |
| PPE×PPFD                  | **                  | **                | NS                        |  |  |  |  |
| Geranium                  |                     |                   |                           |  |  |  |  |
| $B_{32}+R_{64}$           | 44.2 a              | 3.6               | 17.8 a                    |  |  |  |  |
| $B_{32}+R_{64}+FR_{32}$   | 43.7 a              | 3.6               | 17.8 a                    |  |  |  |  |
| $B_{32}+R_{64}+FR_{64}$   | 41.3 ab             | 3.8               | 17.6 a                    |  |  |  |  |
| $B_{32}+R_{256}$          | 40.6 ab             | 3.6               | 17.7 a                    |  |  |  |  |
| $B_{32}+R_{256}+FR_{128}$ | 35.1 b              | 3.6               | 16.0 a                    |  |  |  |  |
| $B_{32}+R_{256}+FR_{256}$ | 34.3 b              | 3.6               | 15.3 a                    |  |  |  |  |
| Significance              |                     |                   |                           |  |  |  |  |
| PPE                       | *                   | NS                | NS                        |  |  |  |  |
| PPFD                      | ***                 | NS                | *                         |  |  |  |  |
| PPE×PPFD                  | NS                  | NS                | NS                        |  |  |  |  |

<sup>&</sup>lt;sup>a</sup>Means with different letters are significantly different by Tukey's honestly significant difference test (P < 0.05).

<sup>&</sup>lt;sup>b</sup>NS, \*, \*\*, or \*\*\* Nonsignificant or significant at P < 0.05, 0.01, or 0.001, respectively.

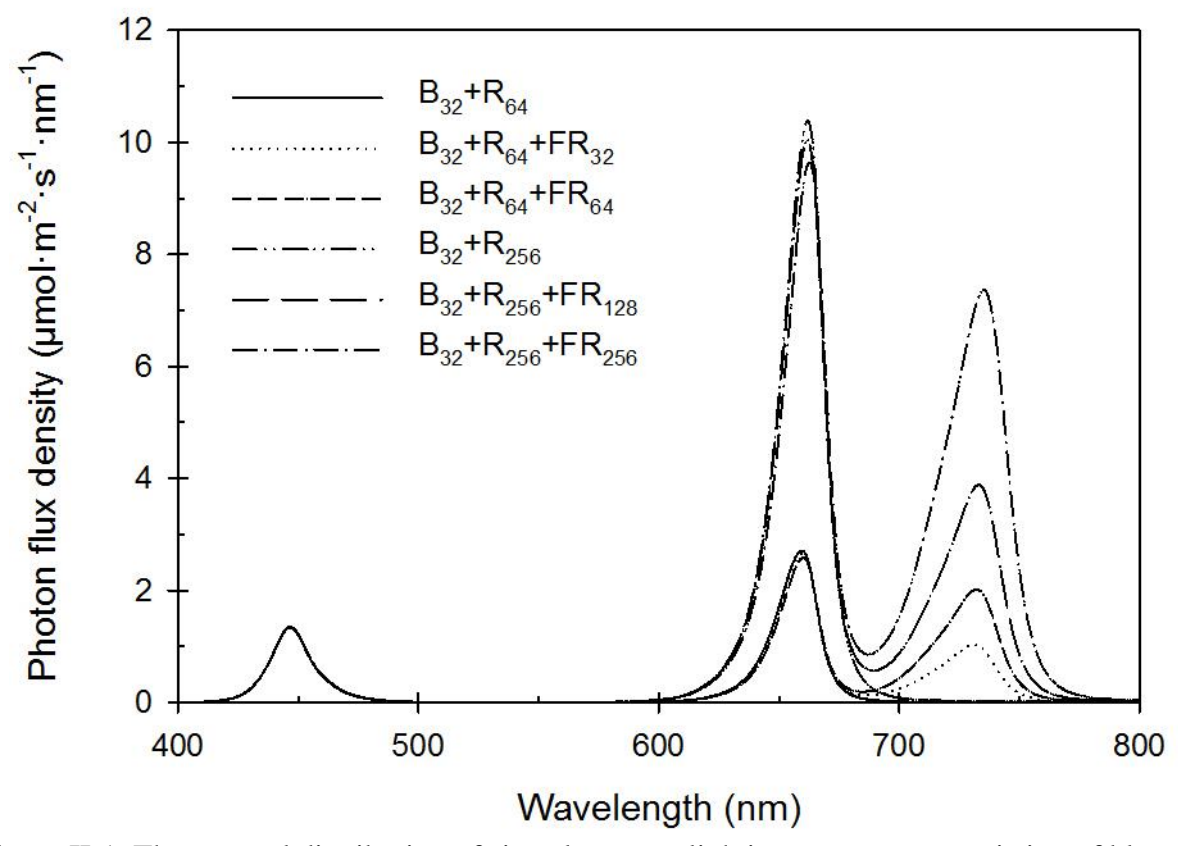


Figure II-1. The spectral distribution of six sole-source lighting treatments consisting of blue (B, 400-500 nm), red (R, 600-700 nm), and far-red (FR, 700-800 nm) radiation delivered by light-emitting diodes. The value after each waveband indicate its photon flux density in  $\mu$ mol·m<sup>-2</sup>·s<sup>-1</sup>.

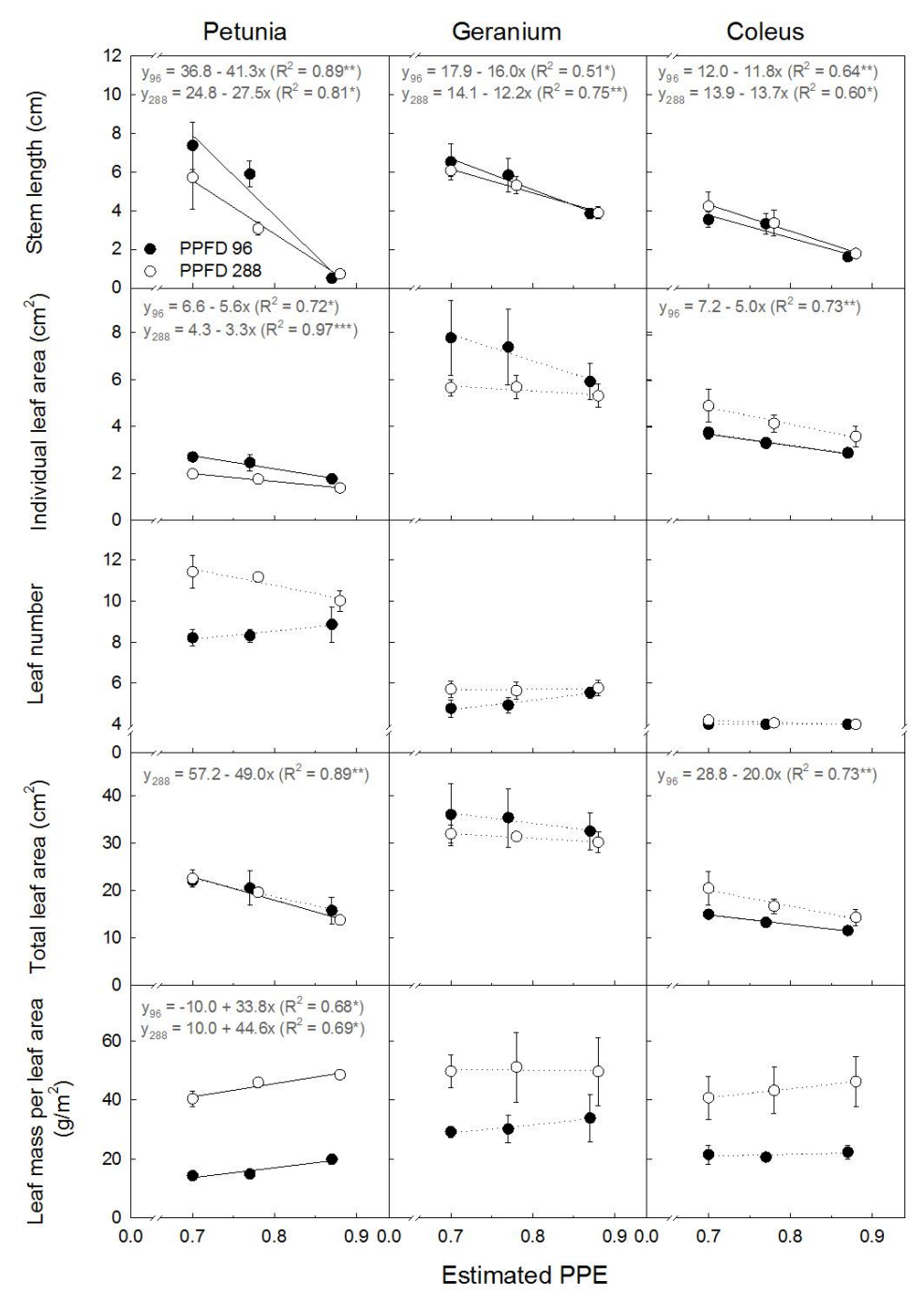


Figure II-2. Influence of the estimated phytochrome photoequilibria (PPE) of sole-source lighting treatments on stem length and leaf characteristics of seedlings grown under a photosynthetic photon flux density (PPFD) of 96 or 288  $\mu$ mol·m<sup>-2</sup>·s<sup>-1</sup>. Each data point represents the mean and standard error of two replications for petunia and three replications for geranium and coleus with 10 subsamples (plants) per replication per species. Associated correlation coefficients (R<sup>2</sup>) and regression equations are presented when statistically significant (solid line) but not when not significant (dotted line). \*, \*\*, or \*\*\* indicate significant at P < 0.05, 0.01, or 0.001, respectively.

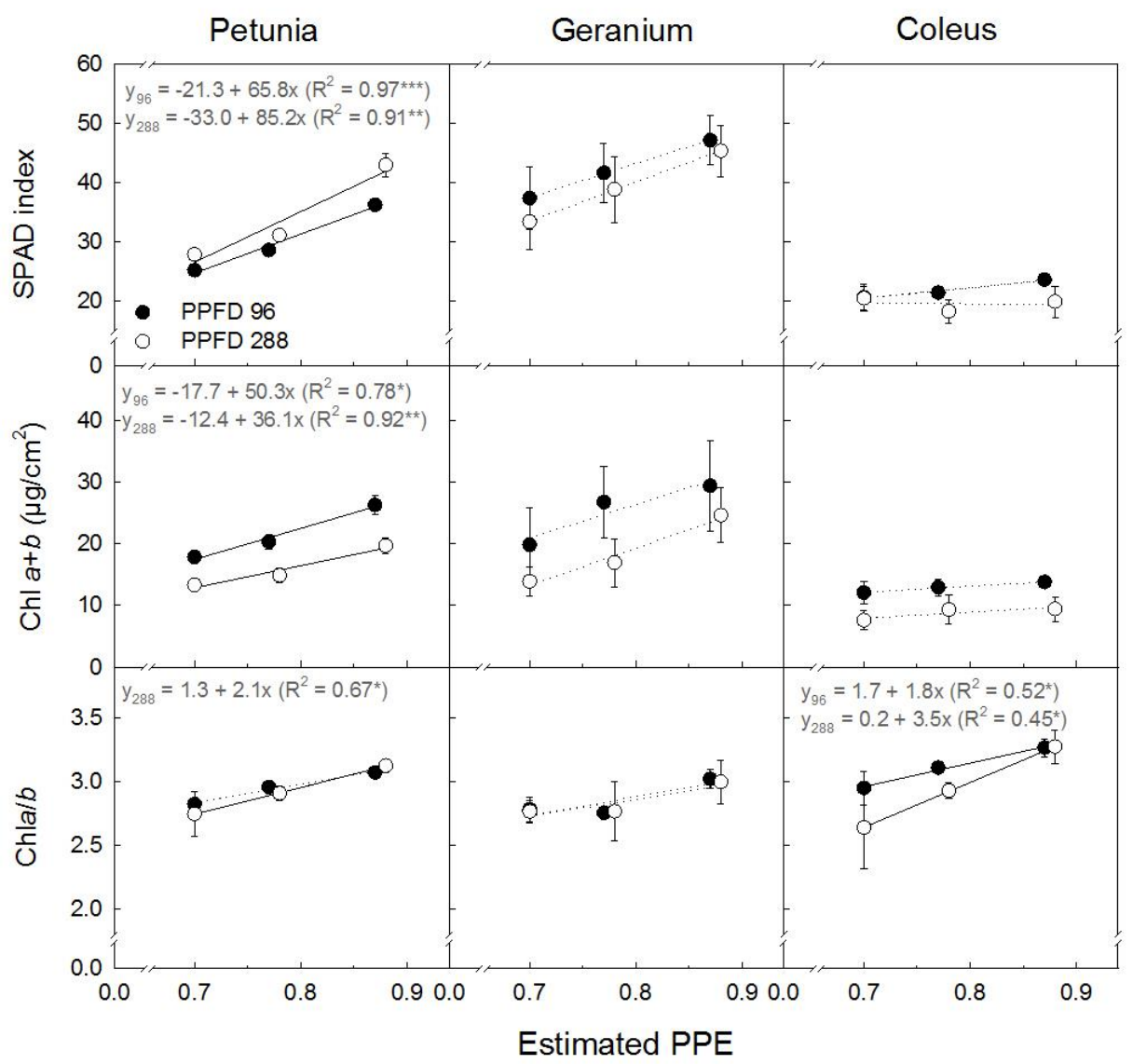


Figure II-3. Influence of the estimated phytochrome photoequilibria (PPE) of sole-source lighting treatments on SPAD index, leaf chlorophyll (Chl) a+b, and Chl a/b of seedlings grown under a photosynthetic photon flux density (PPFD) of 96 or 288  $\mu$ mol·m<sup>-2</sup>·s<sup>-1</sup>. Each data point represents the mean and standard error of two replications for petunia and three replications for geranium and coleus with 10 subsamples (plants) per replication per species for SPAD index and 5 subsamples per replication per species for Chl a+b and Chl a/b. Associated correlation coefficients (R<sup>2</sup>) and regression equations are presented when statistically significant (solid line) but not when not significant (dotted line). \*, \*\*, or \*\*\* indicate significant at P < 0.05, 0.01, or 0.001, respectively.

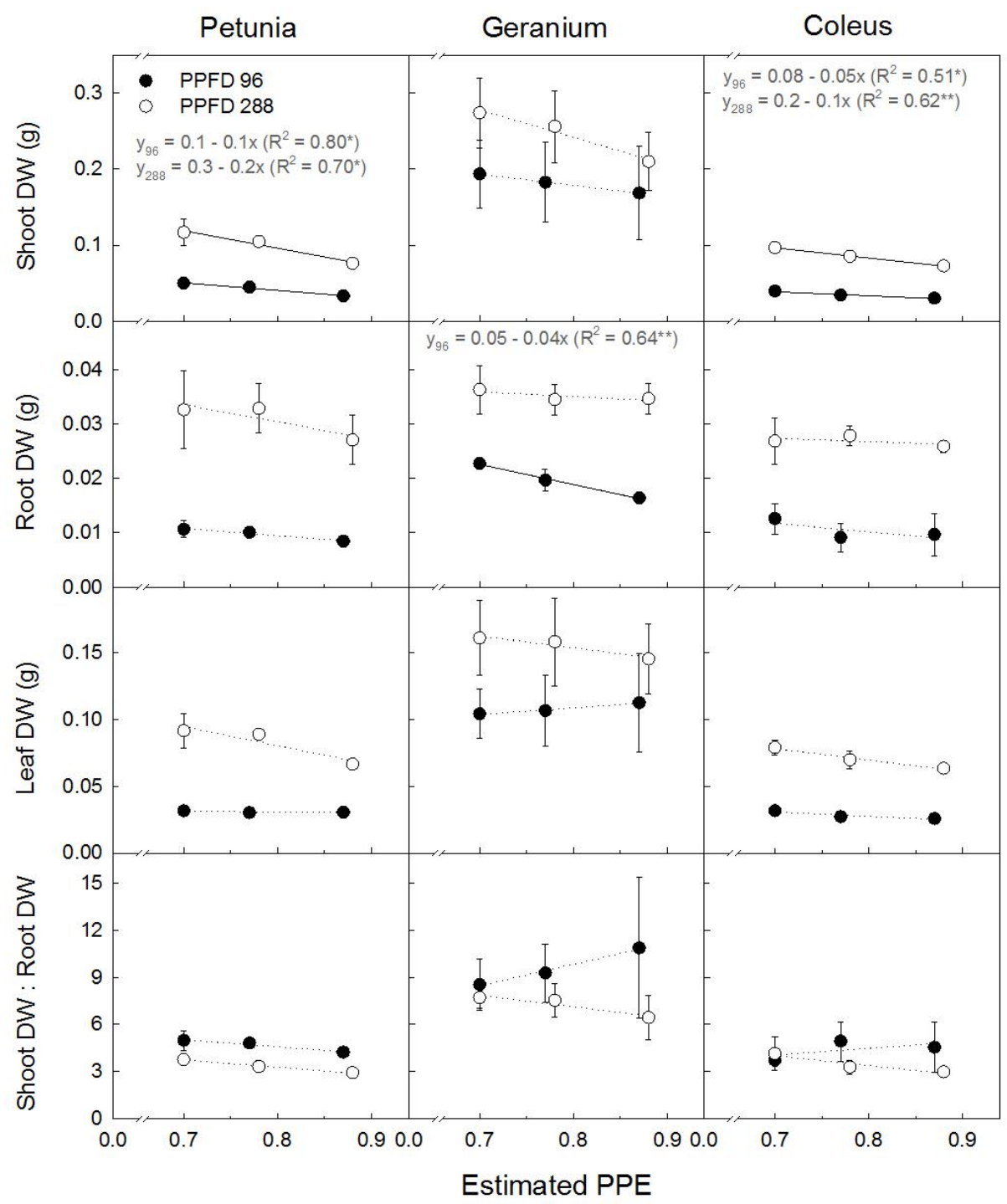


Figure II-4. Influence of the estimated phytochrome photoequilibria (PPE) of sole-source lighting treatments on dry weights of seedlings grown under a photosynthetic photon flux density (PPFD) of 96 or 288  $\mu$ mol·m<sup>-2</sup>·s<sup>-1</sup>. Each data point represents the mean and standard error of two replications for petunia and three replications for geranium and coleus with 10 subsamples (plants) per replication per species. Associated correlation coefficients (R<sup>2</sup>) and regression equations are presented when statistically significant (solid line) but not when not significant (dotted line). \* or \*\* indicate significant at P < 0.05 or 0.01, respectively.

LITERATURE CITED

#### LITERATURE CITED

- Anderson, J.M., W.S. Chow, and Y.I. Park. 1995. The grand design of photosynthesis: acclimation of the photosynthetic apparatus to environmental cues. Photosynth. Res. 46:129–139.
- Ballaré, C.L., R.A. Sanchez, A.L. Scopel, J.J. Casal, and C.M. Ghersa. 1987. Early detection of neighbour plants by phytochrome perception of spectral changes in reflected sunlight. Plant Cell Environ. 10:551–557.
- Ballaré, C.L., A.L. Scopel, and R.A. Sánchez. 1991. Photocontrol of stem elongation in plant neighbourhoods: effects of photon fluence rate under natural conditions of radiation. Plant Cell Environ. 14:57–65.
- Briggs, W.R., E. Mosinger, and E. Shafer. 1988. Phytochrome regulation of greening in barley-effects on chlorophyll accumulation. Plant Physiol. 86:435–440.
- Bugbee, B. 2016. Toward an optimal spectral quality for plant growth and development: The importance of radiation capture. Acta Hortic. 1134:1–12.
- Buisson, D. and D.W. Lee. 1993. The development responses of papaya leaves to simulated canopy shade. Amer. J. Bot. 80:947–952.
- Cao, K, L. Cui, X. Zhou, L. Ye, Z. Zou, and S. Deng. 2016. Four tomato FLOWERING LOCUS T-like proteins act antagonistically to regulate floral initiation. Front. Plant Sci. 6:1213.
- Carabelli, M., M. Possenti, G. Sessa, A. Ciolfi, M. Sassi, G. Morelli, and I. Ruberti. 2007. Canopy shade causes a rapid and transient arrest in leaf development through auxininduced cytokinin oxidase activity. Genes Dev. 21:1863–1868.
- Carvalho, R.F., M.L. Campos, L.E. Pino, S.L. Crestana, A. Zsögön, J.E. Lima, V.A. Benedito, and L.E. Peres. 2011. Convergence of developmental mutants into a single tomato model system: 'Micro-Tom' as an effective toolkit for plant development research. Plant Methods 7:18.
- Casal, J.J. 2012. Shade avoidance. The Arabidopsis Book 10:e0157.
- Casal, J.J. 2013. Photoreceptor signaling networks in plant responses to shade. Annu. Rev. Plant Biol. 64:403–27.
- Casal, J.J., P.J. Aphalo, and R.A. Sanchez. 1987. Phytochrome effects on leaf growth and chlorophyll content in *Petunia axillaris*. Plant Cell Environ. 10:509–514.

- Castro Marín, I., I. Loef, L. Bartetzko, I. Searle, G. Coupland, M. Stitt, and D. Osuna. 2011. Nitrate regulates floral induction in *Arabidopsis*, acting independently of light, gibberellin and autonomous pathways. Planta 233:539–552.
- Cope, K.R. and B. Bugbee. 2013. Spectral effects of three types of white light-emitting diodes on plant growth and development: absolute versus relative amounts of blue light. HortScience 48:504–509.
- Craig, D.S. and E.S. Runkle. 2016. An intermediate phytochrome photoequilibria from night-interruption lighting optimally promotes flowering of several long-day plants. Environ. Exp. Bot. 121:132–138.
- Djakovic-Petrovic T, M. de Wit, L.A.C.J. Voesenek, and R. Pierik. 2007. DELLA protein regulation in growth responses to canopy signals. Plant J. 51:117–126.
- Dougher T.A. and B. Bugbee. 2001. Evidence for yellow light suppression of lettuce growth. Photochem. Photobiol. 73:208–212.
- Erwin, J., N. Mattson, and R. Warner. 2017. Light effects on bedding plants. In: Lopez, R. and E.S. Runkle. (eds.) Light management in controlled environments. Meister Media Worldwide, Willoughby, OH, pp.119–134.
- Evans, J.R. and J.M. Anderson. 1987. Absolute absorption and relative fluorescence excitation spectra of the 5 major chlorophyll protein complexes from spinach thylakoid membranes. Biochim. Biophys. Acta 892:75–82.
- Evans J.R. and H. Poorter. 2001. Photosynthetic acclimation of plants to growth irradiance: the relative importance of specific leaf area and nitrogen partitioning in maximizing carbon gain. Plant Cell Environ. 24:755–761.
- Feng, P., H. Guo, W. Chi, X. Chai, X. Sun, X. Xu, J. Ma, J.D. Rochaix, D. Leister, H. Wang, C. Lu, and L. Zhang. 2016. Chloroplast retrograde signal regulates flowering. Proc. Natl. Acad. Sci. 113:10708–10713.
- Ferjani, A., S. Yano, G. Horiguchi, and H. Tsukaya. 2008. Control of leaf morphogenesis by long- and short-distance signaling: differentiation of leaves into sun or shade types and compensated cell enlargement. In Bögre, L. and G. Beemster (eds.) Plant Growth Signaling. Springer, Berlin, Heidelberg, pp. 47–62.
- Franklin K.A. 2008. Shade avoidance. New Phytol. 179:930–944.
- Franklin, K.A. and P.H. Quail. 2010. Phytochrome functions in *Arabidopsis* development. J. Exp. Bot. 61:11–24.
- Gommers, C.M.M., E.J.W., Visser, K.R. St Onge, L.A.C.J. Voesenek, and R. Pierik. 2013. Shade tolerance: when growing tall is not an option. Trends Plant Sci.18:65–71.

- Gong, W., P. Qi, J. Du, X. Sun, X. Wu, C. Song, W. Liu, Y. Wu, X. Yu, T. Young, X. Wang, F. Yang, Y. Yan, and W. Yang. 2014. Transcriptome analysis of shade-induced inhibition on leaf size in relay intercropped soybean. PLoS ONE 9:e98465.
- Heraut-Bron, V., C. Robin, C. Varlet-Grancher, D. Afif, and A. Guckert. 1999. Light quality (red:far-red ratio): does it affect photosynthetic activity, net CO<sub>2</sub> assimilation, and morphology of young white clover leaves? Can. J. Bot. 77:1425–1431.
- Hogewoning, S.W., E. Wientjes, P. Douwstra, G. Trouwborst, W. van Ieperen, R. Croce, and J. Harbinson. 2012. Photosynthetic quantum yield dynamics: from photosystems to leaves. Plant Cell 24:1921–1935.
- Huq, E., B. Al-Sady, M. Hudson, C. Kim, K. Apel, and P.H. Quail. 2004. Phytochrome-interacting factor 1 is a critical bHLH regulator of chlorophyll biosynthesis. Science 305:1937–1941.
- Inagaki, N., K. Kinoshita, T. Kagawa, A. Tanaka, O. Ueno, H. Shimada, and M. Takano. 2015. Phytochrome B mediates the regulation of chlorophyll biosynthesis through transcriptional regulation of ChlH and GUN4 in rice seedlings. PLoS One 10:e0135408.
- Jang, I.C., R.Henriques, H.S. Seo, A. Nagatani, and N.H. Chua. 2010. Arabidopsis PHYTOCHROME INTERACTING FACTOR proteins promote phytochrome B polyubiquitination by COP1 E3 ligase in the nucleus. Plant Cell 22:2370–2383.
- Kami, C., S. Lorrain, P. Hornitschek, and C. Fankhauser. 2010. Light-regulated plant growth and development. Curr. Top. Dev. Biol. 91:29–66.
- Keller, M.M., Y. Jaillais, U.V. Pedmale, J.E. Moreno, J. Chory, and C.L. Ballaré. 2011. Cryptochrome 1 and phytochrome B control shade-avoidance responses in *Arabidopsis* via partially independent hormonal cascades. Plant J. 67:195–207.
- Keuskamp D.H., R. Sasidharan, I. Vos, A.J.M. Peeters, L.A.C.J. Voesenek, and R. Pierik. 2011. Blue-light-mediated shade avoidance requires combined auxin and brassinosteroid action in *Arabidopsis* seedlings. Plant J. 67:208–217.
- Kim, G.T., S. Yano, T. Kozuka, and H. Tsukaya. 2005. Photomorphogenesis of leaves: shade-avoidance and differentiation of sun and shade leaves. Photochem. Photobiol. Sci. 4:770–774.
- Kozuka, T., G. Horiguchi, G.-T. Kim, M. Ohgishi, T. Sakai, and H. Tsukaya. 2005. The different growth responses of the *Arabidopsis thaliana* leaf blade and the petiole during shade avoidance are regulated by photoreceptors and sugar. Plant Cell Physiol. 46:213–223.
- Kurepin, L.V., R.J. Emery, R.P. Pharis, and D.M. Reid. 2007. Uncoupling light quality from light irradiance effects in *Helianthus annuus* shoots: putative roles for plant hormones in leaf and internode growth. J. Exp. Bot. 58:2145–2157.

- Levy, Y.Y. and C. Dean. 1998. The transition to flowering. Plant Cell 10:1973–1989.
- Li, J., G. Li, H. Wang, and X.W. Deng. 2011. Phytochrome signaling mechanisms. The Arabidopsis Book e0148.
- Lopez, R.G. and E.S. Runkle. 2008. Photosynthetic daily light integral during propagation influences rooting and growth of cuttings and subsequent development of New Guinea impatiens and petunia. HortScience 43:2052–2059.
- Lopéz-Juez, E., J.R. Bowyer, and T. Sakai. 2001. Distinct leaf developmental and gene expression responses to light quantity depend on blue-photoreceptor or plastid-derived signals, and can occur in the absence of phototropins. Planta 227:113–123.
- McCormac, A.C. and M.J. Terry. 2002. Light-signalling pathways leading to the co-ordinated expression of *HEMA1* and *Lhcb* during chloroplast development in *Arabidopsis thaliana*. Plant J. 32:549–559.
- McCree, K.J. 1972. The action spectrum, absorbance and quantum yield of photosynthesis in crop plants. Agr. Meteorol. 9:191–216.
- Meng, Q. and E.S. Runkle. 2014. Controlling flowering of photoperiodic ornamental crops with light-emitting diode lamps: A coordinated grower trial. HortTechnology 24:702–711.
- Mitchell, C., A.-J. Both, M. Bourget, J. Burr, C. Kubota, R. Lopez, R. Morrow, and E. Runkle. 2012. LEDs: the future of greenhouse lighting!. Chronica Hort. 52:6–11.
- Mizoguchi, T., K. Niinuma, and R. Yoshida. 2007. Day-neutral response of photoperiodic flowering in tomatoes: possible implications based on recent molecular genetics of *Arabidopsis* and rice. Plant Biotechnol. 24:83–86.
- Murchie, E.H. and P. Horton. 1997. Acclimation of photosynthesis to irradiance and spectral quality in British plant species: chlorophyll content, photosynthetic capacity and habitat preference. Plant Cell Environ. 20:438–448.
- Okada, K., Y. Inoue, K. Satoh, and S. Katoh. 1992. Effects of light on degradation of chlorophyll and proteins during senescence of detached rice leaves. Plant Cell Physiol. 33:1183–1191.
- Pantin, F., T. Simmonneau, G. Rolland, M. Dauzat, and B. Muller. 2011. Control of leaf expansion: A developmental switch from metabolic to hydraulics. Plant Physiol. 156: 803–815.
- Park, Y. and E.S. Runkle. 2017. Far-red radiation promotes growth of seedlings by increasing leaf expansion and whole-plant net assimilation. Environ. Exp. Bot. 136:41–49.

- Patel, D., M. Basu, S. Hayes, I. Majlath, F.M. Hetherington, T.J. Tschaplinski, and K.A. Franklin. 2013. Temperature-dependent shade avoidance involves the receptor-like kinase ERECTA. Plant J. 73:980–992.
- Pierik, R., G.C. Whitelam, L.A.C.J. Voesenek, H. de Kroon, and E.J.W. Visser. 2004. Canopy studies on ethylene-insensitive tobacco identify ethylene as a novel element in blue light and plant-plant signalling. Plant J. 38:310–319.
- Pierik, R., T. Djakovic-Petrovic, D.H. Keuskamp, M. de Wit, and L. Voesenek. 2009. Auxin and ethylene regulate elongation responses to neighbor proximity signals independent of gibberellin and DELLA proteins in *Arabidopsis*. Plant Physiol. 149:1701–1712.
- Pierik, R. and M. de Wit. 2014. Shade avoidance: phytochrome signalling and other aboveground neighbour detection cues. J. Exp. Bot. 65:2815–2824.
- Pons, T.L. and Y. De Jong-van Berkel. 2004. Species-specific variation in the importance of the spectral quality gradient in canopies as a signal for photosynthetic resource partitioning. Ann. Bot. 94:725–732.
- Pramuk, L.A. and E.S. Runkle. 2005. Photosynthetic daily light integral during the seedling stage influences subsequent growth and flowering of *Celosia*, *Impatiens*, *Salvia*, *Tagetes*, and *Viola*. HortScience 40:1336–1339.
- Rousseaux, M.C., A.J. Hall, and R.A. Sánchez. 1996. Far-red enrichment and photosynthetically active radiation level influence leaf senescence in field-grown sunflower. Physiol. Plant. 96:217–224.
- Runkle, E.S. and R.D. Heins. 2001. Specific functions of red, far red, and blue light in flowering and stem extension of long-day plants. J. Amer. Soc. Hort. Sci. 126:275–282.
- Runkle, E.S. and R.D. Heins. 2003. Photocontrol of flowering and extension growth in the long-day plant pansy. J. Amer. Soc. Hort. Sci. 128:479–485.
- Sager, J.C., W.O. Smith, J.L. Edwards, and K.L. Cyr. 1988. Photosynthetic efficiency and phytochrome photoequilibria determination using spectral data. Trans. Amer. Soc. Agr. Eng. 31:1882–1889.
- Sasidharan, R., C.C. Chinnappa, L.A.C.J. Voesenek, and R. Pierik. 2008. The regulation of cell wall extensibility during shade avoidance: a study using two contrasting ecotypes of Stellaria longipes. Plant Physiol. 148:1557–1569.
- Sheehan, M.J., L.M. Kennedy, D.E. Costich, and T.P. Brutnell. 2007. Subfunctionalization of PhyB1 and PhyB2 in the control of seedling and mature plant traits in maize. Plant J. 49: 338–353.

- Smith, H. and M.G. Holmes. 1977. The function of phytochrome in the natural environment. III. Measurement and calculation of phytochrome photoequilibirum. Phytochem. Photobiol. 25:547–550.
- Smith, H. 1982. Light quality, photoreception, and plant strategy. Ann. Rev. Plant Physiol. 33:481–518.
- Smith, H. 1994. Sensing the light environment: The functions of the phytochrome family. In Kendrick, R.E. and Kronenberg, G.H.M. (eds.) Photomorphogenesis in plants, 2nd edn. Dordrecht, the Netherlands: Kluwer Academic Publishers, pp.377–416.
- Smith, H. and G.C. Whitelam. 1997. The shade avoidance syndrome: multiple responses mediated by multiple phytochromes. Plant Cell Environ. 20:840–844.
- Snowden, M.C., K.R. Cope, and B. Bugbee. 2016. Sensitivity of seven diverse species to blue and green light: interactions with photon flux. PLoS One 11:e0163121.
- Stephenson, P.G. and M.J. Terry. 2008. Light signalling pathways regulating the Mg-chelatase branchpoint of chlorophyll synthesis during de-etiolation in *Arabidopsis thaliana*. Photochem. Photobiol. Sci. 7:1243–1252.
- Su, H., S.D. Abernathy, R.H. White, and S.A. Finlayson. 2011. Photosynthetic photon flux density and phytochrome B interact to regulate branching in *Arabidopsis*. Plant Cell Environ. 34:1986–1998.
- Sullivan, J.A. and X.W. Deng. 2003. From seed to seed: the role of photoreceptors in *Arabidopsis* development. Dev. Biol. 260:289–97.
- Terashima, I. and Y. Inoue. 1985. Vertical gradient in photosynthetic properties of spinach chloroplasts dependent on intra-leaf light environment. Plant Cell Physiol. 26:781–785.
- Vernon, A.J. and J.C.S. Allison. 1963. A method of calculating net assimilation rate. Nature 200:814.
- Wagner, R., L. Dietzel, K. Bräutigam, W. Fischer, and T. Pfannschmidt. 2008. The long-term response to fluctuating light quality is an important and distinct light acclimation mechanism that supports survival of *Arabidopsis thaliana* under low light conditions. Planta 228:573–587.
- Walters, R.G. and P. Horton. 1994. Acclimation of *Arabidopsis thaliana* to the light environment: changes in composition of the photosynthetic apparatus. Planta 195:248–256.
- Walters, R.G. 2005. Towards an understanding of photosynthetic acclimation. J. Exp. Bot. 56:435–447.

- Wellburn, A.R. and H. Lichtenthaler. 1984. Formulae and program to determine total carotenoids and chlorophylls a and b of leaf extracts in different solvents. In: Sybesma, C. (ed.) Advances in photosynthesis research. Springer, Netherlands, pp 9–12.
- Weston, E., K. Thorogood, G. Vinti, and E. Lopéz-Juez. 2000. Light quantity controls leaf-cell and chloroplast development in *Arabidopsis thaliana* wild-type and blue-light-perception mutants. Planta 211:807–815.
- Wiese, A., M.M. Christ, O. Virnich, U. Schurr, and A. Walter. 2007. Spatiotemporal leaf growth patterns of *Arabidopsis thaliana* and evidence for sugar control of the diel leaf growth cycle. New Phytol. 174:752–761.
- Wollaeger, H.M. and E.S. Runkle. 2013. Growth responses of ornamental annual seedlings under different wavelengths of red light provided by light-emitting diodes. HortScience 48:1478–1483.
- Wollaeger, H.M. and E.S. Runkle. 2014. Growth of impatiens, petunia, salvia, and tomato seedlings under blue, green, and red light-emitting diodes. HortScience 49:734–740.
- Wollaeger, H.M. and E.S. Runkle. 2015. Growth and acclimation of impatiens, salvia, petunia, and tomato seedlings to blue and red light. HortScience 50:522–529.
- Wollenberg, A.C., B. Strasser, P.D. Cerdan, and R.M. Amasino. 2008. Acceleration of flowering during shade avoidance in *Arabidopsis* alters the balance between FLOWERING LOCUS C-mediated repression and photoperiodic induction of flowering. Plant Physiol. 148:1681–1694.

## **SECTION III**

BLUE RADIATION ATTENUATES THE PROMOTIVE EFFECTS OF FAR-RED RADIATION ON EXTENSION GROWTH BUT NOT ON FLOWERING

Blue Radiation Attenuates the Promotive Effects of Far-red Radiation on Extension Growth but

not on Flowering

Yujin Park<sup>1</sup> and Erik S. Runkle<sup>2</sup>

Department of Horticulture, 1066 Bogue Street, Michigan State University, East Lansing, MI

48824

This research was supported by Osram Opto Semiconductors; the USDA-ARS Floriculture and

Nursery Research Initiative; the USDA National Institute of Food and Agriculture, Hatch project

192266; Michigan State University's (MSU) AgBioResearch and Project GREEEN; and

horticulture companies supportive of MSU floriculture research. We thank C. Raker & Sons for

donation of plant material and Nate DuRussel for technical assistance. We thank Chun-Lung Lee

(Statistical Consulting Center, CANR Biometry Group, MSU) and Dr. Bert Cregg (Department

of Horticulture, MSU) for statistical advice.

<sup>1</sup>Graduate student.

<sup>2</sup>Corresponding author. E-mail address: runkleer@msu.edu.

76

#### **Abstract**

Blue (B, 400 to 500 nm) and far-red (FR, 700 to 800 nm) radiation have somewhat opposite effects on stem elongation; B typically suppresses extension growth while FR promotes it. Although the effects of B and FR radiation on plant growth have been investigated independently, little research has been published on how they interact to regulate growth and development. We postulated that FR radiation with a moderately high B photon flux density would promote flowering with minimal extension growth. We grew seedlings of geranium (Pelargonium ×hortorum), petunia (Petunia ×hybrida), and coleus (Solenostemon scutellariodes) at 20 °C under six sole-source LED lighting treatments with an 18-h photoperiod. All treatments provided a photosynthetic photon flux density of 160 µmol·m<sup>-2</sup>·s<sup>-1</sup> with the following photon flux densities (subscript in  $\mu$ mol·m<sup>-2</sup>·s<sup>-1</sup>) of B (peak = 447 nm), red (R, peak = 660 nm), or/and FR radiation (peak = 731 nm):  $B_{80}R_{80}$ ,  $B_{80}R_{80}FR_{10}$ ,  $B_{80}R_{80}FR_{80}$ ,  $R_{160}$ ,  $R_{160}FR_{20}$ , and  $R_{160}FR_{160}$ . Seedlings were then transplanted and subsequently grown in a common greenhouse environment at 20 °C with a 16-hour photoperiod. Stem length of all species increased linearly with additions of FR [as the R:FR or estimated phytochrome photoequilibrium (PPE) decreased]. When R was partly substituted with B light (B<sub>80</sub>R<sub>80</sub>), stem length of shade-avoiding petunia and geranium also increased linearly with decreasing PPE, but substantially less (55-85%) than under  $R_{160}$ . In shade-tolerant coleus, there was little to no effect of PPE on stem elongation under B<sub>80</sub>R<sub>80</sub>. In geranium, shoot dry weight decreased linearly with increasing PPE similarly under R<sub>160</sub> and  $B_{80}R_{80}$ , while in petunia, similar trends occurred only under  $R_{160}$ . In the long-day plant petunia, decreasing the PPE promoted subsequent flowering by 7 to 11 d, regardless of the B and R flux density. We conclude that a moderately high B photon flux density attenuates the effects of FR

radiation on extension growth but has no apparent effect on the promotive effects of FR radiation on subsequent flowering in at least some long-day plants.

Keywords: light quality, red to far-red ratio, sole-source lighting

Abbreviations:

B, blue radiation; Cry, cryptochrome; DLI, daily light integral; DW, dry weight; FR, far-red radiation; LEDs, light-emitting diodes; LMA, leaf mass per area; PPE, phytochrome photoequilibrium; PPFD, photosynthetic photon flux density; Pr, R-radiation-absorbing phytochrome; Pfr, FR-radiation-absorbing phytochrome; Phy, phytochrome; PIF, phytochrome interacting factors; R, red; TPFD, total photon flux density; YPFD, yield photon flux density.

#### Introduction

Several families of photoreceptors mediate responses of plants to lighting, ranging from UV-B (280–315 nm) to far-red (FR, 700–800 nm) (Kami et al., 2010). In arabidopsis (*Arabidopsis thaliana*), five classes of photoreceptors are identified according to their light absorption properties, including phytochromes (phyA-E), cryptochromes (cry1, cry2), phototropins (phot1, phot2), Zeitlupe family (ZTL, FKF1, and LKP2), and UV resistance locus 8 (UVR8) (Li et al., 2011; Christie et al., 2015). These photoreceptors coordinately control many aspects of plant growth and development (Mazzella and Casal, 2001; Kami et al., 2010). In particular, the functions of phytochromes and cryptochromes overlap extensively in regulating photomorphogenic and photoperiodic responses, including stem elongation, chlorophyll synthesis, and flowering time (Casal, 2000; Mas et al., 2000; Usami et al., 2004). However, the

effects of B and FR radiation on plant growth have often been investigated independently, and relatively little research has been published on how they interact to regulate growth and development, especially outside of model crops.

Phytochromes are the primary photoreceptors that perceive red (R, 600–700 nm) and FR radiation, and R/FR photoreversibility allows the phytochrome molecules to perform their regulatory functions (Sharrock, 2008; Li et al., 2011). Phytochromes exist in two spectral forms, a biologically inactive R-absorbing form ( $P_r$ ) and an active FR-absorbing form ( $P_{fr}$ ) (Fankhauser, 2001; Rockwell et al. 2006). Upon absorption of R radiation,  $P_r$  converts into  $P_{fr}$ , which accumulates in the nucleus and modulates gene expression. FR radiation, in turn, can convert  $P_{fr}$  back to  $P_r$  (Fankhauser, 2001; Rockwell et al. 2006). The relative portion of R and FR radiation (or R:FR) establishes the relative portion of the active  $P_{fr}$  form in the total phytochrome pool, which is the phytochrome photoequilibrium (PPE) (Smith and Holmes, 1977). In general, a higher R:FR of incident radiation establishes a higher PPE within the plant (Smith and Holmes, 1977; Smith, 1982). The PPE under any radiation spectrum can be estimated using models that are based upon the absorption of  $P_r$  and  $P_{fr}$  and the spectral distribution of incident radiation (Sager et al., 1988).

Stem elongation commonly shows an inverse linear relationship with estimated PPE and a linear relationship with leaf chlorophyll concentration (Morgan and Smith, 1978; Smith, 1982; Runkle and Heins, 2001; Park and Runkle, 2017). In some long-day plants, flowering time exhibits a quadratic relationship with the estimated PPE (Craig and Runkle, 2016). In addition, the most effective PPE value for promoting flowering in long-day plants is similar under night interruption lighting (0.63–0.80) (Craig and Runkle, 2016) and sole-source lighting (0.65–0.85) (Park and Runkle, 2017). Therefore, although different phytochrome-regulated plant responses

show different relationships with the estimated PPE, the estimated PPE is a useful indicator to predict the effects of R:FR ratio on specific phytochrome-regulated responses. In general, a radiation spectrum with a relatively low R:FR (establishing a low to intermediate PPE), promotes extension growth and flowering while decreasing leaf chlorophyll concentration.

Cryptochromes regulate a variety of blue (B, 400–500 nm) radiation-mediated plant responses, including de-etiolation, shade-avoidance responses, and photoperiodic flowering (Yu et al., 2010; Liu et al., 2011). In darkness, cryptochromes remain unphosphorylated and inactive, but upon absorption of B radiation, cryptochromes undergo conformational changes accompanied by phosphorylation, altering their physical interactions with signaling proteins (Shalitin et al., 2002, 2003). The phosphorylated cryptochromes represent their physiologically active form, which initiate B radiation-induced signal transduction (Christie et al. 2015). The level of phosphorylation of cryptochromes was dependent on photon flux density of B radiation (Batschauer, 2005) and also, correlated closely with the biological function of cryptochromes (Liu et al. 2011).

The effects of B radiation at regulating some cyptochrome-mediated responses depend on its flux density. For example, increasing B radiation from 11 to 28% [at a photosynthetic photon flux density (PPFD) of 500  $\mu$ mol·m<sup>-2</sup>·s<sup>-1</sup>] inhibited stem length (by 20–24%) and leaf area index (by 24–37%) while increasing chlorophyll concentration (by 14–23%) in tomato, cucumber, and pepper (Snowden et al., 2016). In a separate study, plant height and leaf area of cucumber decreased linearly and chlorophyll concentration increased linearly with increasing B radiation from 10% to 75% (at PPFD of 100  $\mu$ mol·m<sup>-2</sup>·s<sup>-1</sup>) (Hernández and Kubota, 2016). In addition, the number of flower buds of impatiens increased with increasing B radiation from 0% to 100% (at PPFD of 160  $\mu$ mol·m<sup>-2</sup>·s<sup>-1</sup>) (Wollaeger and Runkle, 2015). Thus, increasing B radiation inhibits

extension growth and promoted chlorophyll concentration and flowering in a quantitative manner.

Although phytochromes and cryptochromes primarily detect and mediate responses to the R:FR and B radiation, respectively, their signalling processes are integrated to regulate overlapping developmental processes in plants (Su et al., 2017). For example, phytochrome interacting factors (PIFs) integrate phyB and cry1/2 signals to promote stem growth (Pedmale et al., 2016; de Wit et al., 2017). The inactivation of both phyB and cry1/2 by low R:FR and low B, respectively, enhanced PIFs action and elongation more than the inactivation of phyB alone (de Wit et al., 2017). In photoperiodic flowering, the antagonistic action of phyB and cry2 regulates the accumulation of CONSTANS (CO) proteins, which promotes the transcription of FLOWERING LOCUS T (FT) and subsequent flowering (Guo et al. 1998).

Thus, plant responses under the control of both photoreceptors are determined, at least in part, by complicated interactions of their antagonistic, redundant, or synergetic effects (Lin, 2002; Su et al., 2017). However, the effects of R:FR (or PPE) and B radiation on plant growth and development have often been investigated individually, and how they interact to regulate growth is less clear. Here, we quantified the effects of PPE on plant architecture, growth, and flowering without and with a moderately high intensity of B radiation (80 µmol·m<sup>-2</sup>·s<sup>-1</sup>) to further understand how plant responses to PPE are controlled by B radiation. We postulated that a moderately high intensity of B radiation would suppress the promotive effects of FR radiation on stem elongation and leaf expansion but have little or no subsequent effect on flowering.

#### **Materials and Methods**

Plant materials

Petunia (*Petunia* ×*hybrida* 'Wave Blue'), geranium (*Pelargonium* ×*hortorum* 'Pinto Premium Orange Bicolor'), and coleus (Solenostemon scutellariodes 'Wizard Golden') were used for study considering their commercial significance, shade tolerance, and photoperiodic flowering response. Petunia and geranium are shade-avoiding species while coleus is shadetolerant; and petunia, geranium, and coleus are long-day, day-neutral, and short-day plants, respectively (Erwin et al., 2017). The experiment was performed three times for petunia and geranium and twice for coleus. In each replication, seeds of each species were sown in 128-cell  $(2.7 \times 2.7\text{-cm}; 12.0\text{-mL volume})$  plug trays by a commercial young plant producer (C. Raker and Sons, Inc., Litchfield, MI). Trays were moved to Michigan State University (East Lansing, MI) on the following number of days after seed sow (rep 1, 2, 3): petunia (7, 10, 9), geranium (7, 8, 8), and coleus (7, 8). Each plug tray of geranium was cut into three sections (each with  $\geq 40$ seedlings) and petunia and coleus trays were cut into four sections (each with  $\geq 30$  seedlings). Seedlings were thinned to one plant per cell and immediately placed under radiation treatments when they had fully expanded cotyledons and as the first true leaf was emerging. Radiation treatments and growth conditions

Six radiation treatments were developed using six LED modules described by Wollaeger and Runkle (2013). Each module was fitted with a new panel that contained 80 B (peak = 447 nm), R (peak = 660 nm), and FR (peak = 731 nm) m) LEDs. To test three R:FR ratios (1:0, 8:1, and 1:1) without and with 80  $\mu$ mol·m<sup>-2</sup>·s<sup>-1</sup> of B radiation, each module delivered a PPFD of 160  $\mu$ mol·m<sup>-2</sup>·s<sup>-1</sup> with the following photon flux densities (subscript in  $\mu$ mol·m<sup>-2</sup>·s<sup>-1</sup>) of B, R, or/and FR radiation: B<sub>80</sub>R<sub>80</sub>, B<sub>80</sub>R<sub>80</sub>FR<sub>10</sub>, B<sub>80</sub>R<sub>80</sub>FR<sub>80</sub>, R<sub>160</sub>, R<sub>160</sub>FR<sub>20</sub>, and R<sub>160</sub>FR<sub>160</sub> (Fig. 1). The

photoperiod was 18 h [creating a daily light integral (DLI) of 10.4 mol·m<sup>-2</sup>·d<sup>-1</sup>] as controlled by a data logger (CR10; Campbell Scientific, Logan, UT). For each replication, the radiation treatments were delivered following methods previously described (Park and Runkle, 2017), and the plug trays were rotated daily inside each LED module to mitigate any positional effects. For each radiation treatment, the percentage of each waveband and R:FR was calculated using 100-nm wavebands; the PPE was estimated as described by Sager et al. (1988); and the yield photon flux density (YPFD; the product of photon flux density and relative quantum efficiency), was calculated based on McCree (1972) and Sager et al. (1988) (Table 1).

The six LED modules were located inside a refrigerated walk-in growth chamber at a constant temperature set point of 20 °C. In each LED module, air and plant canopy temperature and radiation intensity was monitored and recorded as described by Park and Runkle (2017). Average air/canopy temperatures (°C) during the experimental periods were 20.5/20.5, 20.5/20.7, 21.0/21.3, 20.5/20.5, 20.9/21.0, and 20.7/20.8 for the  $B_{80}R_{80}$ ,  $B_{80}R_{80}FR_{10}$ ,  $B_{80}R_{80}FR_{80}$ ,  $R_{160}$ ,  $R_{160}FR_{20}$ , and  $R_{160}FR_{160}$ , respectively. All temperatures had standard deviations (SD)  $\leq \pm 1.0$  °C. Plants were irrigated as described by Park and Runkle (2017) and the EC and pH of the nutrient solution was 0.43 mS·cm<sup>-1</sup> and 6.2, respectively.

## Data collection for seedling growth

In each replication, seedling growth data were collected on 10 random plants of each species in each treatment, usually excluding outer guard rows, at the end of the seeding stage on the following number of days after seed sow (rep 1, 2, 3): geranium (30, 35, 36), petunia (34, 39, 38), and coleus (31, 35). The data collection date was determined when the seedlings were ready for transplanting (when the roots had grown sufficiently so that the seedlings could be easily pushed out of the trays with the entire root zone intact) and varied presumably because of

differences in seed vigor. The following data were collected: leaf (at node) number, total leaf area, SPAD index, plant height (from media level to apical meristem), and shoot, leaf, and root dry weight (DW). Each growth parameter was evaluated as described by Park and Runkle (2017). The leaf mass per area (LMA; leaf DW divided by total leaf area) and net assimilation (plant DW divided by total leaf area) were calculated for all three species.

Growth conditions and data collection after transplant

The effects of the sole-source lighting treatments during the seedling stage on subsequent flowering were evaluated during the first and second replications. At the end of the seedling stage, ten seedlings per treatment per species were randomly selected and transplanted into 10-cm pots containing a 70% peatmoss, 21% perlite, and 9% vermiculite potting media (SUREMIX; Michigan GrowerProducts, Inc., Galesburg, MI). Pots were randomly placed on benches and grown in an environmentally controlled greenhouse at a constant temperature set point of 20 °C. Supplemental lighting provided by 400-W high-pressure sodium lamps delivered a PPFD of 79 (SD  $\pm$  9.4)  $\mu$ mol·m<sup>-2</sup>·s<sup>-1</sup> at plant height and a 16-h photoperiod. Supplemental lighting was controlled as described by Park and Runkle (2017). In petunia and geranium, the following data were collected when each plant flowered: date, flower bud or inflorescence number, and length of the primary stem. For coleus, the length of the primary stem was measured from the media surface to the apical meristem 34 d after transplant for both replications.

## Statistical analysis

The experiment was designed as a randomized complete block design: each replication was regarded as a block; each LED module was regarded as the experimental unit for the radiation treatment; and within each LED module, each individual seedling per species was the sub-sample or observational unit. Data were pooled between replications and analyzed with SAS

software (version 9.4; SAS Institute, Inc., Cary, NC). Two-way analysis of variance (ANOVA) was used to assess the effects of PPE, B, and their interaction on plant growth and flowering parameters using PROC MIXED procedure [with two fixed factors for B and PPE, two random factors of blocks (or replications) and interaction between blocks, B, and PPE]. A simple linear regression analysis was conducted to relate the seedling growth parameters to the estimated PPE for each B level treatment ( $R_{160}$  and  $B_{80}R_{80}$ ) using PROC REG. For regression analysis, the mean for each replication was treated as single data point and included nine data points (3 replications  $\times$  3 different PPEs) for petunia and geranium and six data points (2 replications  $\times$  3 different PPEs) for coleus at each B level. When there was a linear relationship between the estimated PPE and the data parameter at both B levels, analysis of covariance (ANCOVA) was performed by using PROC MIXED to test differences between the slopes of the regression lines for the two B levels (P < 0.05).

#### **Results**

Among the 13 measured growth and flowering parameters, there were significant main effects of both PPE and B in at least two species for stem length, individual leaf area, and SPAD index (Table 2). However, there was an interaction between PPE and B only for stem length in geranium and coleus, and (total and individual) leaf area and LMA in coleus. In at least two species, PPE influenced shoot DW, plant DW, and days to flower while B radiation affected total leaf area, LMA, and root DW.

## Stem extension

In petunia and geranium, stem length decreased linearly as the estimated PPE increased from 0.69 to 0.89 (Table 2; Fig. 2). With 80 μmol·m<sup>-2</sup>·s<sup>-1</sup> of B radiation, the magnitude of

increase in stem length of petunia and geranium in response to decreasing PPE was 85% and 55% less, respectively, than without B radiation. In coleus, stem length decreased by 44% with increasing PPE without B radiation; with B radiation, stem length at each PPE was 68–78% shorter than without B.

Leaf characteristics and photosynthesis

SPAD index, which is an indicator for chlorophyll concentration per unit leaf area, of petunia and geranium increased linearly by 68% and 31%, respectively. as the estimated PPE increased without and with B radiation (Table 2; Fig. 2). In coleus, there was little to no effect of PPE on SPAD value with or without B radiation. Independent of PPE, B radiation increased SPAD index at each PPE by 14–38%, 18–28%, and 96–125% in petunia, geranium, and coleus, respectively.

In petunia and coleus, the addition of FR radiation (or the estimated PPE) had little to no effect on total leaf area with or without B radiation (Table 3). In geranium, the addition of 160  $\mu$ mol·m<sup>-2</sup>·s<sup>-1</sup> FR to a B-deficient environment (PPE = 0.70) increased total leaf area by 22% compared to no FR (PPE = 0.89). Independent of PPE, B radiation decreased total leaf area of geranium at each PPE by 21–25%. In coleus, B radiation decreased total leaf area by 54% only without FR radiation. PPE and B radiation did not affect leaf number except for geranium, in which plants grown with B radiation had 0.1–0.6 more leaves than those grown without B (P = 0.002; data not shown). With few effects of radiation treatments on leaf number, individual leaf area in all species showed similar patterns as with total leaf area (data not shown).

In petunia and geranium, LMA and net assimilation were similar among radiation treatments (Table 3). In coleus and in a B-deficient environment, LMA and net assimilation increased by 65% and 88%, respectively, with the addition of FR radiation (PPE = 0.70)

compared to without FR (PPE = 0.89). B radiation increased LMA and net assimilation of coleus at each estimated PPE by 39-142% or 50-101%, respectively, except for net assimilation at PPE of 0.69.

### Plant dry weight

Without B radiation, shoot DW of petunia and geranium decreased linearly by 29 or 34%, respectively, as the estimated PPE increased (Table 2; Fig. 3). With B radiation, only shoot DW of geranium decreased linearly by 28% with increasing PPE. B radiation decreased the shoot DW of petunia by 24–28% independently of PPE, while shoot DW of geranium was similar without and with B radiation. In coleus, shoot DW was similar among radiation treatments.

At each PPE, B radiation increased the root DW of geranium and coleus by 19–26% and 73–102%, respectively (Table 2; Fig. 3). In all species, there was little to no effect of PPE on root DW without and with B radiation. In all species, because root DW is relatively small compared to shoot DW, plant (shoot+root) DW showed responses similar those of shoot DW (data not shown).

#### Subsequent flowering responses

In both long-day petunia and day-neutral geranium, B radiation during the seedling stage did not affect subsequent flowering (Table 2 and 4). In long-day petunia, the addition of FR (PPE  $\leq$  0.70) accelerated subsequent flowering by 7 to 10 d, regardless of the presence of B radiation. In day-neutral geranium, plants grown under  $R_{160}FR_{160}$  flowered 3 d earlier compared to those grown under  $B_{80}R_{80}$ . Only in petunia, the flowering promotion with the addition of FR radiation was accompanied by a decrease in number of flower buds without B radiation. In coleus, plants grown under  $R_{160}FR_{160}$  were taller than those grown under  $B_{80}R_{80}$  or  $B_{80}R_{80}FR_{10}$ .

#### **Discussion**

FR and B radiation have somewhat antagonistic effects in regulating stem elongation. Extension growth of a wide range of species increases linearly with FR, which decreases the R:FR and PPE (Smith, 1982). In contrast, increasing B photon flux density often inhibits stem elongation (Cope and Bugbee, 2013; Wollaeger and Runkle, 2015; Snowden et al., 2016). Consistently in this study, stem length increased linearly with a decreasing PPE without or with B radiation, except for coleus with B radiation, and stem length was shorter with B radiation compared to without B (Table 2; Fig. 2). In addition, in shade-avoiding petunia and geranium, the rate of increase in stem length with decreasing PPE was much lower in the presence of B radiation (at 80 μmol·m<sup>-2</sup>·s<sup>-1</sup>), while in shade-tolerant coleus, PPE did not influence stem length. This suggests that the antagonistic effects of decreasing R:FR and increasing B photon flux density on stem elongation are not additive or independent but rather, interactive, and that a moderately high B photon flux density suppresses elongation responses to PPE.

In arabidopsis, the active form of phyB and crys interact with and inactivate PIFs, which promote the expression of genes mediating elongation growth (Franklin, 2008; Keller et al., 2011; Pedmale et al., 2016). Under a low R:FR, phyB is inactive and increases the stability of PIFs to promote cell elongation (Franklin, 2008). When a low R:FR (0.3) was combined with low B radiation (1 μmol·m<sup>-2</sup>·s<sup>-1</sup>), PIF5 increased and suppressed transcription factor LONG HYPOCOTYL IN FAR-RED 1 (HFR1), which is a negative regulator of PIFs, subsequently increasing elongation compared to a higher flux density (17 μmol·m<sup>-2</sup>·s<sup>-1</sup>) of B radiation (de Wit et al., 2016). Under the higher B radiation, a low R:FR increases active PIFs, but crys and HFR1 inhibit PIF activity and elongation responses (de Wit et al., 2016; Franklin, 2016; Pedmale et al.,

2016; Su et al., 2017). This suggests that  $80 \, \mu mol \cdot m^{-2} \cdot s^{-1}$  of B radiation used in this study increased the activation of crys and HFR and repressed PIF function, subsequently attenuating the low R:FR-induced elongation responses.

Plants propagated by seed often have a juvenile phase in which they are not competent to initiate flowers (Adams et al., 1999). Once the plants are capable of responding to inductive stimuli, photoperiod regulates flowering of a wide range of ornamental crops. In addition to stem elongation, FR and B radiation can regulate photoperiodic flowering (Mockler et al., 2003). The juvenile phase of petunia (*Petunia* ×hybrida 'Express Blush Pink') grown at 21.3 °C ended 13 d after seedling emergence (Adams et al., 1999). In our study, petunia seedlings were grown under sole-source lighting for 24 d after seedling emergence, and the addition of FR (and decrease in PPE) in sole-source lighting during the 18-h photoperiod promoted subsequent flowering, indicating petunia seedlings were sensitive to spectral quality of photoperiod to initiate flowering. In addition, regardless of the presence of B radiation, the effective PPE values to promote flowering of long-day petunia in this study (0.69–0.70) were within those most effective for night interruption lighting (0.63-0.80) or for sole-source lighting (0.65-0.85) in long-day plants, including petunia and snapdragon (Antirrhinum majus) (Craig and Runkle, 2016; Park and Runkle, 2017). However, the partial substitution of R radiation with B radiation during the seedling stage did not influence subsequent flowering of the long-day plant petunia.

The effects of B radiation on flowering promotion are primarily mediated by cry2 (Guo et al. 1998). The function of cry2 on flowering promotion was partly via antagonizing phyB-mediated R radiation suppression of floral initiation (Guo et al., 1998; Mockler et al., 1999). In arabidopsis, wild-type plants grown under continuous B+R radiation at  $60-80 \mu \text{mol} \cdot \text{m}^{-2} \cdot \text{s}^{-1}$  (R:B = 2-3) flowered later than plants grown under a similar photon flux density of B radiation

(75–85  $\mu$ mol·m<sup>-2</sup>·s<sup>-1</sup>), suggesting that the R-radiation dependent phyB inhibited floral initiation (Guo et al. 1998). Although the R:B (1) of the B<sub>80</sub>R<sub>80</sub> treatments in this study was lower, the photon flux density of R radiation was higher, and thus, it is possible that the effects of 80  $\mu$ mol·m<sup>-2</sup>·s<sup>-1</sup> of R radiation on flowering inhibition may override the effect of B radiation on flowering promotion.

Alternatively, little influence of B radiation on subsequent flowering in long-day plant petunia could be a combined consequence of the effects of B on inhibiting seedling growth and promoting flowering. Previous studies showed high ornamental seedling quality (including high dry mass accumulation and well-developed roots) at transplant stage decreased subsequent flowering time (Lopez and Runkle, 2008; Oh et al., 2010). For example, seedlings of petunia 'Tiny Tunia Violet Ice' and 'Supertunia Mini Purple' grown under higher DLI had larger shoot dry mass (by 106–147%), and they flowered earlier at their finishing stage (by 21–22 d) (Lopez and Runkle, 2008). In this study, DLI was identical for  $B_{80}R_{80}$  and  $R_{160}$  treatments, but shoot dry mass of petunia seedling grown under  $B_{80}R_{80}$  treatments were lower by 37–38% than those grown under  $R_{160}$  treatments (Table 2; Fig. 2). The lower carbohydrate status under  $B_{80}R_{80}$  treatments might contribute to the increase in flowering time, diminishing the promotive effects of B radiation on flowering.

In summary, this study show that a moderately high intensity of B radiation can attenuate the effects of FR radiation on extension growth while the promotive effects of FR on subsequent flowering was not influenced by B radiation. In addition, in the regulation of leaf chlorophyll concentration, the antagonistic effects of FR and B were independent. These results indicate that the relative contribution of the effects of FR and of B radiation can differ among plant processes. In addition, these results suggest that a radiation spectrum that includes FR radiation with a

moderately high intensity of B can produce compact plants with greener leaves while promoting flowering in at least some crop species.

# **APPENDIX**

Table III-1. Spectral characteristics of six radiation treatments. The values after each LED type (B=blue; R=red; FR=far red) indicate their intensity in  $\mu$ mol·m<sup>-2</sup>·s<sup>-1</sup>. Symbols are those used in Fig. 2 - Fig. 8.

| Radiation treatment      | Symbol | PPFD <sup>1</sup> | $TPFD^2$ | YPFD <sup>3</sup> | R:FR <sup>4</sup> | PPE <sup>5</sup> |
|--------------------------|--------|-------------------|----------|-------------------|-------------------|------------------|
| $R_{160}$                | •      | 160               | 160      | 150               | 1:0               | 0.89             |
| $R_{160}FR_{20}$         | •      | 160               | 180      | 152               | 8:1               | 0.86             |
| $R_{160}FR_{160}$        | •      | 160               | 320      | 172               | 2:1               | 0.70             |
| ${ m B}_{80}{ m R}_{80}$ | 0      | 160               | 160      | 134               | 1:0               | 0.86             |
| $B_{80}R_{80}FR_{10}$    | 0      | 160               | 170      | 135               | 8:1               | 0.83             |
| $B_{80}R_{80}FR_{80}$    | 0      | 160               | 240      | 145               | 2:1               | 0.69             |

<sup>&</sup>lt;sup>T</sup>PPFD: Photosynthetic photon flux density (photon flux integral between 400 and 700 nm, in μmol·m<sup>-2</sup>·s<sup>-1</sup>).

<sup>&</sup>lt;sup>2</sup>TPFD: Total photon flux density (photon flux integral between 400 and 800 nm, in  $\mu$ mol·m<sup>-2</sup>·s<sup>-1</sup>).

 $<sup>^{3}</sup>$ YPFD: Yield photon flux density, which is the product of TPFD and relative quantum efficiency (in  $\mu$ mol·m<sup>-2</sup>·s<sup>-1</sup>) based on McCree (1972) and Sager et al. (1988).

<sup>&</sup>lt;sup>4</sup>R:FR: Ratio of photon flux integral of red (R; 600-700 nm) and far red (FR; 700-800 nm) radiation.

<sup>&</sup>lt;sup>5</sup>PPE: Phytochrome photoequilibria, which is the estimated  $P_{FR}/P_{R+FR}$  following Sager et al. (1988).

Table III-2. Analysis of variance for the effects of the estimated phytochrome photoequilibria (PPE), blue radiation (B, 400-500 nm), or their interaction on plant growth and flowering parameters of petunia, geranium, and coleus.

|                           | Petunia |     | Geranium  |     | Coleus |           |     |     |           |
|---------------------------|---------|-----|-----------|-----|--------|-----------|-----|-----|-----------|
| Factor                    | PPE     | В   | PPE<br>×B | PPE | В      | PPE<br>×B | PPE | В   | PPE<br>×B |
| Stem length               | *       | *   | NS        | *** | ***    | ***       | *   | *** | *         |
| SPAD index                | ***     | *** | NS        | **  | ***    | NS        | NS  | *** | NS        |
| Leaf number               | NS      | NS  | NS        | NS  | **     | NS        | NS  | NS  | NS        |
| Individual leaf area      | *       | **  | NS        | *** | ***    | NS        | NS  | *** | *         |
| Total leaf area           | NS      | **  | NS        | **  | ***    | NS        | NS  | *** | *         |
| Leaf mass per area        | NS      | NS  | NS        | NS  | **     | NS        | NS  | *** | *         |
| Net assimilation          | NS      | NS  | NS        | NS  | **     | NS        | *   | *** | *         |
| Plant dry weight (DW)     | ***     | *** | NS        | *** | NS     | NS        | *   | NS  | NS        |
| Shoot DW                  | ***     | *** | NS        | *** | NS     | NS        | *   | NS  | NS        |
| Root DW                   | NS      | NS  | NS        | NS  | *      | NS        | **  | *** | NS        |
| Days to flower            | **      | NS  | NS        | **  | NS     | NS        | _a  | _   | _         |
| Flower no.                | *       | NS  | NS        | NS  | NS     | NS        | _   | _   | _         |
| Plant height at flowering | NS      | NS  | NS        | NS  | NS     | NS        | NS  | **  | NS        |

NS, \*, \*\*, or \*\*\* Nonsignificant or significant at P < 0.05, 0.01 or 0.001, respectively.  $^a$ –, not determined.

Table III-3. Influence of the estimated phytochrome photoequilibria (PPE) and blue (B, 400-500 nm) photon flux density of sole-source lighting treatments on total leaf area, leaf mass per area (LMA), and net assimilation of seedlings. The values after each LED type (B=blue; R=red; FR=far red) indicate their photon flux density in  $\mu$ mol·m<sup>-2</sup>·s<sup>-1</sup>. Data represent the mean of two replications for coleus and three replications for petunia and geranium with 10 subsamples (plants) per replication and species.

|                       | _                                  | _                      | Net                |  |  |  |  |
|-----------------------|------------------------------------|------------------------|--------------------|--|--|--|--|
| Radiation treatment   | Total leaf area (cm <sup>2</sup> ) | LMA $(g \cdot m^{-2})$ | assimilation       |  |  |  |  |
|                       |                                    |                        | $(g \cdot m^{-2})$ |  |  |  |  |
| Petunia               |                                    |                        |                    |  |  |  |  |
| $R_{160}$             | 14.0                               | 43.9                   | 48.6               |  |  |  |  |
| $R_{160}FR_{20}$      | 15.8                               | 42.3                   | 46.6               |  |  |  |  |
| $R_{160}FR_{160}$     | 17.3                               | 40.7                   | 51.6               |  |  |  |  |
| $B_{80}R_{80}$        | 10.3                               | 38.1                   | 42.8               |  |  |  |  |
| $B_{80}R_{80}FR_{10}$ | 10.9 39.0                          |                        | 44.1               |  |  |  |  |
| $B_{80}R_{80}FR_{80}$ | 13.5                               | 39.2                   | 46.4               |  |  |  |  |
| Geranium              |                                    |                        |                    |  |  |  |  |
| $R_{160}$             | $27.4 b^{a}$                       | 40.1                   | 87.4               |  |  |  |  |
| $R_{160}FR_{20}$      | 29.2 ab                            | 42.3                   | 92.7               |  |  |  |  |
| $R_{160}FR_{160}$     | 33.3 a                             | 41.9                   | 94.0               |  |  |  |  |
| $B_{80}R_{80}$        | 21.3 c                             | 48.9                   | 65.5               |  |  |  |  |
| $B_{80}R_{80}FR_{10}$ | 21.9 c                             | 49.8                   | 68.3               |  |  |  |  |
| $B_{80}R_{80}FR_{80}$ | 26.2 bc                            | 48.3                   | 77.2               |  |  |  |  |
| Coleus                |                                    |                        |                    |  |  |  |  |
| $R_{160}$             | 14.2 a                             | 13.3 c                 | 17.8 b             |  |  |  |  |
| $R_{160}FR_{20}$      | 12.4 ab                            | 17.5 bc                | 23.2 b             |  |  |  |  |
| $R_{160}FR_{160}$     | 11.4 abc                           | 21.9 b                 | 33.5 a             |  |  |  |  |
| $B_{80}R_{80}$        | 6.6 c                              | 32.1 a                 | 35.7 a             |  |  |  |  |
| $B_{80}R_{80}FR_{10}$ | 8.7 bc                             | 31.0 a                 | 34.7 a             |  |  |  |  |
| $B_{80}R_{80}FR_{80}$ | 9.6 abc                            | 30.4 a                 | 35.1 a             |  |  |  |  |

<sup>&</sup>lt;sup>a</sup>Means with different letters are significantly different by Tukey's honestly significant difference test (P < 0.05).

Table III-4. Influence of sole-source lighting treatments on subsequent flowering characteristics of seedlings. The values after each LED type (B=blue; R=red; FR=far red) indicate their photon flux density in  $\mu$ mol·m<sup>-2</sup>·s<sup>-1</sup>. Data represent the mean of two replications for petunia and coleus and three replications for geranium with 10 subsamples (plants) per replication and species.

| Radiation treatment      | Days to flower    | Flower bud or     | Plant height at |  |  |  |  |
|--------------------------|-------------------|-------------------|-----------------|--|--|--|--|
|                          | Days to nower     | inflorescence no. | flowering (cm)  |  |  |  |  |
|                          |                   | Petunia           |                 |  |  |  |  |
| $R_{160}$                | 25 a <sup>a</sup> | 42.2 a            | 9.4             |  |  |  |  |
| $R_{160}FR_{20}$         | 21 ab             | 24.1 ab           | 8.3             |  |  |  |  |
| $R_{160}FR_{160}$        | 14 b              | 9.9 b             | 8.9             |  |  |  |  |
| $B_{80}R_{80}$           | 25 a              | 37.1 ab           | 8.3             |  |  |  |  |
| $B_{80}R_{80}FR_{10}$    | 24 ab             | 36.7 ab           | 7.5             |  |  |  |  |
| $B_{80}R_{80}FR_{80}$    | 18 b              | 23.4 ab           | 6.9             |  |  |  |  |
|                          |                   | Geranium          |                 |  |  |  |  |
| $R_{160}$                | 39 ab             | 2.9               | 15.9            |  |  |  |  |
| $R_{160}FR_{20}$         | 38 ab             | 3.1               | 15.4            |  |  |  |  |
| $R_{160}FR_{160}$        | 36 b              | 3.3               | 14.6            |  |  |  |  |
| $B_{80}R_{80}$           | 39 a              | 3.2               | 16.7            |  |  |  |  |
| $B_{80}R_{80}FR_{10}$    | 38 ab             | 3.9               | 15.2            |  |  |  |  |
| $B_{80}R_{80}FR_{80}$    | 37 ab             | 3.3               | 13.4            |  |  |  |  |
| Coleus                   |                   |                   |                 |  |  |  |  |
| $R_{160}$                | _b                | _                 | 14.7 ab         |  |  |  |  |
| $R_{160}FR_{20}$         | _                 | _                 | 14.6 ab         |  |  |  |  |
| $R_{160}FR_{160}$        | _                 | _                 | 15.4 a          |  |  |  |  |
| ${ m B}_{80}{ m R}_{80}$ | _                 | _                 | 12.8 b          |  |  |  |  |
| $B_{80}R_{80}FR_{10}$    | _                 | _                 | 12.7 b          |  |  |  |  |
| $B_{80}R_{80}FR_{80}$    | _                 | _                 | 13.4 ab         |  |  |  |  |

<sup>&</sup>lt;sup>a</sup>Means with different letters are significantly different by Tukey's honestly significant difference test (P < 0.05).

b-, not determined.

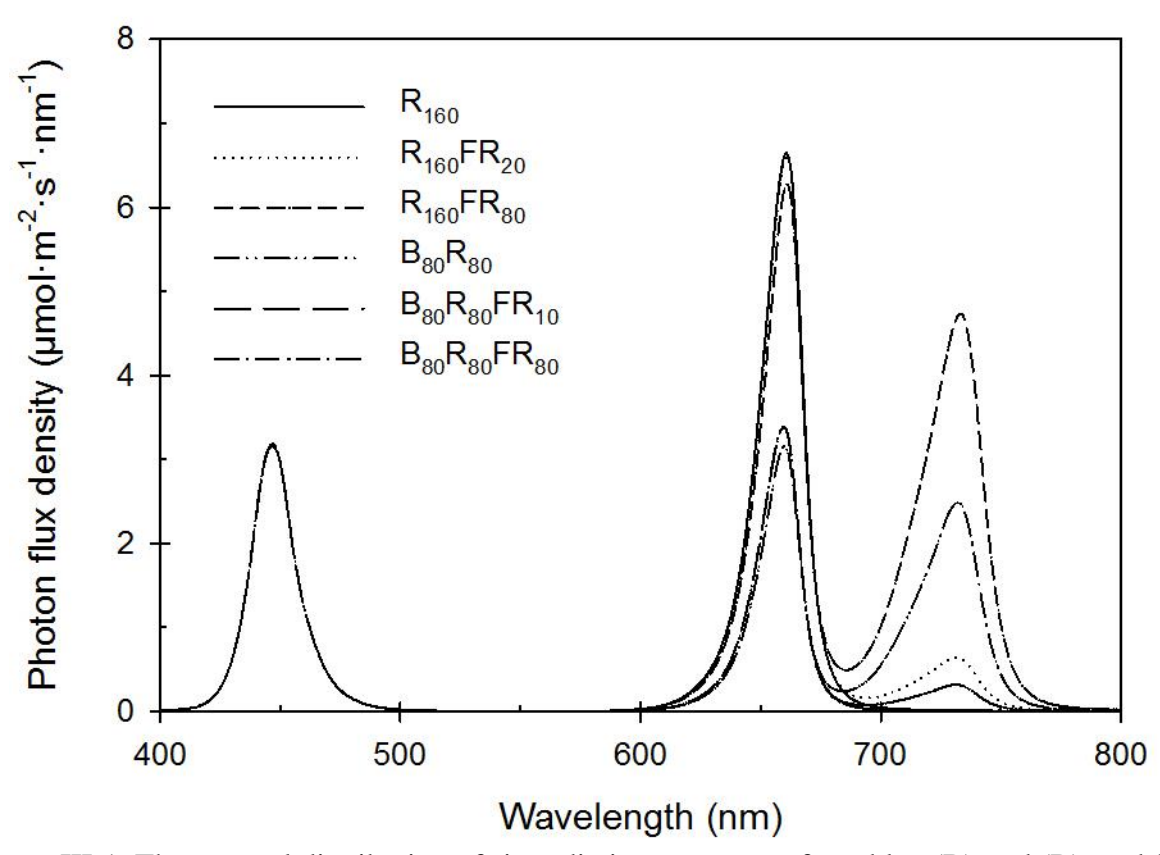


Figure III-1. The spectral distribution of six radiation treatments from blue (B), red (R), and farred (FR) light-emitting diodes (LEDs). The values after each LED type indicate their photon flux density in  $\mu$ mol·m<sup>-2</sup>·s<sup>-1</sup>.

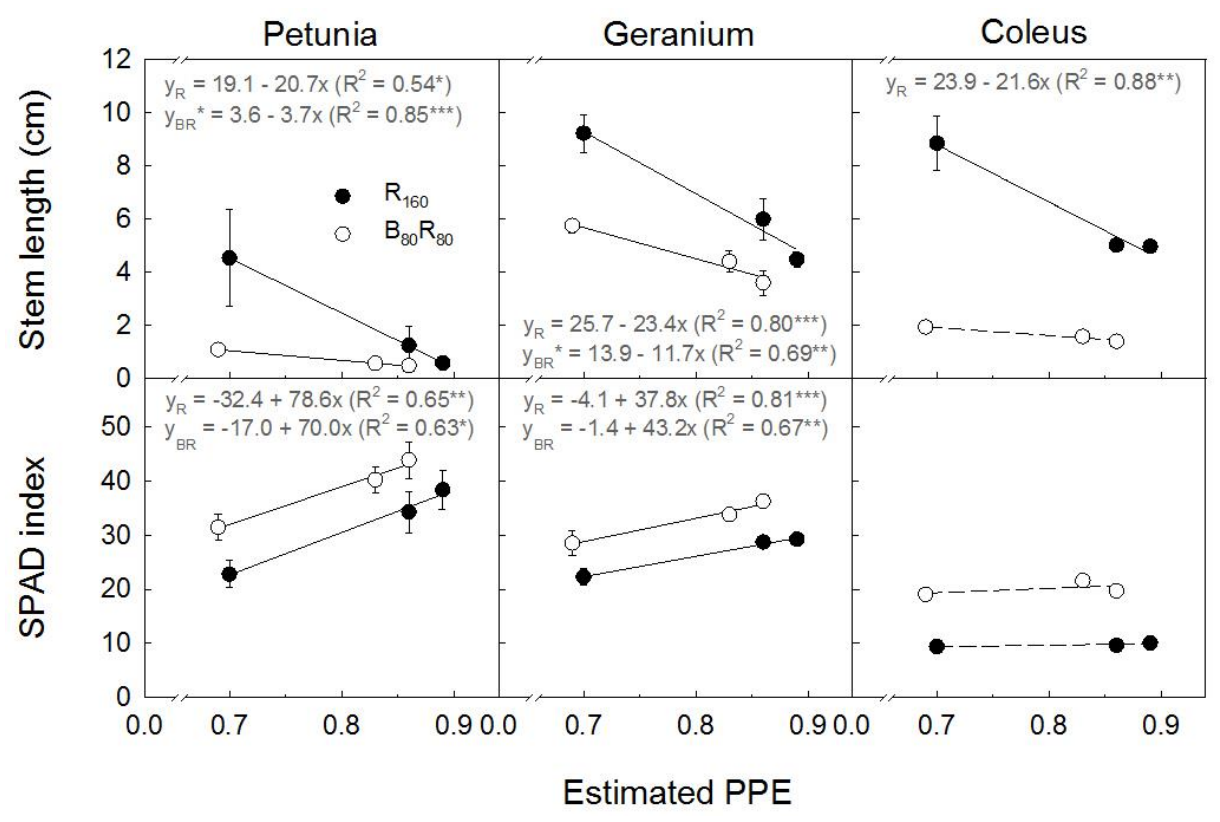


Figure III-2. Influence of the estimated phytochrome photoequilibria (PPE) of sole-source lighting on stem length and SPAD index of seedlings grown under a photosynthetic photon flux density of 160  $\mu$ mol·m<sup>-2</sup>·s<sup>-1</sup> with red (R<sub>160</sub>) or blue and red radiation (B<sub>80</sub>R<sub>80</sub>). Data points represent the means of two replications for coleus and three replications for petunia and geranium, and vertical bars are standard errors of the means (n = 2 for coleus and n = 3 for petunia and geranium). Associated correlation coefficients (R<sup>2</sup>) and regression equations are presented when statistically significant (solid line) but not when not significant (dashed line). \*, \*\*, or \*\*\* indicate significant at P < 0.05, 0.01 or 0.001, respectively.  $y_{BR}$ \* indicates that the slopes of the regression lines are significantly different for the two B levels (P < 0.05).

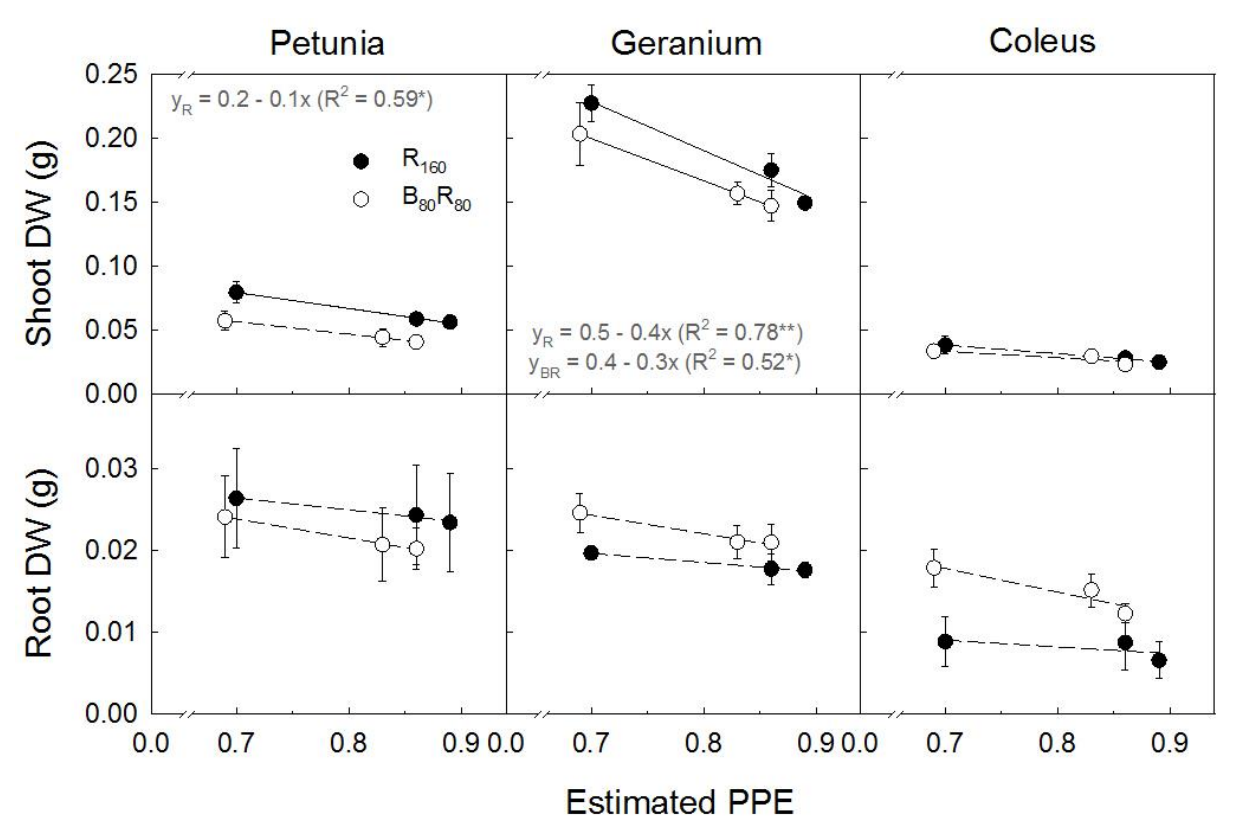


Figure III-3. Influence of the estimated phytochrome photoequilibria (PPE) of sole-source lighting on dry weight (DW) of seedlings grown under a photosynthetic photon flux density of  $160 \ \mu \text{mol} \cdot \text{m}^{-2} \cdot \text{s}^{-1}$  with red (R<sub>160</sub>) or blue and red radiation (B<sub>80</sub>R<sub>80</sub>). Data points represent the means two replications for coleus and three replications for petunia and geranium, and vertical bars are standard errors of the means (n = 2 for coleus and n = 3 for petunia and geranium). Associated correlation coefficients (R<sup>2</sup>) and regression equations are presented when statistically significant (solid line) but not when not significant (dashed line). \* or \*\* indicate significant at P < 0.05 or 0.01, respectively.

LITERATURE CITED

#### LITERATURE CITED

- Adams, S.R., S. Pearson, P. Hadley, and W.M. Patefield. 1999. The effects of temperature and light integral on the phases of photoperiod sensitivity in *Petunia*×*hybrida*. Ann. Bot. 83:263–269.
- Batschauer, A. 2005. Plant cryptochromes: Their genes, biochemistry, and physiological roles. In: Briggs, W.R. and J.L. Spudich. (eds.) Handbook of Photosensory Receptors. Weinheim, Germany: Wiley VCH, pp. 211–258.
- Casal, J.J. 2000. Phytochromes, cryptochromes, phototropin: photoreceptor interactions in plants. Photochem. Photobiol. 71:1–11.
- Christie, J.M., L. Blackwood, J. Petersen, and S. Sullivan. 2015. Plant flavoprotein photoreceptors. Plant Cell Physiol. 56:401–413.
- Cope, K.R. and B. Bugbee. 2013. Spectral effects of three types of white light-emitting diodes on plant growth and development: absolute versus relative amounts of blue light. HortScience 48:504–509.
- Craig, D.S. and E.S. Runkle. 2016. An intermediate phytochrome photoequilibria from night-interruption lighting optimally promotes flowering of several long-day plants. Environ. Exp. Bot. 121:132–138.
- de Wit, M., D.H. Keuskamp, F.J. Bongers, P. Hornitschek, C.M.M. Gommers, E. Reinen, C. Martínez-Cerón, C. Fankhauser, and R. Pierik. 2016. Integration of phytochrome and cryptochrome signals determines plant growth during competition for light. Curr. Biol. 26:3320–3326.
- Erwin, J., N. Mattson, and R. Warner. 2017. Light effects on bedding plants. In: Lopez, R. and E.S. Runkle. (eds.) Light management in controlled environments. Meister Media Worldwide, Willoughby, OH, pp.119–134.
- Fankhauser, C. 2001. The phytochromes, a family of red/far-red absorbing photoreceptors. J. Biol. Chem. 276:11453–11456.
- Franklin K.A. 2008. Shade avoidance. New Phytol. 179:930–944.
- Franklin, K.A. 2016. Photomorphogenesis: Plants feel blue in the shade. Curr. Biol. 26:R1275–R1276.
- Guo, H., H. Duong, N. Ma, and C. Lin. 1998. The Arabidopsis blue light receptor cryptochrome 2 is a nuclear protein regulated by a blue light dependent post-transcriptional mechanism. Plant J. 19:279–287.

- Hernández, R., and C. Kubota. 2016. Physiological responses of cucumber seedlings under different blue and red photon flux ratios using LEDs. Environ. Exp. Bot. 121:66–74.
- Kami, C., S. Lorrain, P. Hornitschek, and C. Fankhauser. 2010. Light-regulated plant growth and development. Curr. Top. Dev. Biol. 91:29–66.
- Keller, M.M., Y. Jaillais, U.V. Pedmale, J.E. Moreno, J. Chory, and C.L. Ballaré. 2011. Cryptochrome 1 and phytochrome B control shade-avoidance responses in *Arabidopsis* via partially independent hormonal cascades. Plant J. 67:195–207.
- Lopez, R.G. and E.S. Runkle. 2008. Photosynthetic daily light integral during propagation influences rooting and growth of cuttings and subsequent development of New Guinea impatiens and petunia. HortScience 43:2052–2059.
- Li, J., G. Li, H. Wang, and X.W. Deng. 2011. Phytochrome signaling mechanisms. The Arabidopsis Book e0148.
- Lin, C. 2002. Blue light receptors and signal transduction. Plant Cell 14:207–225.
- Liu, H., B. Liu, C. Zhao, M. Pepper, and C. Lin. 2011. The action mechanisms of plant cryptochromes. Trends Plant Sci. 16:684–91.
- Mas, P., P.F. Devlin, S. Panda, and S.A. Kay. 2000. Functional interaction of phytochrome B and cryptochrome 2. Nature 408:207–211.
- Mazzella, M., and J. Casal. 2001. Interactive signalling by phytochromes and cryptochromes generates de-etiolation homeostasis in Arabidopsis thaliana. Plant Cell Environ. 24:155–161.
- Meng, Q. and E.S. Runkle. 2015. Low-intensity blue light in night-interruption lighting does not influence flowering of herbaceous ornamentals. Sci. Hort. 186:230–238.
- Meng, Q. and E.S. Runkle. 2017. Moderate-intensity blue radiation can regulate flowering, but not extension growth, of several photoperiodic ornamental crops. Environ. Exp. Bot. 134:12–20.
- Mockler, T., H. Yang, X. Yu, D. Parikh, Y.C. Cheng, S. Dolan, and C. Lin. 2003. Regulation of photoperiodic flowering by Arabidopsis photoreceptors. Proc. Natl. Acad. Sci. USA 100: 2140–2145.
- Mockler, T.C., H. Guo, H. Yang, H. Duong, and C. Lin. 1999. Antagonistic actions of Arabidopsis cryptochromes and phytochrome B in the regulation of floral induction. Development 126:2073–2082.

- Morgan, D.C. and H. Smith. 1978. The relationship between phytochrome-photoequilibrium and Development in light grown *Chenopodium album* L. Planta 142:187–193.
- Oh, W., E.S. Runkle, and R.M. Warner. 2010. Timing and duration of supplemental lighting during the seedling stage influence quality and flowering in petunia and pansy. HortScience 45:1332–1337.
- Park, Y. and E.S. Runkle. 2017. Far-red radiation promotes growth of seedlings by increasing leaf expansion and whole-plant net assimilation. Environ. Exp. Bot. 136:41–49.
- Pedmale, U.V., S.C. Huang, M. Zander, B.J. Cole, J. Hetzel, K. Ljung, P.A.B. Reis, P. Sridevi, K. Nito, J.R., Nery JR *et al.* 2016. Cryptochromes interact directly with PIFs to control plant growth in limiting blue light. Cell 164:233–245.
- Rockwell, N.C., Y.S. Su, and J.C. Lagarias. 2006. Phytochrome structure and signaling mechanisms. Annu. Rev. Plant Biol. 57:837–858.
- Runkle, E.S. and R.D. Heins. 2001. Specific functions of red, far red, and blue light in flowering and stem extension of long-day plants. J. Amer. Soc. Hort. Sci. 126:275–282.
- Runkle, E.S. and R.D. Heins. 2003. Photocontrol of flowering and extension growth in the long-day plant pansy. J. Amer. Soc. Hort. Sci. 128:479–485.
- Sager, J.C., W.O. Smith, J.L. Edwards, and K.L. Cyr. 1988. Photosynthetic efficiency and phytochrome photoequilibria determination using spectral data. Trans. Amer. Soc. Agr. Eng. 31:1882–1889.
- Shalitin, D., Yang, H., Mockler, T.C., Maymon, M., Guo, H., Whitelam, G.C., and Lin, C. 2002. Regulation of Arabidopsis cryptochrome 2 by blue-light-dependent phosphorylation. Nature 417:763–767.
- Shalitin, D., X. Yu, M. Maymon, T. Mockler, and C. Lin. 2003. Blue light-dependent in vivo and in vitro phosphorylation of Arabidopsis cryptochrome1. Plant Cell 15:2421–2429.
- Sharrock, R.A. 2008. The phytochrome red/far-red photoreceptor superfamily. Genome Biol. 9: 230.
- Smith, H. and M.G. Holmes. 1977. The function of phytochrome in the natural environment. III. Measurement and calculation of phytochrome photoequilibirum. Phytochem. Photobiol. 25:547–550.
- Smith, H. 1982. Light quality, photoreception, and plant strategy. Ann. Rev. Plant Physiol. 33:481–518.
- Snowden, M.C., K.R. Cope, and B. Bugbee. 2016. Sensitivity of seven diverse species to blue and green light: interactions with photon flux. PLoS One 11:e0163121.

- Su, J., B. Liu, J. Liao, Z. Yang, C. Lin, and Y. Oka. 2017. Coordination of cryptochrome and phytochrome signals in the regulation of plant light responses. Agronomy 7:25.
- Usami T., N. Mochizuki, M. Kondo, M. Nishimura, and A. Nagatani. 2004. Cryptochromes and phytochromes synergistically regulate Arabidopsis root greening under blue light. Plant Cell Physiol. 45:1798–1808.
- Wollaeger, H.M. and E.S. Runkle. 2013. Growth responses of ornamental annual seedlings under different wavelengths of red light provided by light-emitting diodes. HortScience 48:1478–1483.
- Wollaeger, H.M. and E.S. Runkle. 2015. Growth and acclimation of impatiens, salvia, petunia, and tomato seedlings to blue and red light. HortScience 50:522–529.
- Yu, X., H. Liu, J. Klejnot, and C. Lin. 2010. The cryptochrome blue light receptors. Arabidopsis Book 8:e0135.

## **SECTION IV**

SPECTRAL EFFECTS OF LIGHT-EMITTING DIODES ON PLANT GROWTH, VISUAL COLOR QUALITY, AND PHOTOSYNTHETIC PHOTON EFFICACY

Spectral Effects of Light-emitting Diodes on Plant Growth, Visual Color Quality, and

Photosynthetic Photon Efficacy

Yujin Park<sup>1</sup> and Erik S. Runkle<sup>2</sup>

Department of Horticulture, 1066 Bogue Street, Michigan State University, East Lansing, MI

48824

This research is supported by Osram Opto Semiconductors; the USDA-ARS Floriculture and

Nursery Research Initiative; the USDA National Institute of Food and Agriculture, Hatch project

192266; Michigan State University's (MSU) AgBioResearch and Project GREEEN; and

horticulture companies supportive of MSU floriculture research. We thank C. Raker & Sons for

donation of plant material and Nate DuRussel for technical assistance. We also thank Dr. David

Hamby (OSRAM Sylvania), Rodrigo Pereyra (OSRAM Innovation), and Dr. Chieri Kubota (The

Ohio State University) for valuable input in this manuscript.

<sup>1</sup>Graduate student.

<sup>2</sup>Corresponding author. E-mail address: runkleer@msu.edu.

106

#### **Abstract**

Arrays of blue (B, 400–500 nm) and red (R, 600–700 nm) light-emitting diodes (LEDs) are often used for plant applications, but they make plants appear purplish, causing difficulties in detecting nutritional deficiencies, diseases, and physiological disorders compared to a broad spectrum (white light). Although white (W) LEDs are sometimes used in horticultural lighting fixtures, surprisingly little research has been published using them for sole-source lighting of plants. We postulated that compared to a B+R mixture, using W LEDs in sole-source lighting would elicit similar growth attributes of young plants while enhancing the visual color quality and without an excessive decrease in photosynthetic photon efficacy (PPE). We grew seedlings of begonia (Begonia × semperflorens), geranium (Pelargonium × horturum), petunia (Petunia ×hybrida), and snapdragon (Antirrhinum majus) at 20 °C under six sole-source LED lighting treatments with a photosynthetic photon flux density (PPFD) of 160 µmol·m<sup>-2</sup>·s<sup>-1</sup> using B (peak= 447 nm), green (G, peak= 531 nm), R (peak= 660 nm), and/or mint W (MW, peak=558 nm) LEDs that emitted 15% B, 59% G, and 26% R plus 6 µmol·m<sup>-2</sup>·s<sup>-1</sup> of far-red radiation. The lighting treatments (with percentage from each LED in subscript) were MW<sub>100</sub>, MW<sub>75</sub>R<sub>25</sub>, MW<sub>45</sub>R<sub>55</sub>, MW<sub>25</sub>R<sub>75</sub>, B<sub>15</sub>R<sub>85</sub>, and B<sub>20</sub>G<sub>40</sub>R<sub>40</sub>. At the transplant stage, seedling height, total leaf area, and fresh and dry weight were similar among treatments in all species except for seedling height in snapdragon, which were 26–33% taller under MW<sub>100</sub>, MW<sub>75</sub>R<sub>25</sub> and MW<sub>25</sub>R<sub>75</sub> than under B<sub>15</sub>R<sub>85</sub>. Surprisingly, when petunia seedlings were grown longer (beyond the transplant stage) under sole-source lighting treatments, the primary stem elongated and initiated flower buds earlier under MW<sub>100</sub> and MW<sub>75</sub>R<sub>25</sub> compared to under B<sub>15</sub>R<sub>85</sub>. Among the six radiation treatments, the color rendering index of MW<sub>75</sub>R<sub>25</sub> and MW<sub>45</sub>R<sub>55</sub> were 72, and 77, respectively, which was higher than those of other treatments, which were  $\leq$ 64. The correlated color

temperature of  $MW_{45}R_{55}$  (3018 K) was within the recommended range (2700–4000K) for high quality white light. While PPE of  $B_{15}R_{85}$  (2.25  $\mu$ mol·J<sup>-1</sup>) was higher than the W light treatments (1.51–2.13  $\mu$ mol·J<sup>-1</sup>), the dry weight gain per electric energy consumption (in g·kWh<sup>-1</sup>) of  $B_{15}R_{85}$  was similar to those of  $MW_{25}R_{75}$ ,  $MW_{45}R_{55}$ , and  $MW_{75}R_{25}$  in three species. We conclude that compared to B+R radiation, W radiation had generally similar effects on seedling growth at the same PPFD with similar electric energy consumption, and improved the visual color quality of sole-source lighting. White LEDs can also promote stem elongation and flowering in at least some species.

Keywords: green radiation, LEDs, sole-source lighting, white radiation

Abbreviations:

B, blue radiation; CCT, correlated color temperature; CRI, color rendering index; DLI, daily light integral; DW, dry weight; DWE, dry weight efficacy; FR, far-red radiation; LEDs, light-emitting diodes; LMA, leaf mass per area; PAR, photosynthetically active radiation; PPE, photosynthetic photon efficacy; PPFD, photosynthetic photon flux density; PSS, phytochrome photostationary state; R, red; YPFD, yield photon flux density.

## Introduction

Light-emitting diodes (LEDs) are increasingly being used in the production of specialty crops (e.g., ornamental transplants and leafy greens) grown in controlled environments, including greenhouses and indoor vertical farms. When used indoors, sole-source lighting from LEDs enables one to tailor the radiation spectrum to elicit desirable plant growth attributes. Red

(R, 600–700 nm) radiation is often considered the most efficient at driving photosynthesis based on the quantum yield from instantaneous leaf photosynthesis measurements (McCree, 1972).

Blue (B, 400–500 nm) radiation is added to R for normal photosynthetic functioning and to obtain desired phenotypes (Brown et al., 1995; Dougher and Bugbee, 2001; Yorio et al., 2001; Hogewoning et al., 2010). B and R LEDs also have the highest efficacy values in terms of photosynthetic photons emitted per watt of electricity [or photosynthetic photon efficacy (PPE) in μmol·J<sup>-1</sup>] (Nelson and Bugbee, 2014). Thus, many commercial LED arrays developed for plant applications contain B and R LEDs. Diverse vegetable and floriculture crops have been grown successfully under the B+R sole-source lighting, including lettuce (*Lactuca sativa*), tomato (*Solanum lycopersicum*), cucumber (*Cucumis sativus*), impatiens (*Impatiens walleriana*), salvia (*Salvia splendens*), petunia (*Petunia* × *hybrida*), vinca (*Catharanthus roseus*), geranium (*Pelargonium* × *hortorum*), and French marigold (*Tagetes patula*) (Son and Oh, 2013; Randall and Lopez, 2015; Wollaeger and Runkle, 2015; Hernández and Kubota, 2016).

One limitation of using B+R LEDs is that plants appear purplish to the human eye, causing difficulties in detecting nutritional deficiencies, diseases symptoms, and physiological disorders. One possible solution is to add green (G, 400–500 nm) radiation to a B+R spectrum. Leaves absorb G radiation less effectively (by 16–23%) than B and R radiation (Moss and Lumis, 1951), and two largest peaks of the relative quantum efficiency curve are in B and R radiation region (McCree, 1972). Therefore, G radiation has been considered less efficient at driving photosynthesis than B or R radiation. However, in general, at a constant photosynthetic photon flux density (PPFD), substituting B or R radiation with G radiation does not decrease plant growth. For example, shoot dry weight of impatiens, tomato, salvia, and petunia seedlings was similar under B+R (1:1) and under B+G (1:1) (at PPFD of 160 µmol·m<sup>-2</sup>·s<sup>-1</sup>) (Wollaeger and

Runkle, 2014). Similarly, in cherry tomato (*Lycopersicon esculentum*), plants grown under B+R (1:1) and B+R+G (3:3:1) had similar shoot dry weights (at PPFD of 320 μmol·m<sup>-2</sup>·s<sup>-1</sup>) (Liu et al., 2011). In tomato, cucumber, pepper (*capsicum annum*), soybean (*Glycine max*), lettuce, and wheat (*Triticum aestivium*), substituting R radiation with G from 0% to 30% did not influence dry mass accumulation (at PPFD of 200 and 500 μmol·m<sup>-2</sup>·s<sup>-1</sup>) (Snowden et al., 2016). In addition, the substitution of 24% R radiation with G increased leaf area and dry weight (at PPFD of 150 μmol·m<sup>-2</sup>·s<sup>-1</sup>) (Kim et al., 2004). Therefore, compared to B+R radiation, including G radiation in a sole-source lighting spectrum can have similar effects on plant growth while enabling people to more easily evaluate plant growth.

However, G LEDs are inefficient at converting electricity into photons (referred to as the "green gap") and thus, adding G radiation from G LEDs is currently not practical. Another strategy is to use white LEDs, alone or with R and/or B LEDs, to create a broad spectrum. White LEDs, which are created by adding phosphors to B LEDs to convert some of the B radiation to G and R, have a higher PPE value than G LEDs (Nelson and Bugbee, 2014), and they emit a high portion of G radiation (e.g., 41 to 48%) (Snowden et al., 2016). Mixing these different narrowand broad-band LEDs in various proportions enables control of the portions of B, G, and R radiation for both desirable human vision and plant growth responses.

The main considerations when determining the radiation spectrum of sole-source LED lighting have been its effects on plant growth attributes and its PPE. Meanwhile, a trade-off was made between the PPE of LEDs and its effects on human vision. Therefore, the challenge is to optimize the radiation spectrum for enhancing plant growth and PPE, while improving human vision performance. Here, we used mint white (MW) LEDs, which are rich in G radiation (59% of the PAR), and R LEDs to investigate the effects of different shades of white light on human

vision, PPE, and plant growth and subsequent development of ornamental seedlings compared to a typical mixture of B+R radiation at the same PPFD. We postulated that compared to a typical B+R mixture, delivery of G radiation from MW LEDs would produce young plants with similar growth attributes while improving human vision, and with a minimal decrease in PPE. To evaluate the different colors of our lighting treatments and their effects on human vision, we quantified the correlated color temperature (CCT) and the color rendering index (CRI). We performed an experiment in highly controlled environments to evaluate plant growth attributes including fresh and dry weight, a variety of morphological traits, and subsequent flowering.

#### **Materials and Methods**

Plant materials

Begonia (*Begonia* × *semperflorens* 'Olympia Red'), geranium (*Pelargonium* × *hortorum* 'Deep Rose'), petunia (*Petunia* × *hybrida* 'Wave Blue'), and snapdragon (*Antirrhinum majus* 'Liberty Classic') were selected for study because of their commercial significance and variations in shade tolerance and photoperiodic flowering response. Geranium, petunia, and snapdragon are shade-avoiding species while begonia is shade-tolerant. Geranium and begonia are day neutral; petunia and snapdragon are quantitative long-day plants. Seeds of each species were sown in 128-cell (2.7 × 2.7-cm; 12.0-mL volume) plug trays at a commercial greenhouse (C. Raker and Sons, Inc., Litchfield, MI). They were then transferred to research greenhouses at Michigan State University (East Lansing, MI) with a 16-h photoperiod at 20 °C after the following number of days (rep. 1, 2): begonia (9, 17), geranium (9, 8), petunia (10, 9), and snapdragon (10, 9). The first true leaves emerged after the following number of days from seed sow (rep 1, 2): begonia (21, 19), geranium (9, 10), petunia (14, 14), and snapdragon (14, 14).

Each plug tray was then cut into four sections (each with ≥30 seedlings), thinned to one plant per cell, and placed in each of six LED modules.

Radiation treatments and growth conditions

Six LED modules described by Wollaeger and Runkle (2013) were located inside a refrigerated walk-in growth chamber at a constant temperature set point of 20 °C. Each module was fitted with a new panel that contained 80 B (peak = 447 nm), G (peak = 531 nm), R (peak = 660 nm), and MW (peak = 558 nm) LEDs. The six treatments were designed to investigate the effects of MW with or without R on plant growth compared to a typical B+R radiation spectrum (Table 1). Each module delivered a PPFD of 160 µmol·m<sup>-2</sup>·s<sup>-1</sup> that consisted of the following percentages: MW<sub>100</sub> (100% PPFD from MW LEDs), MW<sub>75</sub>R<sub>25</sub>, MW<sub>45</sub>R<sub>55</sub>, MW<sub>25</sub>R<sub>75</sub>, B<sub>20</sub>G<sub>40</sub>R<sub>40</sub>, and  $B_{15}R_{85}$ . The photoperiod was 18 h [creating a daily light integral (DLI) of 10.4 mol·m<sup>-2</sup>·d<sup>-1</sup>] as controlled by a data logger (CR10; Campbell Scientific, Logan, UT). For each replication, the radiation treatments were delivered following methods described by Park and Runkle (2017), and the plug trays were rotated daily inside each LED module to mitigate any positional effects. For each radiation treatment, the percentage of each waveband and R: far red (FR, 700–800 nm) was calculated using 100-nm wavebands; the phytochrome photostationary state (PSS) was estimated as described by Sager et al. (1988); and the yield photon flux density (YPFD), which is the product of photon flux density and relative quantum efficiency, was calculated based on McCree (1972) and Sager et al. (1988) (Table 1).

The 1931 CIE (x, y) chromaticity coordinates and CRI for each radiation treatment were determined by entering spectrum data into the ColorCalculator software (version 7.23; OSRAM Sylvania, Wilmington, NC, <a href="https://www.osram.us/cb/tools-and-resources/applications/led-colorcalculator/index.jsp">https://www.osram.us/cb/tools-and-resources/applications/led-colorcalculator/index.jsp</a>) (Fig. 2). The CCT for each radiation treatment was derived from the

1931 CIE (x, y) chromaticity coordinates using the following equation (McCamy, 1992): CCT (x, y) =  $-449n^3 + 3525n^2 - 6823.3n + 5520.33$ ; where n = (x - 0.3320)/(y - 0.1858). The PPE of each LED type (at supply amperage of 450 mA) was 1.80, 0.54, 2.33, and 1.52  $\mu$ mol·J<sup>-1</sup> for B, G, R, and MW LEDs (D. Hamby, OSRAM, personal communication in October, 2017), and the PPE of each radiation treatment was estimated by the product of the PPE of each LED type and the percentage of the total PPFD delivered by each LED type (Fig. 2).

In each treatment, air and plant canopy temperature and radiation intensity were monitored and recorded as described by Park and Runkle (2017). Average air/canopy temperatures (°C) during the experimental periods were 21.1/21.0, 21.0/21.0, 21.1/21.2, 20.9/21.3, 20.5/20.7, and 21.0/21.3 for the MW<sub>100</sub>, MW<sub>75</sub>R<sub>25</sub>, MW<sub>45</sub>R<sub>55</sub>, MW<sub>25</sub>R<sub>75</sub>, B<sub>15</sub>R<sub>85</sub>, and B<sub>20</sub>G<sub>40</sub>R<sub>40</sub> treatments, respectively. All temperatures had standard deviations (SD)  $\leq \pm 1.0$  °C. Plants were irrigated as needed, every two or three days, through subsurface irrigation with deionized water supplemented with a water-soluble fertilizer providing (in mg·L<sup>-1</sup>) 50 N, 19 P, 50 K, 23 Ca, 4 Mg, 1 Fe, 0.5 Mn, 0.5 Zn, 0.5 Cu, 0.3 B, and 0.1 Mo (MSU Plug Special; GreenCare Fertilizers, Inc., Kankakee, IL). The EC and pH of the nutrient solution was 0.43 mS·cm<sup>-1</sup> and 6.2, respectively.

#### Data collection and analysis

The experiment was performed twice. In each replication, at the end of the seedling stage, ten random plants of each species in each treatment, usually excluding outer guard rows, were harvested the following number of days after seed sow (rep 1, 2): begonia (51, 52), geranium (33, 32), petunia (31, 34), and snapdragon (36, 37). The harvest times were determined when the seedlings were ready for transplanting (when the roots had grown sufficiently so that the

seedlings could be easily pushed out of the trays with the entire root zone intact) and varied presumably because of differences in seed vigor.

The following data were collected on plants in each treatment: leaf (at node) number, total leaf area, stem length (from media surface to the apical meristem), and root and shoot fresh and dry weight. Petunia typically grows as a rosette and so its stem length was not measured at the transplant stage. A visible leaf that was ≥25% unfolded was counted in leaf number and included in leaf area. Total leaf area per plant was measured using a leaf-area meter (LI-3000; LI-COR). Average individual leaf area was determined by dividing total leaf area by leaf number for each plant. For fresh and dry weight measurements, the shoot was excised at the medium surface, and the medium was carefully washed off to separate the roots. The shoots and roots were placed in separate envelopes and dried in an oven at  $\geq$ 66 °C for  $\geq$ 5 d and weighed using an analytical balance (AB204-S; Mettler Toledo, Columbus, OH). Plant dry and fresh weight was determined by the sum of fresh and dry weight of shoot and root. Net assimilation was determined by dividing plant dry weight gain per unit leaf area for all species (Gregory, 1917; Snowden et al., 2016). For petunia, at the end of the seedling stage, 10 seedlings in each treatment were randomly selected and continuously grown under the LED modules until 59 d after seed sow for both replications. For both replications, date of the first visible bud was recorded for each plant and stem length was measured 53 d after seed sow.

Dry weight gain per electric energy consumption or dry weight efficacy (DWE) (in  $g \cdot kWh^{-1}$ ) for each radiation treatment and species in Table 2 was calculated using the following equation (1):

$$DWE = \frac{DW \times N}{EEC}$$
 (1)

where DW is dry weight (g) per plant for each radiation treatment and species; N is the total

number of plants (128 seedlings) per LED module; and EEC is the electric energy consumption (kWh) per LED module (or each radiation treatment) for each species, which was estimated in the following equation (2):

$$EEC = \frac{PP \times TH}{PPE}$$
 (2)

where PP is the output of photosynthetic photons ( $\mu$ mol·s<sup>-1</sup>) needed for the growing area in each LED module; TH is the total number of hours of sole-source lighting during the experiment, which was calculated by multiplying the photoperiod (18 h·d<sup>-1</sup>) by the period of sole-source lighting treatments (34, 25, 24 and 19 d for begonia, geranium, snapdragon, and petunia, respectively); PPE is photosynthetic photon efficacy ( $\mu$ mol·J<sup>-1</sup> or  $\mu$ mol·s<sup>-1</sup>·W<sup>-1</sup>), which was calculated for each radiation treatment (Table 2) using the following the equation (3);

$$PP = \frac{PPFD \times A}{PUF}$$
 (3)

where PPFD is the PPFD for the sole-source lighting treatments ( $160 \, \mu mol \cdot m^{-2} \cdot s^{-1}$ ); A is the growing area (or the bottom surface area) of each LED module ( $0.8 \, m \times 0.27 \, m = 0.216 \, m^2$ ); and PUE is the photon use efficiency of the LED module, which indicates the proportion of the photon flux received by the growing area (or the bottom surface) compared to that emitted by the LED fixtures. PUE depends on the properties of the LED fixture, such as beam distribution, reflector design, and geometries (Hernandez and Kubota, 2015). In this study, considering the highly reflective walls of each LED module, the PUE was estimated as 0.9.

The experiment used a randomized complete block design with two blocks and ten subsamples per block. Each replication was regarded as a block. Each LED module was regarded as the experimental unit for the radiation treatment. Within each LED module, ten individual seedlings per species were the sub-samples or observational units. Data were analyzed with SAS (version 9.4; SAS Institute, Cary, NC) using the PROC MIXED procedure [with a fixed factor

for radiation treatments, a random factor of blocks (or replications), and a random factor for interaction between blocks and radiation treatments] that provided pairwise comparisons between treatments using Tukey's honestly significant test at  $P \le 0.05$ .

#### **Results and Discussion**

*Visual and color properties* 

CRI evaluates the accuracy of light sources to render human color perception of objects compared to a reference light source (including black body radiation for light sources having CCT <5000 K, or natural daylight for those having CCT  $\geq$ 5000 K) (Ohno, 2005; Pust et al., 2015). The maximum value of CRI is 100, and a light source with a CRI  $\geq$ 80 is typically considered good at rendering the color of objects and elicits a comfortable human visual perception (Sasabe et al., 2013). For example, typical CRI values of common light sources include 100 for incandescent lamps, 89 for fluorescent lamps, and 24 for high-pressure sodium lamps (Thejokalyani and Dhoble, 2014). The CRI values can be negative when light sources have low accuracy of color rendering (Ohno, 2005). In this study, the CRI value of  $B_{15}R_{85}$  was negative, while  $MW_{100}$  had a CRI value of 64 and substituting MW with R LEDs by 25% or 55% increased the CRI to 77 or 72, respectively (Fig. 2). However, when 75% of MW was substituted with R, CRI value decreased to 47, which was lower than  $B_{20}G_{40}R_{40}$  (CRI = 56). The CRI values for all of our white light treatments were lower than the recommended CRI value  $\geq$ 80, but were much higher than a typical B+R spectrum used in horticulture.

The color appearance of light emitted by a light source can be described with CCT (Both et al., 2017). CCT is the absolute temperature of a blackbody radiator, expressed in degrees Kelvin (K), whose chromaticity is closest to that of the light source (Ohta and Robertson, 2006;

Thejokalyani and Dhoble, 2014). Based on CCT value, white light can be categorized as warm white (2500–3500 K), neutral white (3500–4500 K), and cool white (4500–5500 K) (Pust et al., 2015). The MW LEDs used in this study had a CCT of 4657 K and thus can described as cool white. As MW was increasingly substituted with R, the CCT decreased to 1979 K (Fig. 2). Thus, the white light created by  $MW_{75}R_{25}$  (4116 K) and  $MW_{45}R_{55}$  (3018 K) can be categorized into neutral white and warm white, respectively. In addition, the CCT of  $MW_{45}R_{55}$  was within the recommended CCT ranges (2700–4000K) for a natural color perception (Pust et al., 2015). The CCT values for  $B_{15}R_{85}$  (14766 K) and  $B_{20}G_{40}R_{40}$  (9842 K) were outside of the range of white light.

### Plant growth and development

In general, seedling growth characteristics, including plant height, total leaf area, and fresh and dry weight of all species tested in this study were similar among the different shades of white radiation and B+R radiation at the same PPFD, except for seedling height in snapdragon (Fig. 3). In snapdragon, seedlings grown under  $MW_{100}$ ,  $MW_{75}R_{25}$  and  $MW_{25}R_{75}$  were 26–33% taller than those grown under  $B_{15}R_{85}$ . Similarly, when petunia seedlings were grown longer (beyond the transplant stage) under the sole-source lighting treatments, the primary stem elongated and had flower buds earlier under  $MW_{100}$  and  $MW_{75}R_{25}$  compared to under  $B_{15}R_{85}$  (Fig. 4). The differences in radiation spectrum between  $MW_{100}$  and  $MW_{75}R_{25}$  and  $B_{15}R_{85}$  treatments include a higher portion of G radiation and a lower R:FR (Table 1), both of which can affect stem elongation and flowering time.

A few studies showed that G radiation, similar to FR radiation, induces shade-avoidance responses, including elongated hypocotyls and petioles (Folta, 2004; Zhang et al., 2011; Wang et al., 2015). Genetic studies have demonstrated that G radiation reverses B radiation-mediated

inhibition of hypocotyl and stem elongation by inactivating cryptochromes (Banerjee et al., 2007; Bouly et al., 2007; Sellaro et al., 2010). In addition, while the effects on G radiation on flowering are still less clear, the heading of wheat was promoted as the portion of G radiation in the radiation spectrum increased (Kasajima et al., 2007). In this study, the percentage of G radiation (in PAR) of  $MW_{100}$  and  $MW_{75}R_{25}$  was 59% and 45%, respectively while  $B_{15}R_{85}$  had 0% of G radiation (Table 1). Thus, the stem elongation and flowering promotion under  $MW_{100}$  and  $MW_{75}R_{25}$  could be at least partly attributed an increasing percentage of G radiation in the  $MW_{100}$  and  $MW_{75}R_{25}$  treatments.

In addition, increasing the amount of FR radiation (or decreasing the R:FR) stimulates extension growth, creating taller plants (Smith, 1982). For example, in the shade-avoiding geranium, petunia, and snapdragon, stem length increased linearly as the R:FR decreased from 1:0 to 1:1 (Park and Runkle, 2017). The R:FR is also involved in regulating photoperiodic flowering, and an intermediate R:FR of photoperiodic lighting during the finishing stage and sole-source lighting during the seedling stage accelerated flowering in some long-day plants (Sullivan and Deng, 2003; Craig and Runkle, 2016; Park and Runkle, 2017). In this study,  $MW_{100}$  and  $MW_{75}R_{25}$  emitted a small amount of FR radiation (4–6  $\mu$ mol·m<sup>-2</sup>·s<sup>-1</sup>) and thus had a lower R:FR (8:1–17:1) value than other treatments (Table 1). Thus, the stem elongation and flowering promotion under  $MW_{100}$  and  $MW_{75}R_{25}$  could also be influenced by a lower R:FR. Because of the possible interactions of G radiation, the R:FR ratio, and other differences in the spectrum, we cannot attribute the stem elongation and flowering promotion responses under the  $MW_{100}$  and  $MW_{75}R_{25}$  treatments to specific spectral components.

In plant growth analysis, total leaf area and net assimilation determines plant dry weight gain (Gregory, 1917; Casal, 2013; Snowden et al., 2016). Light quality can influence plant dry

mass accumulation by altering leaf expansion and by affecting photosynthesis associated with the wavelength dependence of the quantum yield (Hogewoning et al. 2010; Park and Runkle, 2017). YPFD has been used to quantify the effects of light quality on photosynthesis (Sager et al., 1988; Stutte, 2009). In this study, while MW+R treatments promoted stem elongation in snapdragon and petunia and flowering in petunia compared to B<sub>15</sub>R<sub>85</sub>, spectral differences of lighting treatments had negligible effects on total leaf area in all species (Fig. 3). In addition, because G radiation has a lower average RQE value (0.85) than R radiation (0.91), the calculated YPFD was 1–4% lower in the MW+R treatments and 9% lower in B<sub>20</sub>G<sub>40</sub>R<sub>40</sub> treatment than B<sub>15</sub>R<sub>85</sub> (Table 1). However, the marginally lower YPFD of the MW+R and B<sub>20</sub>G<sub>40</sub>R<sub>40</sub> treatments had little to no effect on whole-plant net assimilation in any species (data not shown). With few significant spectral effects of lighting treatments on leaf expansion and net assimilation, plant dry weight was similar among radiation treatments in all species.

## Photosynthetic photon efficacy

PPE, which describes the PAR photon output per electric energy input (in  $\mu$ mol·J<sup>-1</sup>), is considered as the appropriate metric for electrical efficiency of light sources for plant growth (Nelson and Bugbee, 2014; ANSI/ASABE S640, 2017; Both et al., 2017). In this study,  $B_{15}R_{85}$  had the highest PPE value of 2.25  $\mu$ mol·J<sup>-1</sup> (Table 2). The PPE of MW<sub>100</sub> was 1.52  $\mu$ mol·J<sup>-1</sup>, which was 33% lower than that of  $B_{15}R_{85}$ , but as more MW was substituted with R, the PPE increased to 2.13  $\mu$ mol·J<sup>-1</sup>.  $B_{20}G_{40}R_{40}$  had a comparable PPE (1.51  $\mu$ mol·J<sup>-1</sup>) as the MW<sub>100</sub>. We also calculated dry weight gain per electric energy consumption, or DWE (in g·kWh<sup>-1</sup>). While  $B_{15}R_{85}$  had a higher PPE (in  $\mu$ mol·J<sup>-1</sup>) than the white light treatments, the DWE of  $B_{15}R_{85}$  was similar with those of  $MW_{25}R_{75}$ ,  $MW_{45}R_{55}$ , and  $MW_{75}R_{25}$  in begonia, petunia, and geranium

(Table 2). Only DWE for  $MW_{100}$  and  $B_{20}G_{40}R_{40}$  was 26–38% lower than that of  $B_{15}R_{85}$  in those three species. In snapdragon, DWE was similar among light treatments.

Here, we evaluated different shades of W and B+R radiation in terms of their effects on plant growth, electrical efficiency, and visual and color qualities. Seedling growth was similar under B+R and W radiation treatments at the same PPFD. In addition, W radiation created by mixing MW and R LEDs produced plant dry mass as efficiently as a typical B+R mixture. Using W radiation generally increased the visual quality (or CRI value), and particularly, some mixtures of MW and R LEDs showed higher visual quality and optimum color quality for white light. These results suggest that W radiation can be used for sole-source lighting to produce young plants with similar growth attributes and electric energy consumption while improving human vision.

## **APPENDIX**

Table IV-1. Spectral characteristics of sole-source lighting treatments delivered from mint white (MW), red (R), blue (B), and green (G) light-emitting diodes (LEDs) at total photosynthetic photon flux density (PPFD) =  $160 \mu \text{mol} \cdot \text{m}^{-2} \cdot \text{s}^{-1}$ . The subscript values after each LED type indicate the percentages of the total PPFD delivered from each LED type.

| indicate the percentages of the total FFTD derivered from each LED type. |                  |     |     |        |                   |           |                   |  |  |  |
|--|------------------|-----|-----|--------|-------------------|-----------|-------------------|--|--|--|
| Radiation  | % B <sup>a</sup> | % G | % R | $FR^b$ | R:FR <sup>c</sup> | $PPE^{d}$ | YPFD <sup>c</sup> |  |  |  |
| treatment  |                  |     |     |        |                   |           |                   |  |  |  |
| $MW_{100}$   | 15               | 59  | 26  | 6      | 8                 | 0.84      | 141               |  |  |  |
| $MW_{75}R_{25}$  | 11               | 45  | 44  | 4      | 17                | 0.87      | 142               |  |  |  |
| $MW_{45}R_{55}$  | 7                | 27  | 66  | 3      | 35                | 0.88      | 145               |  |  |  |
| $MW_{25}R_{75}$  | 4                | 16  | 80  | 2      | 57                | 0.88      | 146               |  |  |  |
| $B_{15}R_{85}$   | 15               | 0   | 85  | 1      | 130               | 0.88      | 147               |  |  |  |
| $B_{20}G_{40}R_{40}$   | 20               | 40  | 40  | 1      | 108               | 0.87      | 134               |  |  |  |

<sup>&</sup>lt;sup>a</sup>Percentage of B (400-500 nm), G (500-600 nm), and R (600-700 nm) radiation among total PPFD (400-700 nm).

<sup>&</sup>lt;sup>b</sup>Photon flux integral of FR (700-800 nm) radiation in μmol·m<sup>-2</sup>·s<sup>-1</sup>.

<sup>&</sup>lt;sup>c</sup>R:FR: Ratio of photon flux integral of R (600-700 nm) and FR (700-800 nm) radiation.

<sup>&</sup>lt;sup>d</sup>PPE: Phytochrome photoequilibria following Sager et al. (1988).

<sup>&</sup>lt;sup>e</sup>YPFD: Yield photon flux density, which is the product of TPFD and relative quantum efficiency (in μmol·m<sup>-2</sup>·s<sup>-1</sup>) based on McCree (1972) and Sager et al. (1988).

Table IV-2. Photosynthetic photon efficacy (PPE) and dry weight gain per electric energy consumption (dry weight efficacy) for begonia 'Olympia Red', geranium 'Pinto Premium Deep Rose', snapdragon 'Liberty Classic Yellow', and petunia 'Wave Blue' seedlings grown for 34 d, 25 d, 24 d and 19 d, respectively, under six sole-source lighting treatments delivered by mint white (MW), red (R), blue (B), and green (G) light-emitting diodes. The values after each LED type represent their percentages of the total PPFD.

| Radiation            | PPE                                    | Dry weight efficacy (g·kWh <sup>-1</sup> ) |          |            |          |  |  |
|----------------------|--|--|----------|------------|----------|--|--|
| treatment            | $(\mu \text{mol} \cdot \text{J}^{-1})$ | Begonia                                    | Geranium | Snapdragon | Petunia  |  |  |
| $MW_{100}$           | 1.52                                   | $0.78 b^a$                                 | 2.18 cd  | 1.37       | 1.00 cd  |  |  |
| $MW_{75}R_{25}$      | 1.72                                   | 0.92 ab                                    | 2.44 bcd | 1.53       | 1.12 bcd |  |  |
| $MW_{45}R_{55}$      | 1.88                                   | 1.17 a                                     | 2.70 bc  | 1.58       | 1.30 abc |  |  |
| $MW_{25}R_{75}$      | 2.13                                   | 1.11 a                                     | 3.52 a   | 1.78       | 1.50 a   |  |  |
| $B_{15}R_{85}$       | 2.25                                   | 1.14 a                                     | 3.02 ab  | 1.76       | 1.36 ab  |  |  |
| $B_{20}G_{40}R_{40}$ | 1.51                                   | 0.79 b                                     | 1.88 d   | 1.32       | 0.91 d   |  |  |
| Significance         |  | **b  | **       | NS         | **       |  |  |

<sup>&</sup>lt;sup>a</sup>Means with different letters are significantly different by Tukey's honestly significant difference test (P < 0.05) and lack of mean separation indicates nonsignificance.

<sup>&</sup>lt;sup>b</sup>NS or \*\* Nonsignificant or significant at P < 0.01, respectively.

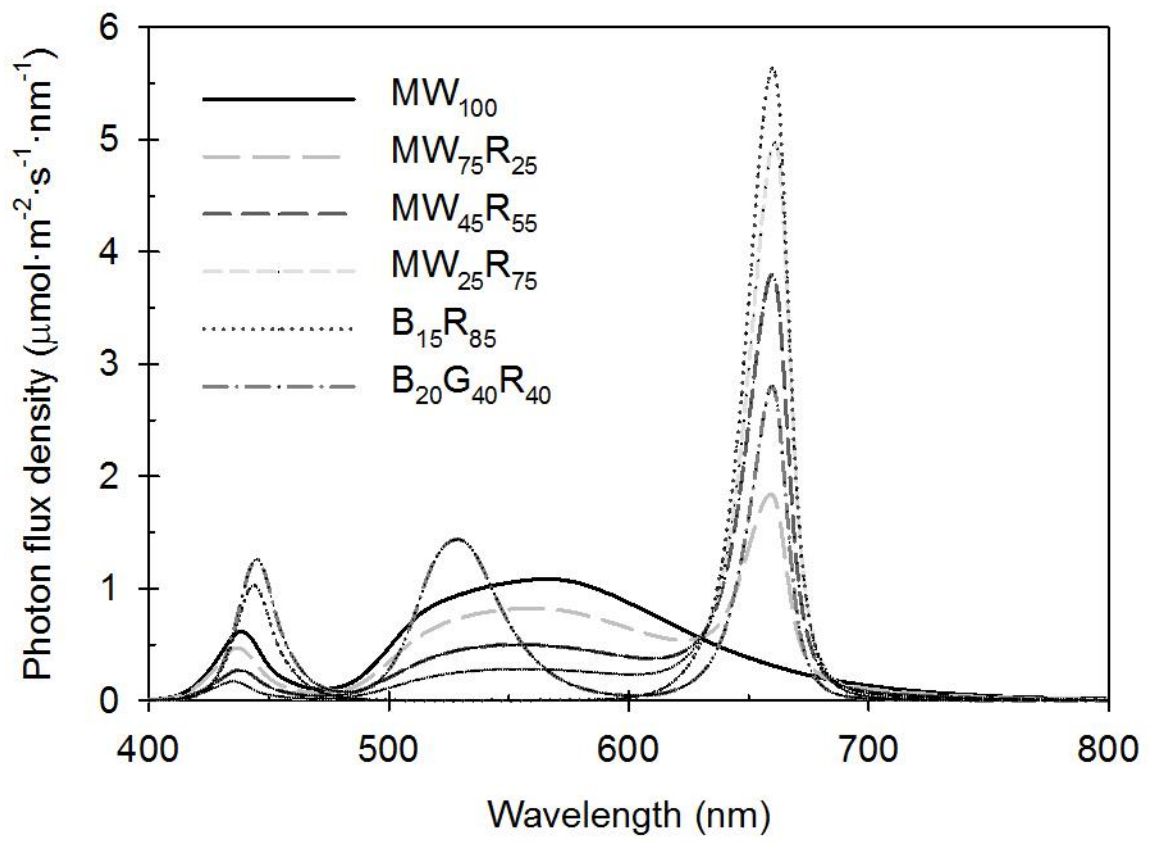


Figure IV-1. The spectral distribution of sole-source lighting treatments delivered from mint white (MW), red (R), blue (B), and green (G) light-emitting diodes (LEDs) at total photosynthetic photon flux density (PPFD) =  $160 \ \mu mol \cdot m^{-2} \cdot s^{-1}$ . The subscript values after each LED type indicate the percentages of the total PPFD delivered from each LED type.

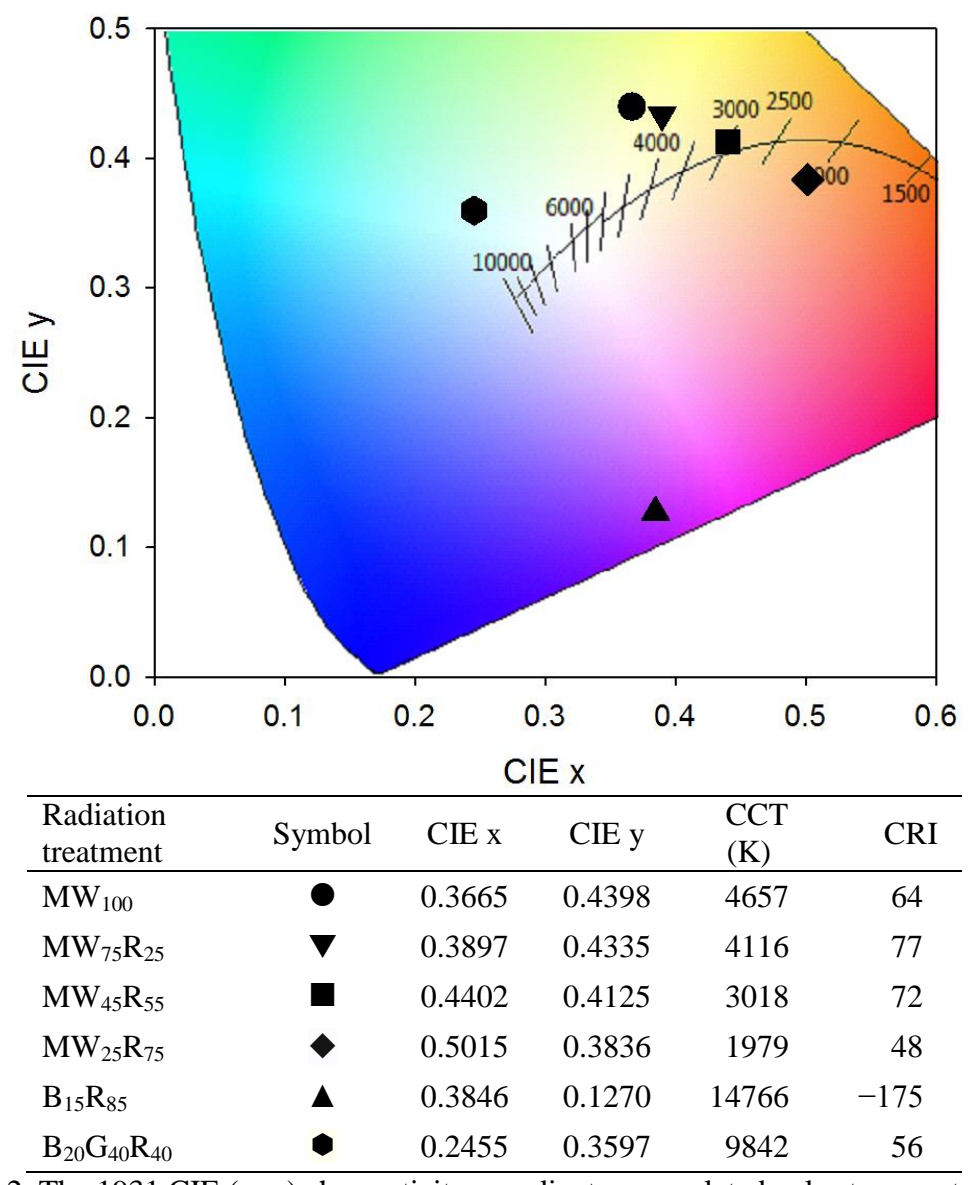


Figure IV-2. The 1931 CIE (x, y) chromaticity coordinates, correlated color temperature (CCT), and color rendering index (CRI) of six sole-source lighting treatments delivered from mint white (MW), red (R), blue (B), and green (G) light-emitting diodes (LEDs) at a total photosynthetic photon flux density (PPFD) =  $160 \mu \text{mol} \cdot \text{m}^{-2} \cdot \text{s}^{-1}$ . The subscript values after each LED type indicate the percentages of the total PPFD delivered from each LED type. Black-body curve (black solid line) and CCT values (K) are presented in CIE 1931 chromaticity coordinates.

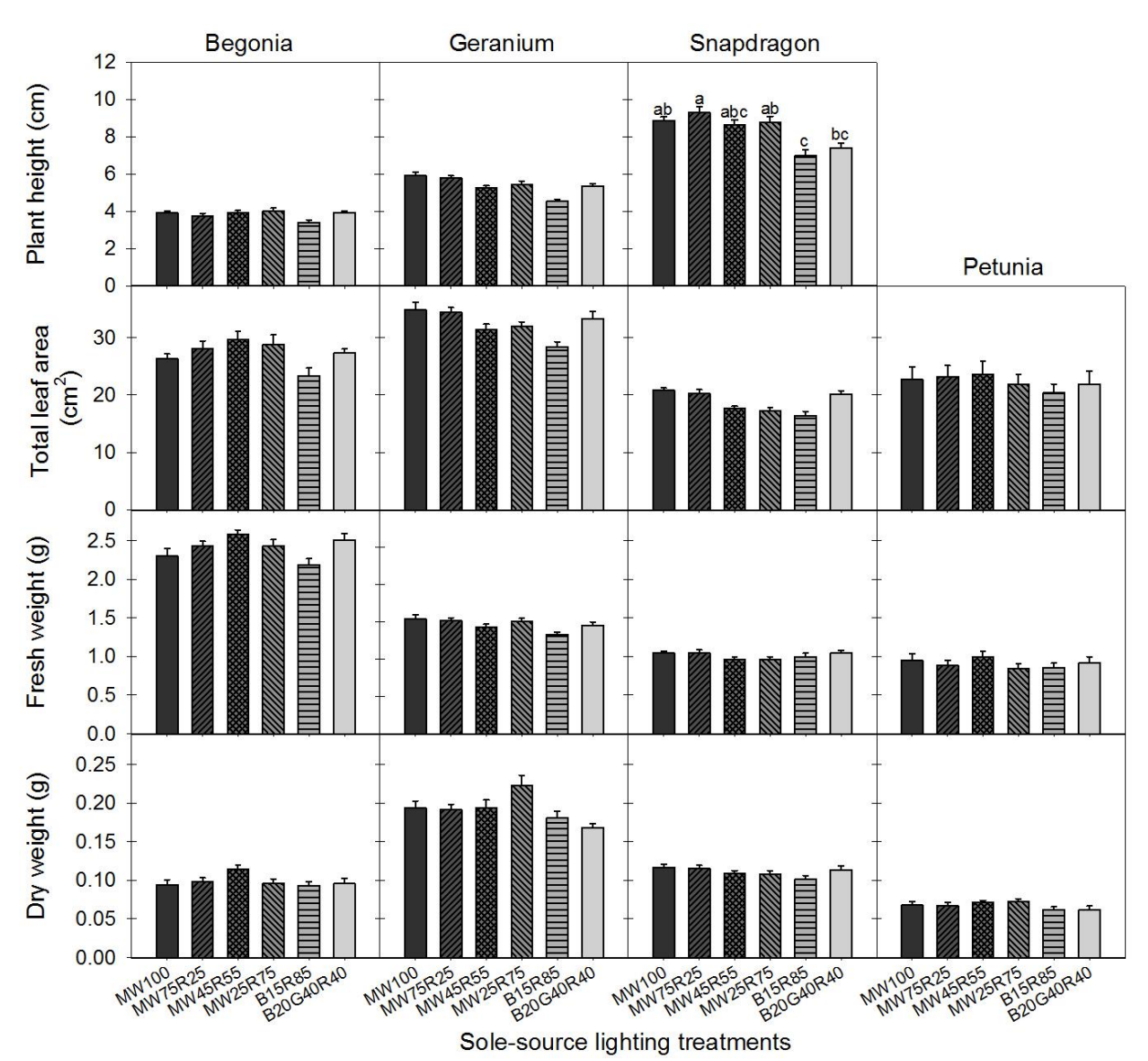
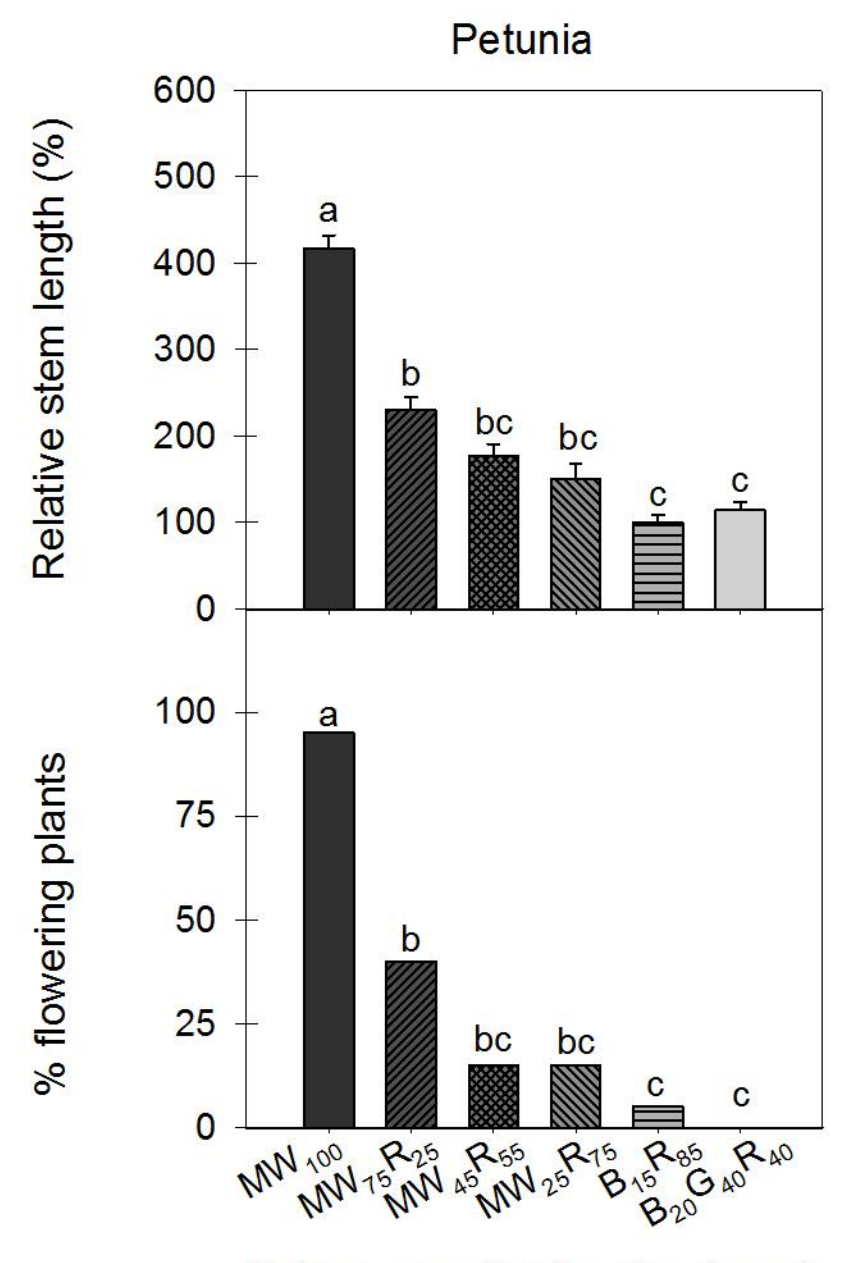


Figure IV-3. Plant height, total leaf area, fresh and dry weight for begonia 'Olympia Red', geranium 'Pinto Premium Deep Rose', snapdragon 'Liberty Classic Yellow', and petunia 'Wave Blue' seedlings grown for 34 d, 25 d, 24 d and 19 d, respectively, under six sole-source lighting treatments delivered by mint white (MW), red (R), blue (B), and green (G) light-emitting diodes. The values after each LED type represent their percentages of the total PPFD. Means with different letters are significantly different by Tukey's honestly significant difference test (P < 0.05) and lack of mean separation indicates nonsignificance. Error bars indicate standard error of two replications with 10 subsamples (plants) per replication per species.



# Sole-source lighting treatments

Figure IV-4. Relative stem length and percent of plants that had visible buds of petunia 'Wave Blue' grown for 39 d and 45 d, respectively, under six sole-source lighting treatments delivered by mint white (MW), red (R), blue (B), and green (G) light-emitting diodes. The values after each LED type represent their percentages of the total PPFD. Means with different letters are significantly different by Tukey's honestly significant difference test (P < 0.05). Error bars indicate standard error of two replications with 10 subsamples (plants) per replication per species.

LITERATURE CITED

#### LITERATURE CITED

- American National Standards Institute/American Society for Agricultural and Biological Engineers (ANSI/ASABE S640). 2017. Quantities and Unites of Electromagnetic Radiation for Plants (Photosynthetic Organisms). Amer. Soc. Agr. Biol. Eng. St. Joseph, MI.
- Banerjee, R., E. Schleicher, S. Meier, R.M. Viana, R. Pokorny, M. Ahmad, R. Bittl, and A. Batschauer. 2007. The signaling state of *Arabidopsis* cryptochrome 2 contains flavin semiquinone. J. Biol. Chem. 282:14916–14922.
- Bouly, J-P, E. Schleicher, M. Dionisio-Sese, F. Vandenbussche, D. Van Der Straeten, N. Bakrim, S. Meier, A. Batschauer, P. Galland, R. Bittl, and M. Ahmad. 2007. Cryptochrome blue light photoreceptors are activated through interconversion of flavin redox states. J. Biol. Chem. 282:9383–9391.
- Both, A.J., B. Bugbee, C. Kubota, R.G. Lopez, C. Mitchell, E.S. Runkle, and C. Wallace. 2017. Proposed product label for electric lamps used in the plant sciences. HortTechnology 27:544-549.
- Brown, C.S., A. Schuerger, and J.C. Sager. 1995. Growth and photomorphogenesis of pepper plants under red LEDs with supplemental blue or far-red lighting. J. Amer. Soc. Hort. Sci. 120:808–813.
- Casal, J.J. 2013. Canopy light signals and crop yield in sickness and in health. ISRN Agron. 2013, 650439.
- Cope, K.R. and B. Bugbee. 2013. Spectral effects of three types of white light-emitting diodes on plant growth and development: absolute versus relative amounts of blue light. HortScience 48:504–509.
- Cope, K.R., Snowden, M.C., Bugbee, B., 2014. Photobiological interactions of blue light and photosynthetic photon flux: effects of monochromatic and broadspectrum light source. Photochem. Photobiol. 90:574–584.
- Craig, D.S. and E.S. Runkle. 2016. An intermediate phytochrome photoequilibria from night-interruption lighting optimally promotes flowering of several long-day plants. Environ. Exp. Bot. 121:132–138.
- Dougher, T.A.O. and B. Bugbee. 2001. Differences in the response of wheat, soybean, and lettuce to reduced blue radiation. Photochem. Photobiol. 73:199–207.
- Folta, K.M. 2004. Green light stimulates early stem elongation, antagonizing light-mediated growth inhibition. Plant Physiol. 135:1407–1416.

- Gregory, F.G. 1917. Physiological conditions in cucumber houses. 3rd Ann. Exp. Res. Stn. Rep. Cheshunt, England, pp. 19–28.
- Hernández, R., and C. Kubota. 2016. Physiological responses of cucumber seedlings under different blue and red photon flux ratios using LEDs. Environ. Exp. Bot. 121:66–74.
- Hogewoning, S.W., Douwstra, P., Trouwborst, G., van Ieperen, W., Harbinson, J., 2010. An artificial solar spectrum substantially alters plant development compared with usual climate room irradiance spectra. J. Exp. Bot. 61:1267–1276.
- Kasajima, S.-Y., N. Inoue, R. Mahmud, K. Fujita, and M. Kato. 2007. Effect of light quality on developmental rate of wheat under continuous light at a constant temperature. Plant Prod. Sci. 10:286–291.
- Kim, H.H., Goins, G.D., Wheeler, R.M. and Sager, J.C. 2004. Green light supplementation for enhanced lettuce growth under red- and blue-light–emitting diodes. HortScience 39: 1617–1622.
- Liu, X.Y., T.T. Chang, S.R. Guo, Z.G. Xu, and J. Li. 2011b. Effect of light quality of LED on growth and photosynthetic character in cherry tomato seedling. Acta Hort. 907:325–330.
- McCamy, C.S. 1992. Correlated color temperature as an explicit function of chromaticity coordinates. Color Res. Appl. 17:142–144.
- McCree, K.J. 1972. The action spectrum, absorbance and quantum yield of photosynthesis in crop plants. Agr. Meteorol. 9:191–216.
- Moss, R.A. and W.E. Loomis. 1952. Absorption spectra of leaves. 1. The visible spectrum. Plant Physiol. 27:370–391.
- Nelson, J.A. and B. Bugbee. 2014. Economic Analysis of Greenhouse Lighting: Light Emitting Diodes vs. High Intensity Discharge Fixtures. PLoS ONE 9:e99010.
- Ohno, Y. 2005. Spectral design considerations for white LED color rendering. Opt. Eng. 44, 11302.
- Ohta, N. and A. Robertson. 2006. Colorimetry: fundamentals and applications. John Wiley & Sons, West Sussex, UK.
- Park, Y. and E.S. Runkle. 2017. Far-red radiation promotes growth of seedlings by increasing leaf expansion and whole-plant net assimilation. Environ. Exp. Bot. 136:41–49.
- Pust, P., P.J. Schmidt, and W. Schnick. 2015. A revolution in lighting. Nat. Mater. 14:454–458.

- Randall, W.C. and R.G. Lopez. 2015. Comparisons of bedding plant seedlings grown under sole source light-emitting diodes (LEDs) and greenhouse supplemental lighting from LEDs and high-pressure sodium lamps. HortScience 50:705–713.
- Sager, J.C., W.O. Smith, J.L. Edwards, and K.L. Cyr. 1988. Photosynthetic efficiency and phytochrome photoequilibria determination using spectral data. Trans. Amer. Soc. Agr. Eng. 31:1882–1889.
- Sasabe, H. and J. Kido. 2013. Development of high performance OLEDs for general lighting. J. Mater. Chem. CMater. Opt. Electron. Devices 1:1699–1707.
- Sellaro, R., M. Crepy, S.A. Trupkin, E. Karayekov, A.S. Buchovsky, C. Rossi and J.J. Casal. 2010. Cryptochrome as a sensor of the blue/green ratio of natural radiation in Arabidopsis. Plant Physiol. 154:401–409.
- Smith, H. 1982. Light quality, photoreception, and plant strategy. Ann. Rev. Plant Physiol. 33:481–518.
- Smith, H. and G.C. Whitelam. 1997. The shade avoidance syndrome: multiple responses mediated by multiple phytochromes. Plant Cell Environ. 20:840–844.
- Stutte, G.W. 2009. Light-emitting diodes for manipulating the phytochrome apparatus. HortScience 44:231–234.
- Sullivan, J.A. and X.W. Deng. 2003. From seed to seed: the role of photoreceptors in *Arabidopsis* development. Dev. Biol. 260:289–97.
- Snowden, M.C., Cope, K.R., Bugbee, B., 2016. Sensitivity of seven diverse species to blue and green light: interactions with photon flux. PLoS One 11:e0163121.
- Son, K.H. and M.M. Oh. 2013. Leaf shape, growth, and antioxidant phenolic compounds of two lettuce cultivars grown under various combinations of blue and red light-emitting diodes. HortScience 48:988–995.
- Thejokalyani N. and S.J. Dhoble. 2014. Novel approaches for energy efficient solid state lighting by RGB organic light emitting diodes—a review. Renew. Sustain. Energy Rev. 32:448–467.
- Wang, Y. and K.M. Folta. 2013. Contributions of green light to plant growth and development. Am. J. Bot. 100:70–78.
- Wang, Y., T. Zhang, K.M. Folta. 2015. Green light augments far-red-light-induced shade response. Plant Growth Regul. 77:147–155.
- Wollaeger, H.M. and E.S. Runkle. 2014. Growth of impatiens, petunia, salvia, and tomato seedlings under blue, green, and red light-emitting diodes. HortScience 49:734–740.

- Wollaeger, H.M. and E.S. Runkle. 2015. Growth and acclimation of impatiens, salvia, petunia, and tomato seedlings to blue and red light. HortScience 50:522–529.
- Yorio, N.C., G. Goins, H. Kagie, R. Wheeler, and J.C. Sager. 2001. Improving spinach, radish, and lettuce growth under red LEDs with blue light supplementation. HortScience 36:380–383.
- Zhang, T., S.A. Maruhnich, and K.M. Folta. 2011. Green light induces shade avoidance symptoms. Plant Physiol.157:1528–1536.